People's Democratic Republic of Algeria

Ministry of Higher Education and Scientific Research

Hamma Lakhdar University of El Oued

Faculty of Technology

Department of Electrical Engineering

End-of-Study Thesis

Submitted in fulfillment of the requirements for the degree of

ACADEMIC MASTER

Specialization: Electrical Control

Topic

Design, Modeling, and Simulation of a DC/DC Boost Converter for MPPT-Based Photovoltaic Systems

Created by: Atoussi Abderrahmane & Khellout Abdraouf

Before the jury composed of:		
Pr.Nadhir Mesbahi	Univ. El Oued	President
Dr.Mahni Tidjani	Univ. El Oued	Examiner
Dr.Bilal Hamidani	Univ. El Oued	Supervisor

Academic year:

2025/2026

DEDICACES

We dedicate this work to:

Our dear parents

Our brothers and sisters

Our friends

And to all our families

Thanks and Appreciation

First and foremost, all praise is due to Allah, who granted us strength, health, and patience, and enabled us to accomplish this work .

We would like to express our sincere thanks and profound gratitude to our supervisor for the valuable guidance, insightful advice, and continuous follow-up that had a significant impact on the completion of this work .

We also extend our sincere thanks to the honorable members of the examination committee for accepting to evaluate this modest work and for enriching it with their valuable academic remarks .

I dedicate this modest work to my beloved parents, in appreciation of their sacrifices and continuous support, to all my dear family members .

Abstract

The increasing demand for renewable energy has led to significant interest in solar photovoltaic (PV) systems as a sustainable and clean energy source. However, the efficiency of PV systems is highly dependent on environmental conditions such as solar irradiance and temperature. To address this challenge, Maximum Power Point Tracking (MPPT) techniques are widely used to ensure that the PV system operates at its optimal power point.

This project focuses on the design, modeling, and implementation of a DC–DC boost converter integrated with an MPPT algorithm for photovoltaic applications. The boost converter is used to step up the low output voltage of the PV panel to a higher and regulated level suitable for the load. An appropriate MPPT technique is applied to maximize the energy extraction from the solar panel under varying environmental conditions.

The system is first modeled and simulated using MATLAB/Simulink to analyze its performance and validate the control strategy. Key parameters such as output voltage, efficiency, and response to changes in irradiance are evaluated. Finally, the implementation aspects of the system are discussed to demonstrate its practical feasibility.

The results show that the integration of the boost converter with MPPT significantly improves the overall efficiency and performance of the photovoltaic system, making it a reliable solution for renewable energy applications.

Keywords: DC/DC Boost Converter - Photovoltaic (PV) System -Maximum Power Point Tracking (MPPT) -Solar Energy

الملخص

أدى الطلب المتزايد على الطاقة المتجددة إلى اهتمام كبير بأنظمة الطاقة الشمسية الكهروضوئية (PV) كمصدر طاقة مستدام ونظيف. ومع ذلك، فإن كفاءة هذه الأنظمة تعتمد بشكل كبير على الظروف البيئية مثل شدة الإشعاع الشمسي ودرجة الحرارة. ولمعالجة هذه المشكلة، تُستخدم تقنيات تتبع نقطة القدرة العظمى (MPPT) على نطاق واسع لضمان عمل النظام عند نقطة القدرة المثلى.

يركز هذا المشروع على تصميم ونمذجة وتنفيذ محول رافع للتيار المستمر (DC–DC Boost Converter) مدمج مع خوارزمية MPPT لتطبيقات الطاقة الشمسية. يُستخدم هذا المحول لرفع الجهد المنخفض الخارج من اللوح الشمسي إلى مستوى أعلى ومنظم مناسب للحمل. كما يتم تطبيق تقنية MPPT مناسبة لتعظيم استخراج الطاقة من اللوح الشمسي تحت ظروف بيئية متغيرة.

يتم أولاً نمذجة النظام ومحاكاته باستخدام MATLAB/Simulink لتحليل أدائه والتحقق من استراتيجية التحكم. ويتم تقييم معلمات رئيسية مثل جهد الخرج، الكفاءة، واستجابة النظام للتغيرات في شدة الإشعاع الشمسي. وأخيرًا، تتم مناقشة جوانب تنفيذ النظام لإظهار قابليته للتطبيق العملي.

تُظهر النتائج أن دمج المحول الرافع مع تقنية MPPT يحسن بشكل كبير الكفاءة العامة وأداء النظام الكهروضوئي، مما يجعله حلاً موثوقًا لتطبيقات الطاقة المتجددة.

الكلمات المفتاحية: نظام الطاقة الكهروضوئية- الطاقة الشمسية- محوّل رافع للجهد - نقطة قدرة العظمى

Résumé

La demande croissante en énergie renouvelable a suscité un intérêt considérable pour les systèmes photovoltaïques (PV) en tant que source d'énergie durable et propre. Cependant, l'efficacité des systèmes PV dépend fortement des conditions environnementales telles que l'irradiation solaire et la température. Pour relever ce défi, des techniques de suivi du point de puissance maximale (MPPT) sont largement utilisées afin de garantir que le système PV fonctionne à son point de puissance optimal.

Ce projet se concentre sur la conception, la modélisation et la mise en œuvre d'un convertisseur élévateur DC–DC (boost) intégré à un algorithme MPPT pour des applications photovoltaïques. Le convertisseur boost est utilisé pour élever la faible tension de sortie du panneau photovoltaïque à un niveau plus élevé et régulé, adapté à la charge. Une technique MPPT appropriée est appliquée afin de maximiser l'extraction d'énergie du panneau solaire dans des conditions environnementales variables.

Le système est d'abord modélisé et simulé à l'aide de MATLAB/Simulink afin d'analyser ses performances et de valider la stratégie de contrôle. Des paramètres clés tels que la tension de sortie, le rendement et la réponse aux variations d'irradiation sont évalués. Enfin, les aspects liés à la mise en œuvre du système sont discutés afin de démontrer sa faisabilité pratique.

Les résultats montrent que l'intégration du convertisseur boost avec le MPPT améliore significativement le rendement global et les performances du système photovoltaïque, ce qui en fait une solution fiable pour les applications d'énergie renouvelable.

List of Abbreviations

PV	Photovoltaic
DC	Direct current
AC	Alternating current
MPPT	Maximum Power Point Tracking
V_{OC}	Open circuit voltage
I_{SC}	Short circuit current
V_{MPP}	Voltage at maximum point
IGBT	Integrated bipolar transistor
INC	Incremental conductance
P&O	The Perturbation and Observation Algorithm
MPP	Maximum Power Point
Pmax	Maximum Power
Vmpp	Voltage at maximum point
Imp	Current at maximum point
Rsh	Shunt Resistance
Rs	Series Resistance
A	Diode ideality factor
α	Short-circuit current temperature coefficient Isc
β	Voltage temperature coefficient Voc

Table of Contents

Dedication i

Thanks and Appreciation ii

Abstract iii

List of Abbreviations vi

Table of Contents vii

List of Figures xii

List of Tables xvi

General Introduction 1

Chapter I: General Overview of Photovoltaic Systems

I.1. Introduction 2

I.2. Photovoltaic systems Foundation and its impact in Algeria 2

I.2.1. Diversification of Energy Sources 2

I.2.2. Economic Development 3

I.2.3. Environmental Conservation 3

I.2.4. Rural Electrification and Social Impact 4

I.2.5. Research and Innovation 4

I.2.6. Energy Export Potential 4

I.2.7. Solar Radiation Patterns and Implemented Solar Installations 4

I.3. Solar Radiation 5

I.4. Types of Solar Radiation 5

I.4.1. Direct Solar Radiation 5

I.4.2. Diffuse Solar Radiation 5

I.4.3. Reflected Solar Radiation 6
I.4.4. Global Solar Radiation 6
I.5. Solar Energy 6
I.6. Types of Solar Energy 8
I .6.1. Thermal solar energy 8
I.6.2. Thermodynamic solar energy 8
I.6.3. Photovoltaic solar energy 8
I.6.3.1. The photovoltaic effect 8
I.7. Photovoltaic cells 9
I.7.1. Operating Principle of Photovoltaic Cells 10
I.8. Different types of photovoltaic cells 11
I.8.1. Mono crystalline cells 11
I.8.2. Polycrystalline cells 12
I.8.3. Amorphous silicon cells 12
I.8.4. Comparison of different technologies 13
I.9. Photovoltaic modules 13
I.9.1. Role of the PV solar module 14
I.10. Connection of photovoltaic modules 14
I.10.1. Series connection 14
I.10.2. Parallel Connection 15
I.10.3. Mixed connection (Series – Parallel) 16
I.11. photovoltaic system 17
I.11.1. Autonomous systems 17
I.11.2. Grid-connected systems 18
I.11.3. Hybrid systems 18

I.12. Power electronic converters 19
I.12.1. DC-DC converters 20
I.12.2. DC-DC Converters for Solar Energy Systems 20
I.12.3. types of DC-DC converters 20
I.13. Advantages and disadvantages of a photovoltaic system 21
I.13.1. Advantages 21
I.13.2. disadvantages 21
I.14. Conclusion 21

Chapter II: Modeling and Analysis of DC–DC Converters

II.1. Introduction 22
II.2. Step-down converter (Buck converter) 22
II.2.1. Principle of operation 23
II.2.2. Mathematical model 23
II.2.3. Conversion and yield report 24
II.2.4. Continuous conduction mode 25
II.2.5. Discontinuous conduction mode 26
II.3. Step-up converter (Boost converter) 26
II.3.1. Principle of operation 27
II.3.2. Equivalent mathematical model 27
II.3.3. Conversion and yield report 28
II.3.4. Continuous conduction mode 29
II.3.5. Discontinuous conduction mode 30
II.4. Buck-Boost Converter 31
II.4.1. Principle of operation 32

II.4.2. Conversion and yield report 33
II.4.3. Continuous conduction mode 33
II.4.4. Discontinuous conduction mode 34
II.5. Simulation results 35
II.5.1. DC/DC Boost converter simulation 35
II.6. Conclusion 37

Chapter III: Maximum Power Point Tracking (MPPT) Principles and Algorithms

III.1. Introduction 39
III.2. Principle of Maximum Power Point Tracking (MPPT) 39
III.3. Classification of (MPPT) algorithms according to the search method 40
III.3.1. Direct methods 40
III.3.2. Indirect methods 40
III.4. MPPT Algorithms 41
III.4.1. Perturb and Observe (P&O) Algorithm 41
III.4.2. Incremental Conductance Algorithm (INC) 42
III.4.3. Constant Voltage Algorithm 44
III.4.4. Constant Current Algorithm 45
III.4.5. Hill Climbing Algorithm 45
III.5. Conclusion 46

Chapter IV: Simulation Results and Comparative Analysis

IV.1. Introduction 48
IV.2. Simulation Results 48
IV.2.1. Open circuit PV Panel Simulation Via MATLAB/Simulink 48

IV.2.1.1. Irradiance variation test 50
IV.2.1.2. Temperature variation test 52
IV.2.2. Effect of Load Resistance on Solar Panel Operating Points and Power Output 54
IV.2.3. Effect of DC/DC Boost Converter Duty Cycle on Solar Panel Operating Point 55
IV.3. Simulation of PV system under Perturb and Observe MPPT method via MATLAB/Simulink 56
IV.3.1. Simulation results 56
IV.4. Simulation of PV system under Incremental Conductance (INC) MPPT algorithm via MATLAB/Simulink 59
IV.4.1. Simulation results 60
IV.5. Simulation of PV system under Hill Climbing (HC) MPPT algorithm via MATLAB/Simulink 63
IV.5.1. Simulation results 63
IV.6. Comparison between Perturb & Observe (P&O), Incremental Conductance (INC), and Hill Climbing methods 66
IV.7. Conclusion 67
Conclusion General 68
List of References 69
Appendix 75

List of Figures

Figure I.1: Diversification of Energy Sources 3

Figure I.2: Solar Irradiation in Algeria 5

Figure I.3: Components of Solar Radiation 6

Figure I.4: Solar spectrum 8

Figure I.5: Working Principle of the Photovoltaic Effect 9

Figure I.6: A photovoltaic cell 10

Figure I.7: Principle of Photovoltaic Cells 11

Figure I.8: Mono crystalline cells 11

Figure I.9: Polycrystalline cells 12

Figure I.10: Amorphous silicon cells 13

Figure I.11: Composition of a photovoltaic (PV) solar module 14

Figure I.12: Series connection of solar cells 15

Figure I.13: Parallel connection of photovoltaic cells 16

Figure I.14: Parallel and series connection of photovoltaic cells 16

Figure I.15: Autonomous photovoltaic installation 17

Figure I.16: Diagram of a grid-connected photovoltaic installation 18

Figure I.17: Autonomous hybrid photovoltaic installation 19

Figure I.18: Symbol of a DC-DC converter 19

Figure I.19: Voltages Ve and Vs in a DC/DC converter 20

Figure II.1: Principle diagram of a Buck converter 22

Figure II.2: Equivalent circuit diagram of the series chopper when t ∈ [0, αTs] ... 23

Figure II.3: the conversion ratio M(d) of a series chopper (DC-DC converter) ... 24

Figure II.4: Current and voltage waveforms in a Buck converter 25

Figure II.5: Evolution with time of the voltages V_0 V_D V_L and the current I_L in an ideal buck converter operating in continuous mode 26

Figure II.6: Basic diagram of a Boost converter 27

Figure II.7: Equivalent circuit diagram of the boost chopper when t ∈ [0; α,Ts] ... 27

Figure II.8: Equivalent circuit of a boost chopper when t ∈ [α,Ts; Ts] 28

Figure II.9: Shape of the conversion ratio as a function of the duty cycle 29

Figure II.10: Current and voltage waveforms in a Boost converter 30

Figure II.11: Waveforms of inductor current and voltage in a boost converter operating in discontinuous mode 31

Figure II.12: Buck-Boost Converter 31

Figure II.13: Equivalent circuit of a Buck-Boost converter when t ∈ [0, αT_s] 32

Figure II.14: Equivalent circuit of a Buck-Boost converter when t ∈ [αT_s, T_s] 32

Figure II.15: Conversion ratio as a function of the duty cycle 33

Figure II.16: Current and voltage waveforms in a Buck-Boost converter 34

Figure II.17: Waveforms of current and voltage in a buck–boost converter operating in discontinuous mode 34

Figure II.18: Block diagram of a Boost converter 35

Figure II.19: Time response of the output voltage Vout under duty cycle step changes compared to the input voltage Vin 35

Figure III.1: Power characteristic curve of a PV generator 39

Figure III.2: Principle diagram of an MPPT converter 40

Figure III.3: Search for the MPP using the P&O method. 41

Figure III.4: Flowchart of the P&O algorithm 42

Figure III.5: Positioning of the operating point according to the value of $\Delta I_{pv}/\Delta V_{pv}$ on the(I-V) characteristics 43

Figure III.6: Flowchart of the INC algorithm 44

Figure III.7: Flowchart of the Hill Climbing Algorithm 45

Figure IV.1: Simulation scheme of Open circuit PV Panel 48

Figure IV.2: Characteristic Curves of a PV Module: Current-Voltage (I-V) and Power-Voltage (P-V) at Standard Test Conditions (STC) 49

Figure IV.3: I-V Characteristics of the PV module under Solar Irradiance Variation with constant temperature 50

Figure IV.4: P-V characteristics of the PV module under solar irradiance variation with constant temperature 51

Figure IV.5: I-V Characteristics of a PV module under temperature variation with constant solar irradiance 52

Figure IV.6: P-V Characteristics of a PV module under temperature variation with constant solar irradiance 53

Figure IV.7: I-V characteristics of the PV panel and operating points with different resistors loads 54

Figure IV.8: Effect of the DC/DC Boost Converter duty cycle on the operating point of the PV solar panel 55

Figure IV.9 : Simulation block diagram of a PV solar system under (P&O),(INC),(HC) algorithm 56

Figure IV.10 : Solar irradiance curve 56

Figure IV.11: Dynamic Power curve with variable irradiance under P&O algorithm 57

Figure IV.12: voltage curve with variable irradiance under P&O algorithm 58

Figure IV.13: current curve with variable irradiance under P&O algorithm 58

Figure IV.14: Dynamic Power curve with variable irradiance under INC algorithm 60

Figure IV.15: Dynamic voltage curve with variable irradiance under INC algorithm 61

Figure IV.16: Dynamic current curve with variable irradiance under INC algorithm 62

Figure IV.17: Dynamic power curve with variable irradiance under Hill Climbing (HC) algorithm 63

Figure IV.18: Dynamic voltage curve with variable irradiance under Hill Climbing (HC) algorithm 64

Figure IV.19: Dynamic current curve with variable irradiance under Hill Climbing (HC) algorithm 65

Figure IV.20: Dynamic power comparison between P&O, INC and Hill Climbing MPPT algorithms under varying irradiance 66

Figure IV.21: Dynamic voltage comparison between P&O, INC and Hill Climbing MPPT algorithms under varying irradiance 67

List of Tables

Table I.1: Power, and Tariffs for the two energy sources Wind, Solar PV 3

Table I.2: Comparison of different cell technologies 13

General Introduction

The increasing global demand for electrical energy and the environmental problems caused by fossil fuels have accelerated the search for clean and renewable energy sources. Among the available renewable technologies, photovoltaic (PV) systems have become one of the most promising solutions due to their reliability, sustainability, and ability to directly convert solar energy into electrical energy. However, the efficiency of PV systems is highly affected by environmental conditions such as solar irradiance and temperature, which leads to continuous variations in the output power of the system.

To improve the performance of photovoltaic systems, power electronic converters and Maximum Power Point Tracking (MPPT) techniques are widely used. DC–DC converters play an essential role in adapting and regulating the output voltage of PV generators, while MPPT algorithms ensure the extraction of the maximum available power under changing climatic conditions. The integration of these techniques significantly enhances the overall efficiency, stability, and reliability of solar energy systems.

This work focuses on the study, modeling, and simulation of a photovoltaic system associated with a DC–DC Boost converter and MPPT control techniques. The objective is to analyze the behavior of the PV system and evaluate the performance of different MPPT algorithms under varying environmental conditions.

This dissertation is organized into four chapters:

The first chapter presents a general overview of photovoltaic systems, including their operating principles, components, characteristics, and applications.

The second chapter focuses on DC–DC converters, particularly the Boost converter, its operating principles, and mathematical modeling.

The third chapter discusses Maximum Power Point Tracking (MPPT) techniques and introduces the most commonly used algorithms for extracting maximum power from photovoltaic systems.

The fourth chapter is dedicated to the modeling and simulation of the photovoltaic system using MATLAB/Simulink, as well as the comparative analysis of different MPPT algorithms under varying irradiance and temperature conditions.

Finally, the work concludes with a summary of the obtained results and perspectives for future improvements in photovoltaic energy conversion systems.

CHAPTER I:

GENERAL OVERVIEW OF PHOTOVOLTAIC SYSTEMS

I.1. Introduction

In the realm of renewable energy solutions, photovoltaic systems stand as pivotal entities, drawing their power from sunlight, the quintessential source of energy. This chapter delves into the intricate world of photovoltaic systems, illuminating their importance in the contemporary landscape of sustainable energy [1]. Amidst the urgency of the global climate crisis, the imperative for clean, renewable energy has never been more pronounced. Photovoltaic systems, commonly known as solar power systems, exemplify human innovation, encapsulating our pursuit of a sustainable tomorrow [2].

Photovoltaic systems represent one of the most prominent modern technologies in the field of renewable energy generation. They rely on the direct conversion of solar energy into electrical energy in a clean and silent manner, without the need for moving mechanical parts. This technology is based on the physical properties of semiconductor materials, particularly silicon, which has the ability to generate an electric current when exposed to solar radiation. This process produces direct current (DC), which can later be converted into alternating current (AC) through specialized devices in order to meet the requirements of various electrical applications.

Photovoltaic systems are characterized by their wide range of applications. They can be used to power small electronic devices such as watches and calculators, and they also play a significant role in supplying electricity to remote areas that are not connected to the electrical grid. In addition, they are used in telecommunications systems and can be integrated with public power grids. The ease of installation, low maintenance requirements, quiet operation, and environmentally friendly nature of these systems make them an ideal choice for both residential and commercial building applications.

In essence, this chapter embarks on an odyssey, tracing the evolution of an idea into a cornerstone of clean energy. It is a voyage through time, science, and engineering, where sunlight becomes more than illumination; it becomes the life force propelling sustainable progress. As we delve deeper into the ensuing chapters, the narrative woven here will serve as the foundation, grounding us in the profound significance of photovoltaic systems and their pivotal role in shaping a sustainable future.

I.2. Photovoltaic systems Foundation and its impact in Algeria

Algeria, a nation endowed with abundant sunlight, has astutely recognized the potential of solar energy as a transformative solution to its energy challenges [3]. Photovoltaic systems, often referred to as solar power systems, have emerged as pioneering technologies, significantly reshaping Algeria in several fundamental dimensions.

I.2.1. Diversification of Energy Sources

Historically reliant on finite fossil fuels, Algeria has strategically diversified its energy mix by investing in photovoltaic systems [4]. The vast desert expanses, notably the Sahara, receive intense sunlight throughout the year, making them ideal locations for solar power projects. By integrating photovoltaic systems into its energy grid, Algeria has substantially reduced its dependence on finite fossil fuels, thereby enhancing energy security and sustainability [5] as illustrated in Fig.1.

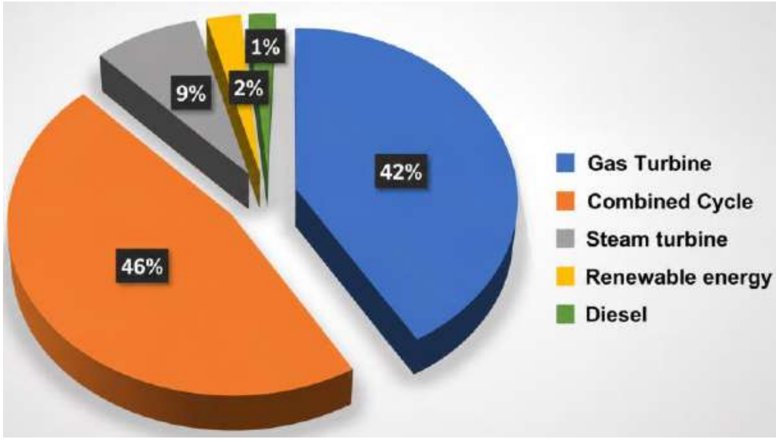

Figure I.1: Diversification of Energy Sources

I.2.2. Economic Development

The adoption of photovoltaic systems has catalyzed economic growth in Algeria. The establishment and maintenance of solar power plants have generated employment opportunities, stimulating local economies [6]. Additionally, the decreased reliance on imported fuels for electricity generation has alleviated financial burdens, allowing redirected funds to vital sectors such as education, healthcare, and infrastructure projects [7]. In 2014, the Algerian government introduced a feed-in tariff mechanism, a pivotal initiative in the country's energy sector, incentivizing renewable energy adoption [8]. Algeria has also instituted a structured pricing scale for electricity generated from various sources, creating a framework for sustainable energy production and consumption [9] as shown in Table 1.

Table I.1: Power, and Tariffs for the two energy sources Wind, Solar PV[75]

Energy source	Power (MW)	Feed-In Tariff (DZD/KWh)	
		5 initial Years	15 Remaining Years
Wind	1-5	13.10	9.55-16.66
	≥ 5	10.48	7.64-13.33
Solar PV	1-5	15.94	11.80-20.08
	≥ 5	12.75	9.44-16.06

I.2.3. Environmental Conservation

Algeria's commitment to photovoltaic systems aligns with global efforts to combat climate change. By generating electricity from renewable sources, particularly solar power, Algeria has significantly reduced its carbon footprint. This transition to clean energy has mitigated the adverse environmental effects associated with fossil fuel combustion, leading to improved air quality and diminished greenhouse gas emissions [10].

I.2.4. Rural Electrification and Social Impact

In numerous remote and rural areas of Algeria, access to electricity was once a luxury. Photovoltaic systems, especially in the form of off-grid solar installations, have facilitated rural electrification [11]. By bringing electricity to these regions, these systems have elevated the quality of life for residents. Access to electricity has enabled enhanced healthcare, education, and communication, fostering social development and empowerment [12].

I.2.5. Research and Innovation

The implementation of photovoltaic systems has stimulated research and innovation in Algeria. Academic institutions and research centres are delving into solar technology, aiming to enhance efficiency and reduce costs [13]. This focus on research not only enriches Algeria’s knowledge base but also contributes valuable insights to the global solar energy community.

I.2.6. Energy Export Potential

Algeria's strategic investment in photovoltaic systems positions the country as a potential energy exporter in the future. With advancements in energy storage technology, surplus solar energy can be stored and transported to neigh boring regions, creating economic opportunities and strengthening diplomatic ties through energy cooperation [14].

I.2.7. Solar Radiation Patterns and Implemented Solar Installations

As illustrated in Fig.2, In Algeria, solar photovoltaic technology stands as the most viable energy solution, primarily due to the country's extensive solar exposure, covering approximately 90% of its vast landmass spanning 2,382 million km^2 [15]. The region benefits from an estimated annual sunshine duration of 3000 hours and daily energy absorption of up to 5 kWh per square meter on most horizontal surfaces. However, the uneven and variable distribution of solar irradiation poses a challenge, varying significantly from one geographical location to another [16].

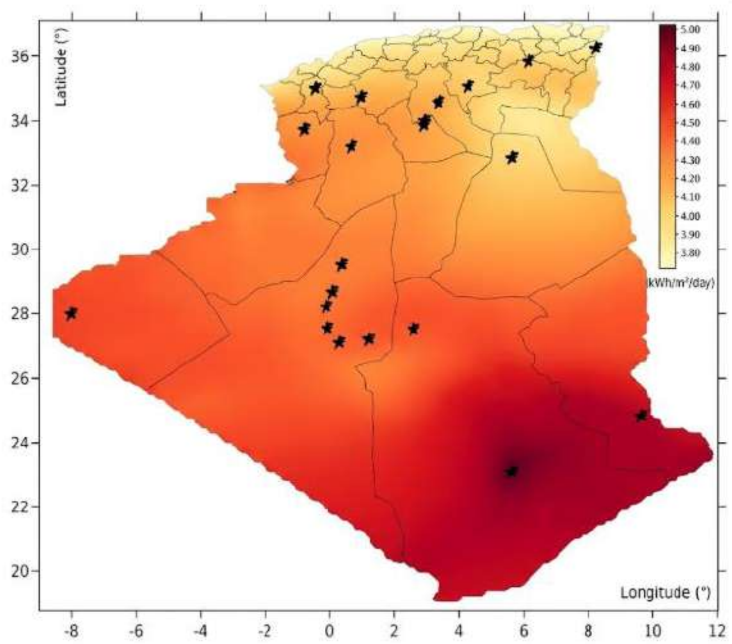

Figure I.2: Solar Irradiation in Algeria

I.3. Solar Radiation

The energy that reaches the ground is less than 1354 W/m² (the solar constant) because part of the solar radiation is absorbed by the atmosphere (about 15%) and re-emitted in all directions in the form of diffuse radiation. The atmosphere also reflects a portion of the solar radiation back into space (about 6%). Thus, the global radiation at ground level is the sum of direct radiation and diffuse radiation. The energy received by a surface depends on several factors such as the season, altitude, weather conditions, terrain, pollution, the orientation of the surface, etc. At ground level, several components are distinguished [17].

I.4. Types of Solar Radiation

I.4.1. Direct Solar Radiation

It is received directly from the sun, without being scattered by the atmosphere. It is the difference between global radiation and diffuse radiation [18].

I.4.2. Diffuse Solar Radiation

It consists of light scattered by the atmosphere (air, cloudiness, aerosols). Scattering is the phenomenon that divides a parallel beam into a multitude of beams spreading in all directions. In the sky, air molecules, water droplets (clouds), and dust particles all contribute to this dispersion of the sun's rays. Therefore, it mainly depends on weather conditions [19].

I.4.3. Reflected Solar Radiation

It is the radiation that is reflected by the ground or by objects located on its surface. This albedo can be significant when the ground is particularly reflective (such as water, snow, etc.)[20].

I.4.4. Global Solar Radiation

On a horizontal surface: It is the total solar radiation coming from the sun that reaches a horizontal surface on planet Earth. This therefore includes the vertical component of direct solar radiation as well as diffuse solar radiation.

On an inclined surface: Global radiation on an inclined surface corresponds to the sum of direct, diffuse, and reflected radiation[18].

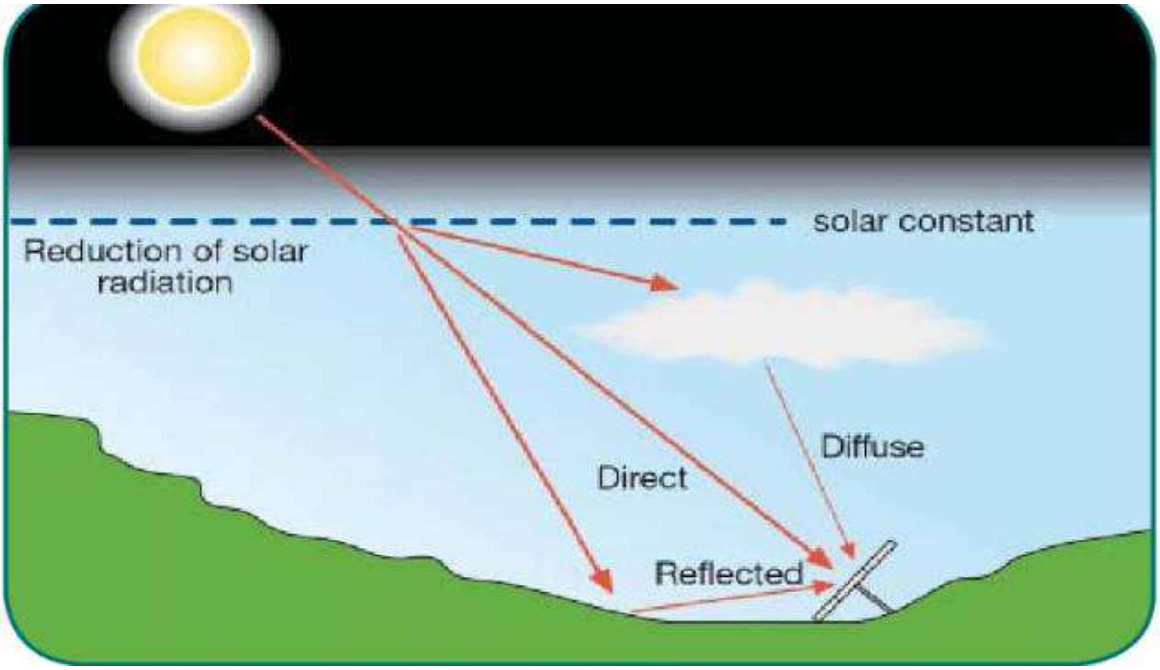

Figure I.3: Components of Solar Radiation

I.5. Solar Energy

The Sun irreversibly transforms every second 564 million tons of hydrogen into 560 million tons of helium. The Sun therefore loses 4 million tons, which are dispersed in the form of radiation. The energy emitted by the Sun each second is therefore about 3.85×10^{26} W. However, only a very small fraction of this power is received by the Earth because of the small solid angle under which our planet is seen from the Sun: approximately two billion times less. This still gives a considerable value (about 1.9×10^{17} W)..

The solar energy received per unit area perpendicular to the Sun's rays, at a Sun–Earth distance equal to its average value, is called the solar constant, which is estimated at 1,367 $W \cdot m^{-2}$ [21][22].

Albert Einstein, while working on the photoelectric effect, discovered that light does not only have a wave nature, but that its energy is also carried by particles called photons. The energy of a photon is given by the relation:

$$\mathbf{E = m \cdot c^2} \tag{1.1}$$

m: mass in kilograms(kg).

c: the speed of light.

Thus, the shorter the wavelength, the greater the energy of the photon.[23] The Sun emits electromagnetic radiation (Figure I.2) within a wavelength band ranging from 0.22 to 10 microns (µm) [24].

The energy associated with this solar radiation is approximately distributed as follows:

- 9% in the ultraviolet band (< 0.4 µm).
- 47% in the visible band (0.4 to 0.8 µm).
- 44% in the infrared band (> 0.8 µm).

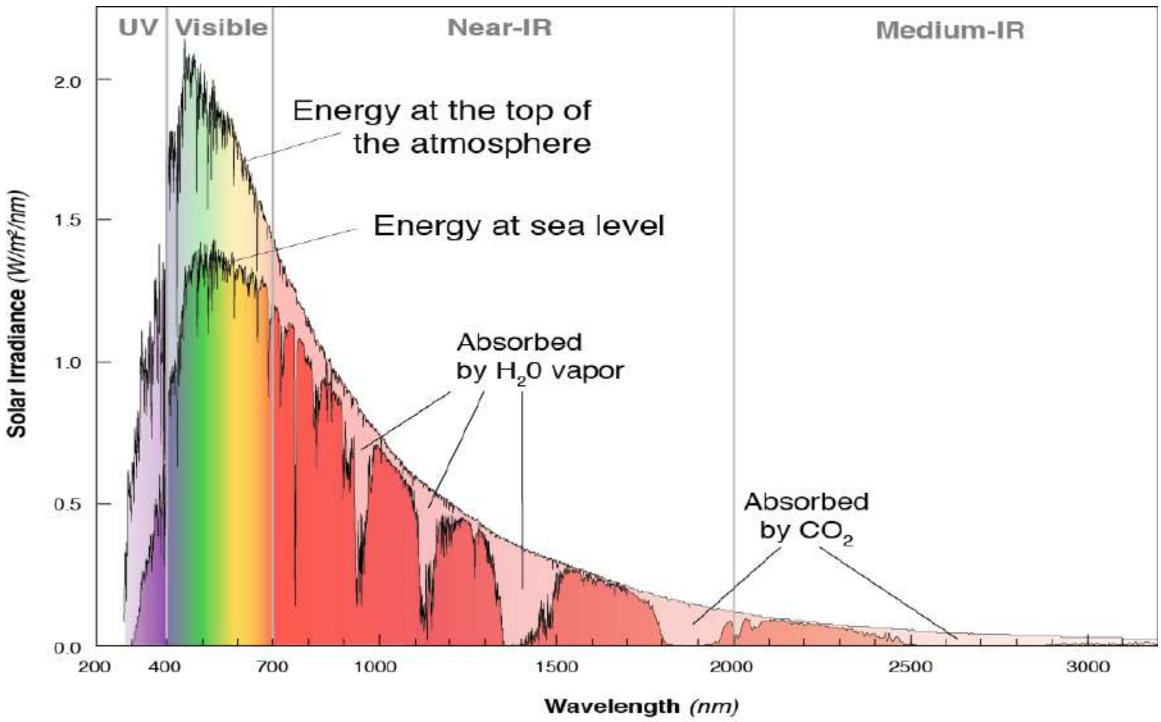

Figure I.4: Solar spectrum [25]

I.6. Types of Solar Energy

I.6.1. Thermal solar energy

This energy is the transformation of the sun's rays into thermal energy (heat). This energy can be used directly either for heating or to obtain hot water. The general principle is to concentrate the sun's rays in one place. They are then trapped by glazed solar thermal collectors, which transfer the solar energy to metallic absorbers [26][27].

I.6.2. Thermodynamic solar energy

These are large power plants equipped with solar ray concentrators, called mirrors, to heat a fluid to high temperatures in order to produce steam through heat exchange, and then use a steam turbine to generate electricity [20].

I.6.3. Photovoltaic solar energy

Photovoltaic solar energy harnesses the sun as a source of light. This energy is captured and converted into electricity using solar panels installed on the façades or roofs of buildings. This conversion process is known as the photovoltaic effect [28][29].

I.6.3.1. The photovoltaic effect

The photovoltaic effect is a process that converts solar energy, emitted in the form of photons, into electrical energy using a semiconductor device called a solar cell [30].

However, this effect can only occur if a potential barrier exists within the semiconductor prior to illumination. Such a barrier appears, for example, at the interface between two differently doped regions, where two types of impurities are introduced at different concentrations, thereby forming a P–N junction. When this material is exposed to light, the incident photons transfer their energy to the electrons in the semiconductor, making them mobile. Under the influence of the potential barrier, the generated electric charges are separated: positive charges move to one side while negative charges move to the other side, which results in the generation of an electric current [30].

Among the materials used in the fabrication of photovoltaic cells, crystalline silicon is the most widely used and currently accounts for approximately 90% of the photovoltaic panels produced worldwide. Nevertheless, other technologies also exist, such as thin-film solar cells, which are already industrialized, as well as other technologies that are still under research and development [31].

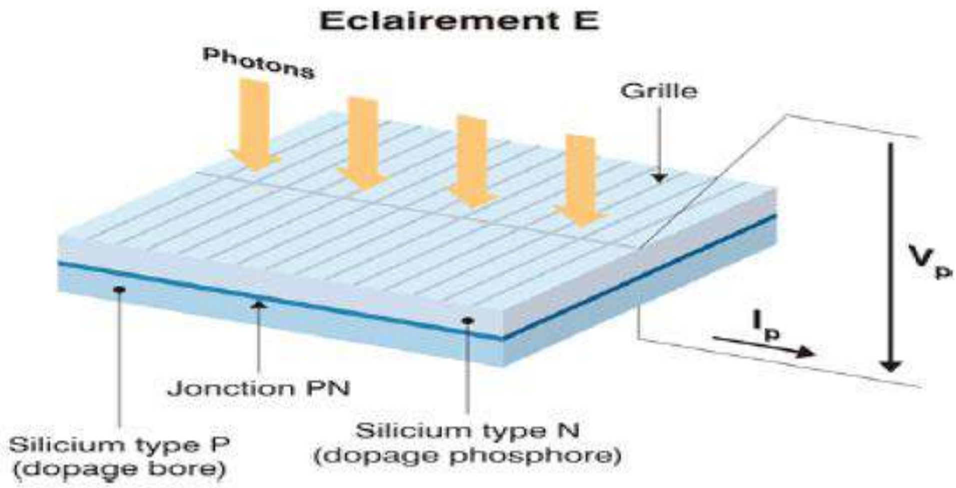

Figure I.5: Working Principle of the Photovoltaic Effect [32]

I.7. Photovoltaic cells

The PV cell, also called a photocell, is the smallest element of a photovoltaic installation. It is composed of semiconductor materials and directly converts light energy into electrical energy [33].

The operation of the photovoltaic cell is based on the photovoltaic effect, generating a voltage that can vary between 0.3 V and 0.7 V depending on the material used, its structure, as well as the temperature and aging of the cell [34].

The energy efficiency performances achieved industrially are 13–14% for mono crystalline silicon cells, 11–12% for polycrystalline silicon, and 7–8% for amorphous silicon thin films. The photocell or solar cell is the basic element of a photovoltaic generator [35].

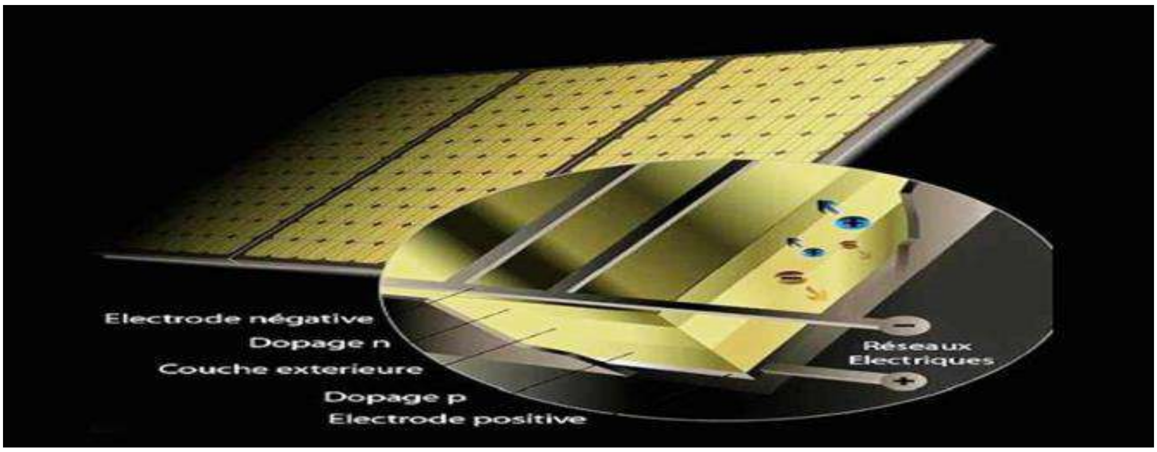

Figure I.6: A photovoltaic cell [36]

I.7.1. Operating Principle of Photovoltaic Cells

A photovoltaic cell can be considered as a photosensitive diode, and its operation is based on the properties of semiconductor materials.

The photovoltaic cell allows the direct conversion of light energy into electrical energy. Its operating principle is based on the photovoltaic effect. A cell is composed of two layers of a semiconductor. These two layers are doped differently. The (N) layer has an excess of valence electrons, while the (P) layer has a deficit of electrons. Thus, the two layers create a potential difference. The energy of the incoming light photons captured by the valence electrons (in the N layer) enables them to cross the potential barrier and generate a direct electric current. To collect this current, electrodes are deposited by screen printing on the two layers of the semiconductor (Figure I.5). The upper electrode is a grid that allows light rays to pass through. An anti-reflection layer is then deposited on this electrode in order to increase the amount of absorbed light [37].

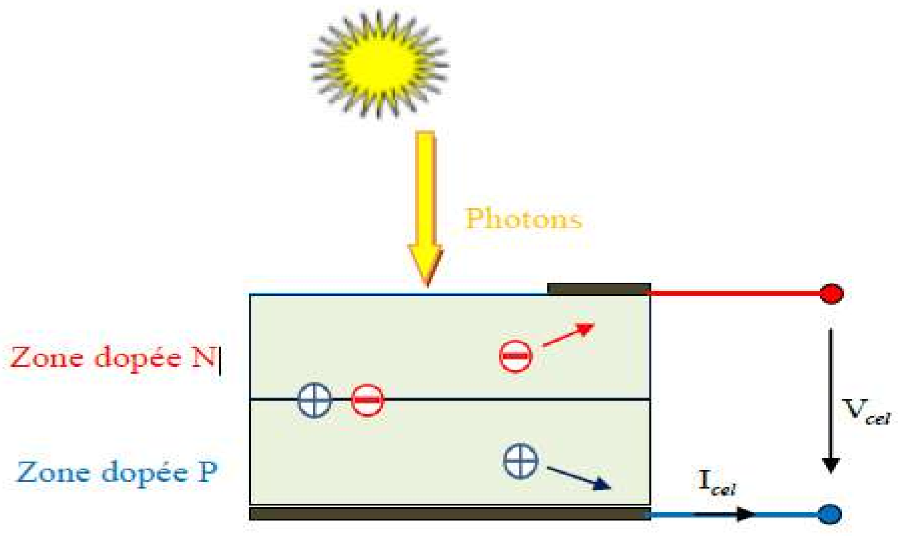

Figure I.7: Principle of Photovoltaic Cells

I.8. Different types of photovoltaic cells

Nowadays, there are several types of cells with diverse and varied characteristics, each suited to a specific function. We will therefore mention the different technologies used in the manufacturing of these cells [30].

I.8.1. Mono crystalline cells

Mono crystalline cells are first-generation photovoltaic cells. They are made from a single block of silicon crystallized into one piece. These cells are generally a uniform blue color. They have good efficiency, typically between 12% and 20% for industrial cells, but the production method is labor-intensive and costly [34].

Figure I.8: Mono crystalline cells [36]

I.8.2. Polycrystalline cells

Polycrystalline cells are made from a block of silicon crystallized into multiple crystals. When viewed closely, the different orientations of the crystals can be seen (different shades). They have an efficiency of about 11% to 13%, but their production cost is lower than that of mono crystalline cells. During the cooling of silicon, several crystals are formed. This type of cell is blue, but not uniform; patterns created by the different crystals can be distinguished [38].

Figure I.9: Polycrystalline cells

I.8.3. Amorphous silicon cells

These cells are composed of a glass or synthetic material substrate on which a thin layer of silicon is deposited (the arrangement of atoms is no longer regular as in a crystal). Their efficiency is around 5–10%, which is lower than that of crystalline cells. They are used in small consumer products (watches, calculators) but are rarely used in solar installations [35].

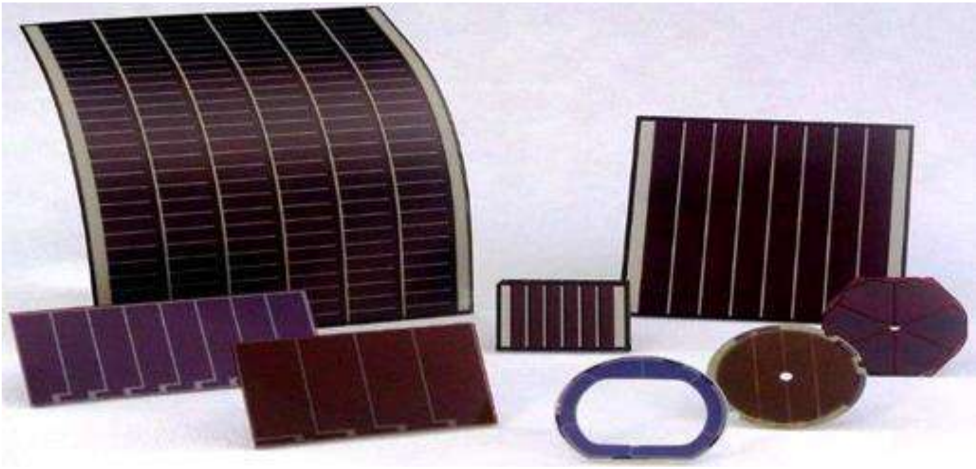

Figure I.10: Amorphous silicon cells [39]

I.8.4. Comparison of different technologies

Table I.2: Comparison of different cell technologies [18]

technologies	Mono crystalline cells	Polycrystalline cells	Amorphous silicon cells
Efficiency	14-17%	12-15%	6-10%
Advantages	• High efficiency for a cell	• High efficiency for a module	• Easy to produce
Disadvantages	• High costs and loss of raw materials during the manufacturing process.	• High costs and loss of raw materials during the manufacturing process	• Low yield, high costs, and loss of raw materials during the manufacturing process
Lifetime	35 Years	35 Years	<10 Years
Power	100 to 150 Wp/m² 7M²/kWp	100Wp/m² 8M²/kWp	50Wp/m² 16M²/kWp
Market share	43%	47%	10%

I.9. Photovoltaic modules

To increase the operating voltage, several photovoltaic cells are connected in series to form a photovoltaic module. The nominal voltage of the module is usually adapted to a 12-volt load, and the module will therefore generally have 36 cells. Moreover, the fragility of the cells to breakage and corrosion requires protection from the environment, and they are generally encapsulated under glass or plastic compound. The whole assembly is called a "photovoltaic module".

Modules can also be connected in series and in parallel to increase the operating voltage and current [40].

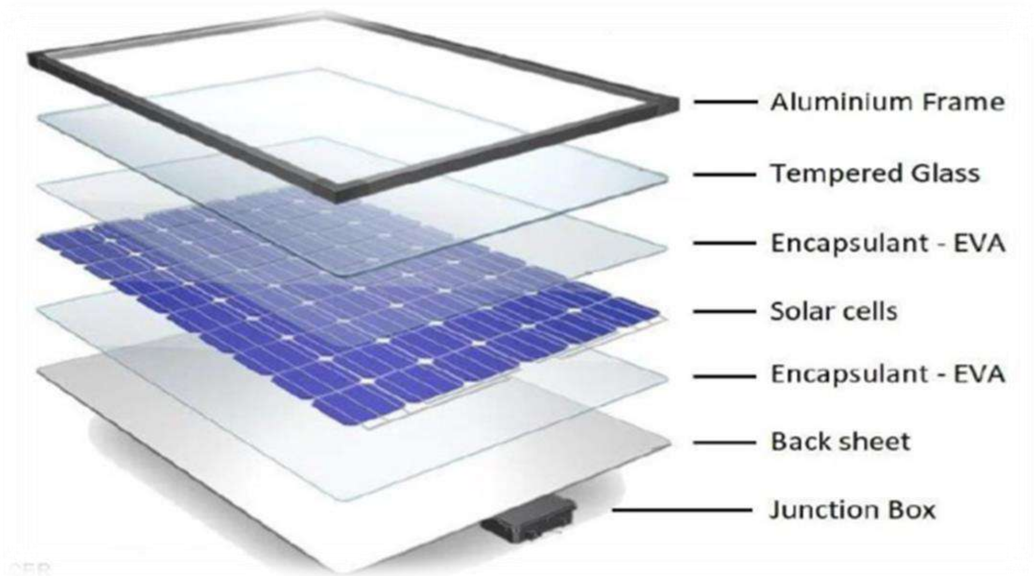

Figure I.11: Composition of a photovoltaic (PV) solar module

I.9.1. Role of the PV solar module

The photovoltaic (PV) solar module is the component of a PV solar system that produces electricity (direct current) when it is exposed to sunlight. The amount of electricity the module can generate depends on the following factors [41].

• The availability of sunlight (direct, diffuse, reflected, night, etc).

• The orientation of the module (whether it faces North-South or not)

• The tilt of the module (angle relative to the horizontal)

• The location where the PV solar module is installed.

I.10. Connection of photovoltaic modules

The association of modules with each other forms photovoltaic panels. The three types of association of photovoltaic modules are [42]:

I.10.1. Series connection

The individual cell, an essential component of a photovoltaic system, produces only a very small amount of electrical power, generally around 0.5 W with a voltage of less than one volt. To increase power output, cells are combined to form a module (or panel) [43]. The series connection of photovoltaic modules delivers a voltage equal to the sum of the individual voltages and a current equal to that of a single module [42].

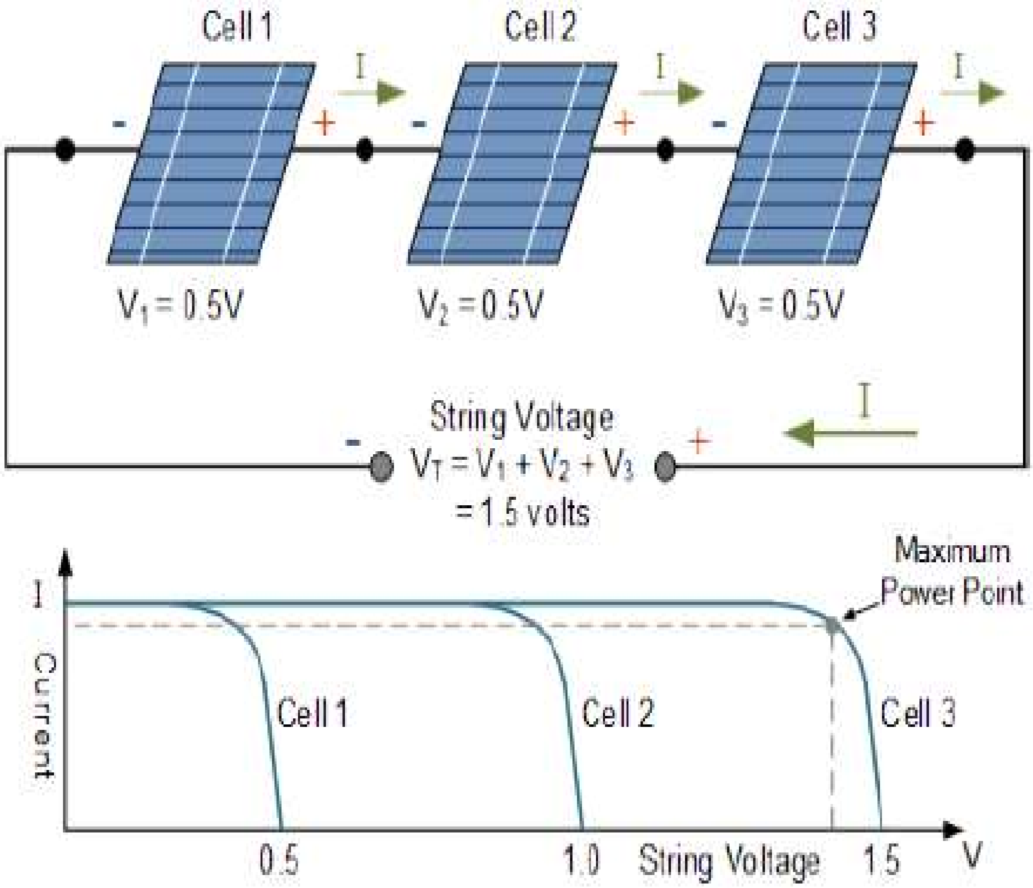

Figure I.12: Series connection of solar cells [44]

I.10.2. Parallel Connection

The parallel connection of photovoltaic modules delivers a current equal to the sum of the individual currents and a voltage equal to that of a single module [42].

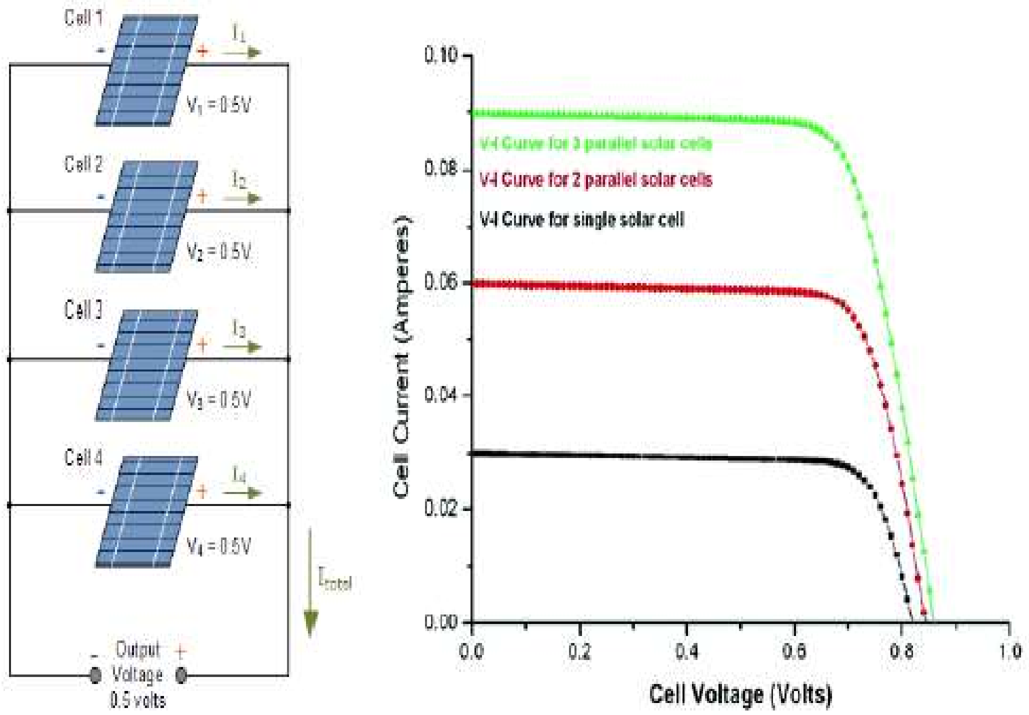

Figure I.13: Parallel connection of photovoltaic cells [44]

I.10.3. Mixed connection (Series – Parallel)

To achieve satisfactory current and voltage, it is necessary to use a mixed arrangement, that is, series-parallel [43].

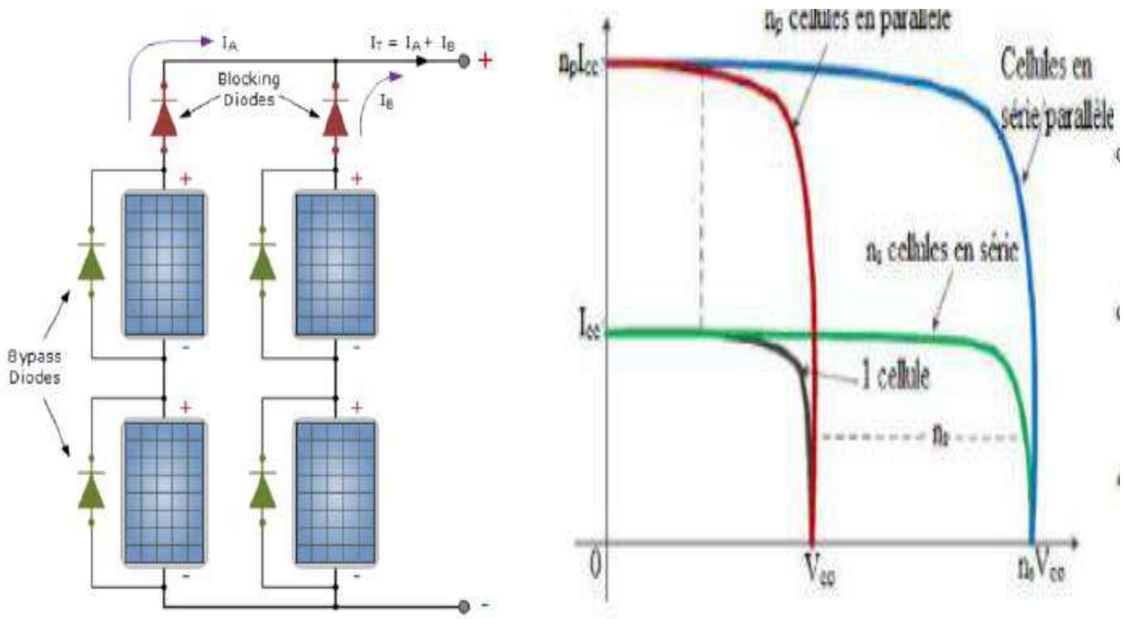

Figure I.14: Parallel and series connection of photovoltaic cells [45]

I.11. photovoltaic system

In addition to the main component, the photovoltaic generator—which represents more than 50% of the total cost of the system—the PV system also includes secondary components such as the storage system and the power conditioning stage.

The storage device often consists of one or more rechargeable batteries. Batteries are very expensive components and must be selected carefully. The power conditioning stage involves a static converter, either DC/DC or DC/AC.

Batteries typically have a lifespan of 8 to 10 years, while PV modules last between 20 and 30 years [46].

I.11.1. Autonomous systems

Autonomous systems play the role of supplying power to one or more consumers in areas far from the electrical grid. A standalone solar panel system consists of a storage system associated with solar generators to ensure continuous power supply at all times and for several days, even in case of production interruption, as well as static converters for the adaptation stage between the solar generator and the loads [47].Two types can be distinguished:

• Sun-tracking (direct-use) systems.

• Systems with storage.

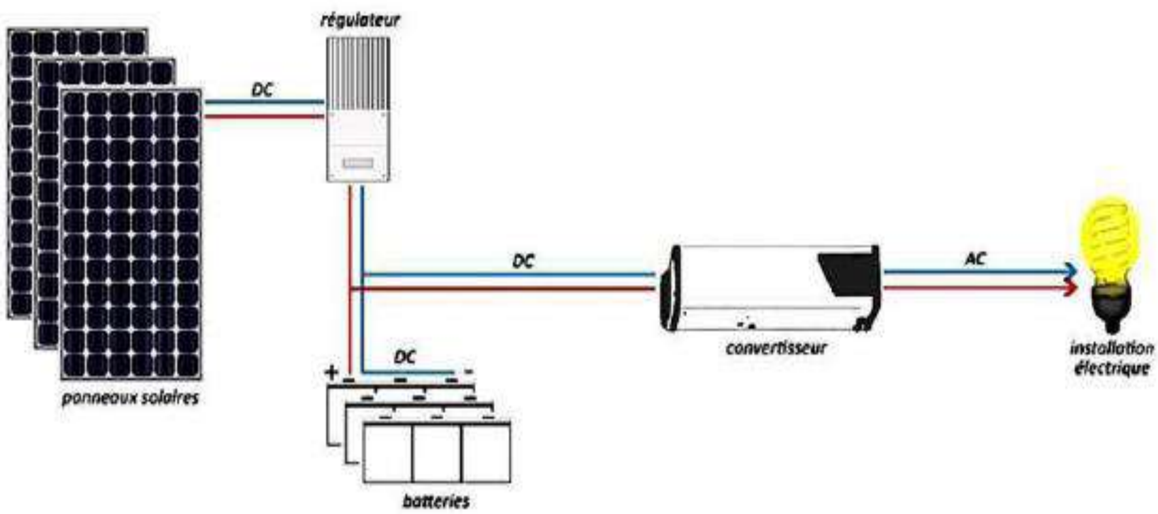

Figure I.15: Autonomous photovoltaic installation [48]

I.11.2. Grid-connected systems

Grid-connected photovoltaic systems are connected to the public grid through an appropriate inverter, because a photovoltaic module only produces direct current (DC).

Grid-connected photovoltaic systems can be divided into two types:

• Decentralized grid-connected photovoltaic systems.

• Centralized grid-connected photovoltaic systems [49].

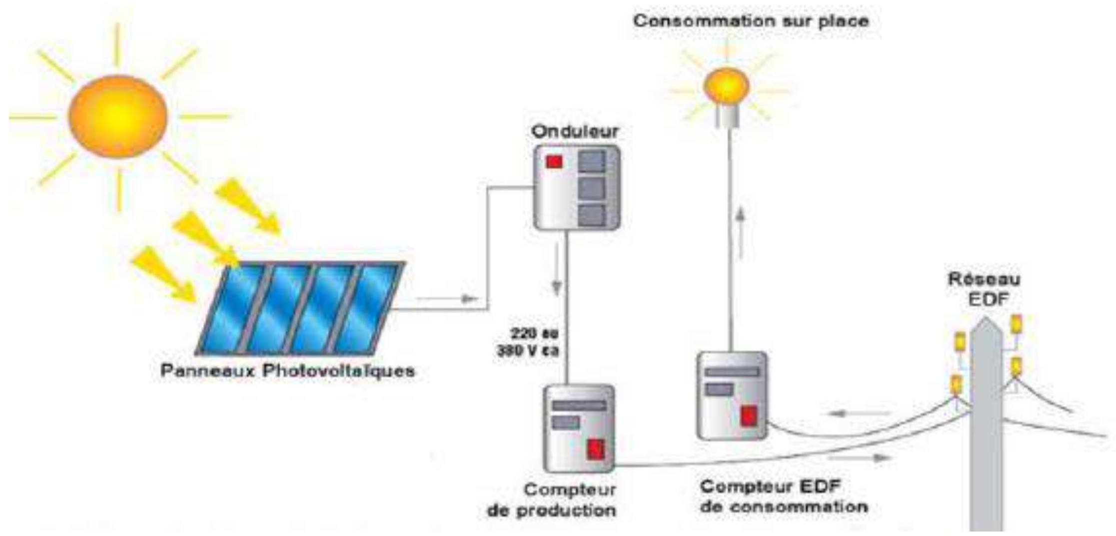

Figure I.16: Diagram of a grid-connected photovoltaic installation [36]

I.11.3. Hybrid systems

Hybrid systems consist of a photovoltaic generator combined with one or more renewable energy sources, a generator, or both simultaneously. In the event of a discharge, these systems may also include batteries that can be recharged by the other source [50].

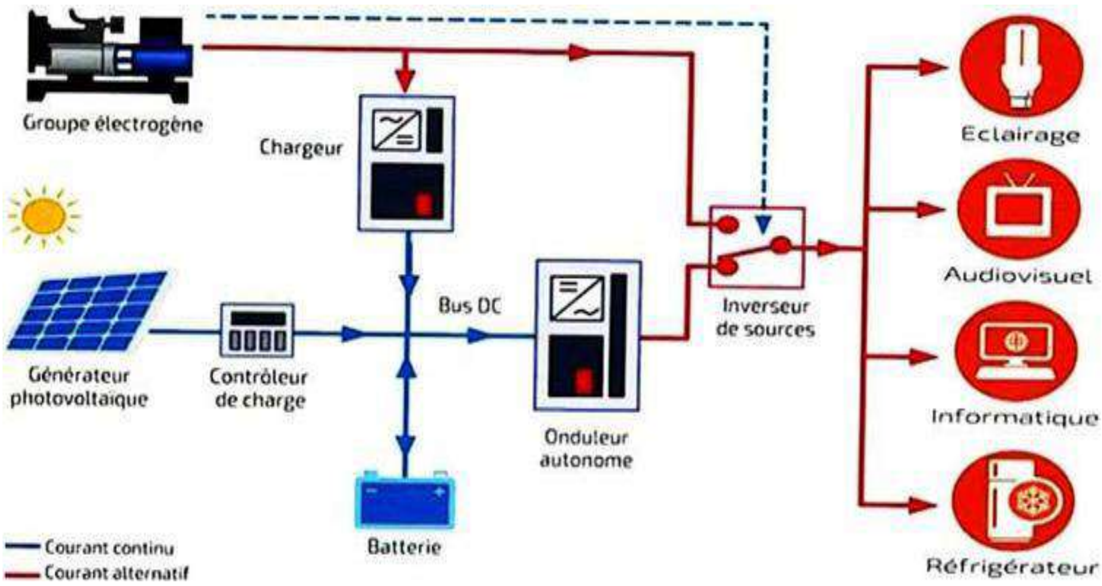

Figure I.17: Autonomous hybrid photovoltaic installation [48]

I.12. Power electronic converters

Power electronic devices play a major in the functioning of photovoltaic system either in stepping up or stepping down DC the voltage generated by the solar panels and these are known as DC-DC converters or during the conversion of direct current to alternating current and these referred to as (DC-AC converters). The choice of these power electronic devices rests entirely on the types of loads used, either AC or DC loads [51].

I.12.1. DC-DC converters

These devices are considered solid-state power electronics, as they are used to step up or step-down direct current (DC) voltage. DC-DC converters operate based on pulse width modulation (PWM) technology, where a high-frequency pulse signal is generated to control the switching on and off of electronic switches, allowing precise control of the output voltage level [51].

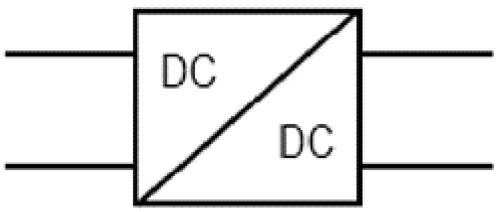

Figure I.18: Symbol of a DC-DC converter [52]

I.12.2. DC-DC Converters for Solar Energy Systems

A chopper can be implemented using a controlled electronic switch (a power transistor operating in 0–1 switching mode), which opens and closes, such as GTO thyristors, bipolar transistors, or insulated-gate field-effect transistors operating in switching (on/off) mode.

The principle of the chopper consists of periodically establishing and interrupting the connection between the source and the load using this electronic switch. This switch must be able to be opened or closed at will in order to obtain an adjustable continuous output voltage.

For this purpose, DC-DC converters (or choppers) are used in solar energy systems to adapt the variable DC source (PV panel) to the load, which generally requires a constant DC voltage [53].

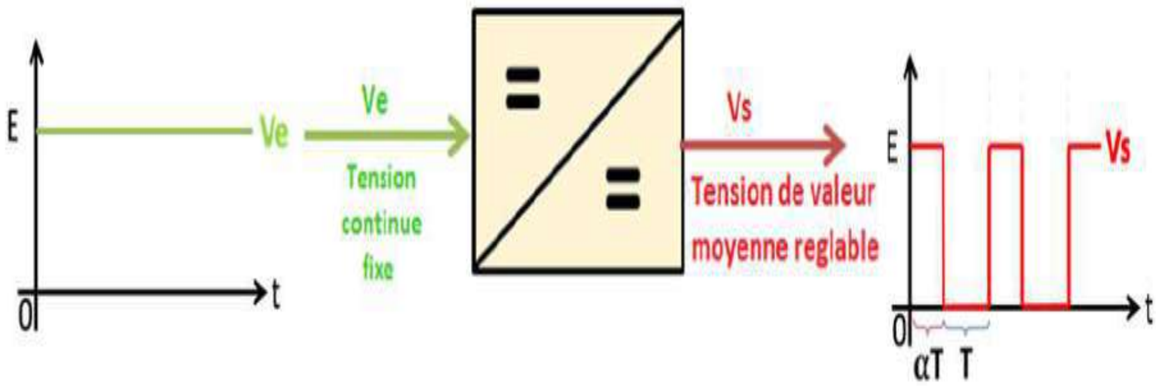

Figure I.19: Voltages Ve and Vs in a DC/DC converter [54]

I.12.3. Types of DC-DC converters

DC-DC converters (or choppers) are used in solar energy systems to adapt a variable-amplitude DC source (PV panel) to a load that generally requires a constant DC voltage. The three basic configurations are [55]:

• Buck converters,

• Boost converters.

• Buck – boost converters.

I.13. Advantages and disadvantages of a photovoltaic system [56][57]

I.13.1. Advantages

• Solar photovoltaic energy generates neither noise, nor harmful emissions, nor polluting gases.

• Reliable and stable systems.

• Its output varies with the days and seasons, but it is relatively predictable.

• Safe and risk-free technology.

I.13.2. disadvantages

• The investment cost is relatively high.

• The efficiency of PV cells remains quite low.

• There is no electricity production in the evening and at night.

I.14. Conclusion

Solar photovoltaic energy is one of the most important global fields in sustainable development. Despite the mastery of solar cell manufacturing technology and their encapsulation, photovoltaic systems are still expensive. Therefore, mastering the technology alone is no longer sufficient to reduce the cost of PV systems; proper design and sizing techniques can also help minimize the cost per watt-peak produced.

In this chapter, the main focus was on the basic components of a photovoltaic system (solar cells and PV modules), as well as the current–voltage (I–V) characteristics of a PV module.

Thus, designing a photovoltaic field requires thorough knowledge of the performance of the photovoltaic generators used and their behavior under different environmental conditions.

CHAPTER II:

MODELING AND ANALYSIS OF DC-DC CONVERTERS

II.1. Introduction

Modern electronic devices must meet several criteria such as high quality, reliability, compact size, light weight, and low cost. Linear power regulators, whose operating principle is based on current or voltage division, can provide a very high-quality output voltage [58]. However, this type of regulator remains inefficient because its main field of application is at low power levels.

Switching regulators, known as DC/DC converters, use electronic switches based on semiconductors such as thyristors, power transistors, or IGBTs, as they generate low power losses during transitions from one state to another. These converters ensure high energy conversion efficiency and can operate at high frequencies. The dynamic characteristics of DC/DC converters improve as the switching frequency increases. High operating frequencies therefore allow for a faster dynamic response to rapid changes in load current or input voltage [59].

II.2. Step-down converter (Buck converter)

The step-down converter (Figure II.1) is often found in the literature under the name Buck converter or series chopper. The latter, which is a switch, can only connect two sources of different types (current/voltage or vice versa).

The use of the Buck converter in photovoltaic conversion systems is quite appropriate, since the photovoltaic generator is a direct current source, while the load generally a battery behaves like a voltage source.

Its typical application is to convert the input voltage into a lower output voltage, where the conversion ratio α = Vo/Vi varies with the duty cycle of the switch [60].

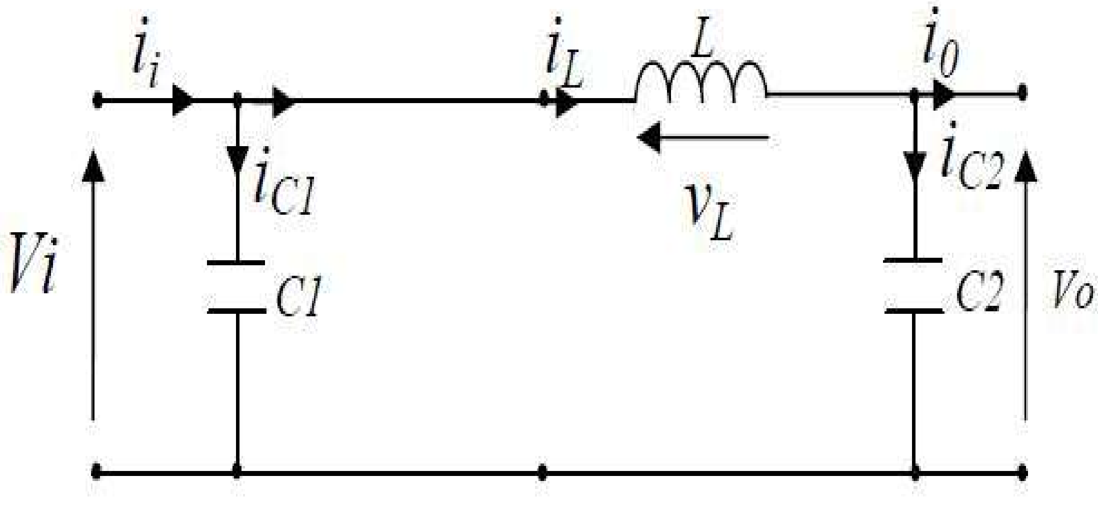

Figure II.1: Principal diagram of a Buck converter

II.2.1. Principle of operation

A buck converter is an electronic circuit used to step down a higher DC voltage to a lower DC voltage with high efficiency. Its operation is based on the rapid switching of an electronic switch (usually a transistor) along with energy storage elements such as an inductor and a capacitor. When the switch is closed (ON state), energy is transferred from the source to the load, and the inductor stores part of this energy in the form of a magnetic field, while the diode is reverse-biased. When the switch is opened (OFF state), the inductor maintains the current flow by releasing its stored energy and supplying it to the load through the diode. This switching process repeats at a high frequency, resulting in a stable output voltage that is lower than the input voltage. The output voltage is controlled by the duty cycle, following the approximate relation Vout = D × Vin. The inductor and capacitor help smooth the signal and reduce ripple, making the buck converter highly efficient and widely used in modern electronic applications.

II.2.2. Mathematical model

To determine the actual behavior of this converter, it is necessary to know its mathematical model in detail. For this purpose, we must represent the equivalent circuit in both states of the switch and then derive the mathematical model that relates the input and output variables.

(Figure II.2) shows the equivalent circuit diagram of a step-down (buck) converter with the switch closed during αTs, while (Figure II.1) represents the step-down converter with the switch open during (1 − α)Ts [61].

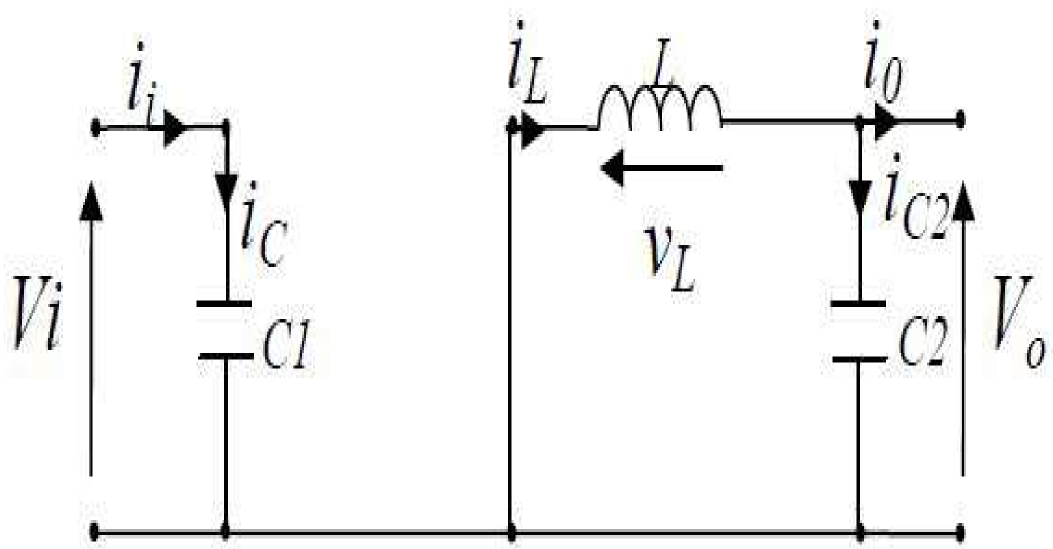

Figure II.2: Equivalent circuit diagram of the series chopper when t ∈ [0, αTs].

When Kirchhoff's law is applied to the circuit above, the following equations are obtained:

$$\begin{cases} i_{c1}(t) = C_1 \dfrac{dv_i(t)}{dt} = i_i(t) - i_L(t) \\ i_{c2}(t) = C_2 \dfrac{dv_0(t)}{dt} = i_L(t) - i_0(t) \\ V_L(t) = L \dfrac{di_L(t)}{dt} = V_i(t) - V_0(t) \end{cases} \tag{2.1}$$

II.2.3. Conversion and yield report

The conversion ratio M is defined as the ratio between the output voltage and the input voltage as follows [62]:

$$M(\alpha) = \frac{V_o}{V_i} = \eta\alpha \tag{2.2}$$

Where η is the efficiency of the converter, defined as the ratio of the output power to the input power:

$$\eta = \frac{P_o}{P_i} = \frac{V_o I_o}{V_i I_i} \tag{2.3}$$

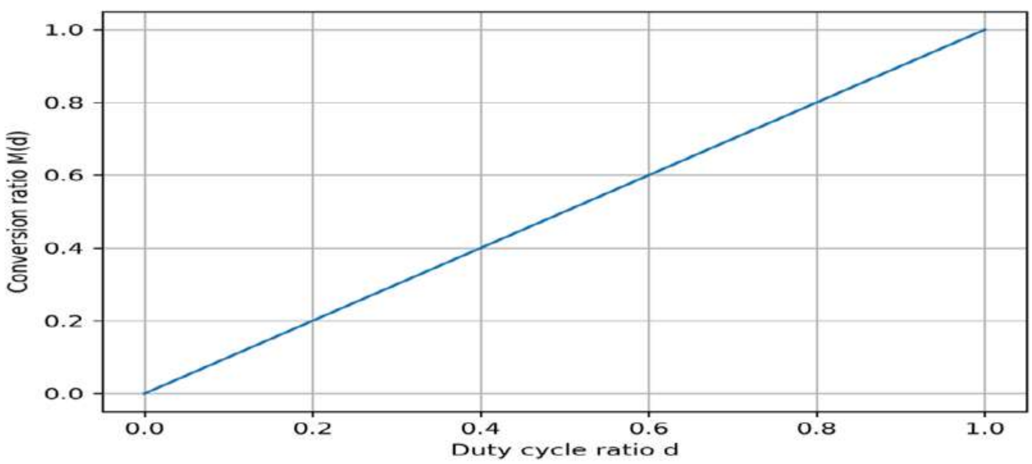

Figure II.3: the conversion ratio M(d) of a series chopper (DC-DC converter)

II.2.4. Continuous conduction mode

The Continuous Conduction Mode (CCM) is the most prevalent and efficient operational state for Buck converters. This mode occurs when the minimum inductor current I_{Lmin} remains strictly greater than zero throughout the entire switching period (T). Physically, this implies that the inductor does not completely discharge its stored energy into the load before the next switching cycle begins, thereby ensuring a continuous flow of current toward the output.

The converter's response in this mode is characterized by two fundamental stages: the first occurs when the electronic switch is closed (Switch ON), where the current increases linearly as the inductor stores energy; the second occurs when the switch is opened (Switch OFF), where the current decreases through the free-wheeling diode to feed the load, while maintaining a positive value.

From a design perspective, CCM is preferred in power applications due to its ability to minimize current ripple, which reduces stress on electrolytic capacitors and enhances the quality of the output voltage. Furthermore, the relationship between input and output voltage in this mode is linear and depends exclusively on the duty cycle (D), according to the following mathematical expression:

$$V_{out} = D * V_{in} \tag{2.4}$$

This linear proportionality significantly simplifies the design of control circuits and closed-loop systems, ensuring higher stability for the converter under various loading conditions.

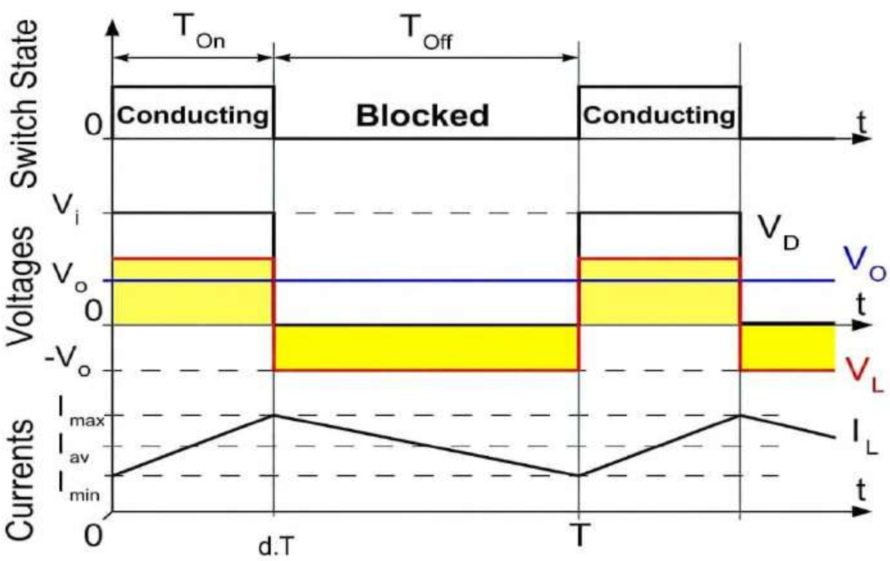

Figure II.4: Current and voltage waveforms in a Buck converter

II.2.5. Discontinuous conduction mode

Discontinuous Conduction Mode (DCM) in a Buck converter is defined as the operating state where the inductor current i_L falls to zero before the end of the switching period T_S This mode typically occurs under light load conditions (high load resistance) or when the inductance value is too small to maintain a continuous current flow. Mechanically, the DCM cycle consists of three distinct intervals: the ON-state, the OFF-state where the current decreases, and a third interval where the inductor current remains at zero. While DCM can lead to higher output voltage ripples and requires a different mathematical approach for modeling, it offers certain advantages such as the elimination of the reverse recovery loss in the diode and a simplified control loop due to the reduction in the system's order.

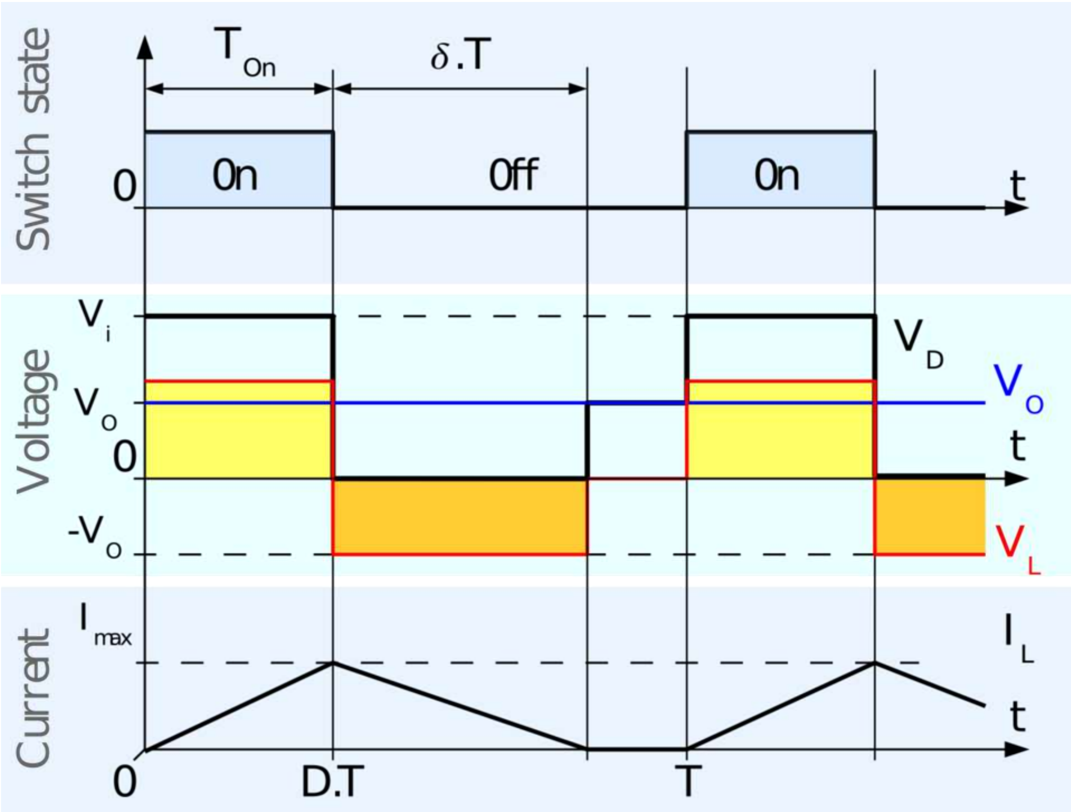

Figure II.5: Evolution of the voltages and currents with time in an ideal buck converter operating in discontinuous mode.

II.3. Step-up converter (Boost converter)

This is a step-up converter, also known as a boost converter or a parallel chopper; it transforms any input voltage into a higher output voltage. Its basic circuit is shown in (Figure II.6)[63].

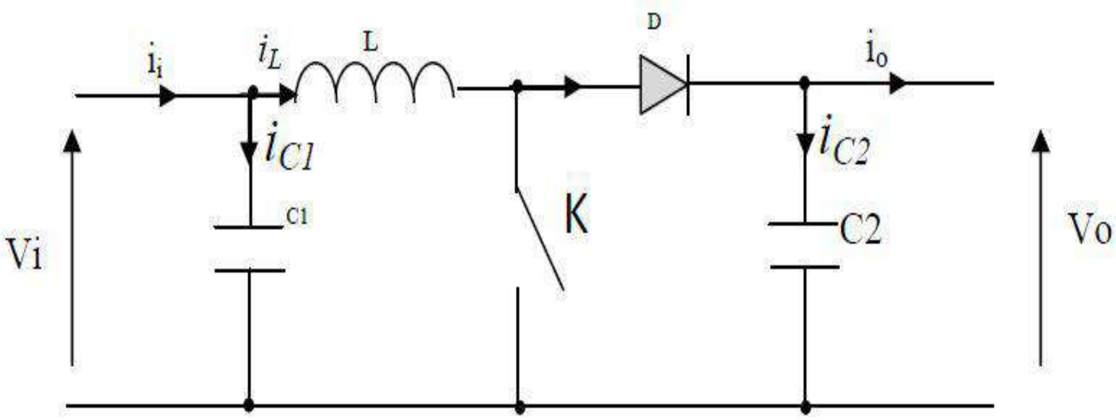

Figure II.6: Basic diagram of a Boost converter

II.3.1. Principle of operation

When switch K is closed, during the period t_{ON}, i.e., t ∈ $[0, \alpha T_S]$, the current gradually increases, allowing the inductor to store more energy throughout the entire closing time of K. Then the switch turns off, i.e., during the period t_{OFF},t ∈ $[\alpha T_S, T_S]$ During this transition from the closed state to the open state, the inductor L opposes the change in the current I_L in its circuit. This variation also causes a change in the magnetic flux in its core, and thus it generates a voltage across its terminals that adds to the source voltage, the whole appearing across the capacitor C_2[64].

II.3.2. Equivalent mathematical model

To be able to synthesize the functions of the boost chopper in steady state, it is necessary to present the equivalent circuit diagrams for each position of switch K. The one in (Figure II.5) presents the equivalent circuit of the boost converter when K is closed, i.e., between [0;α·Ts].[63].

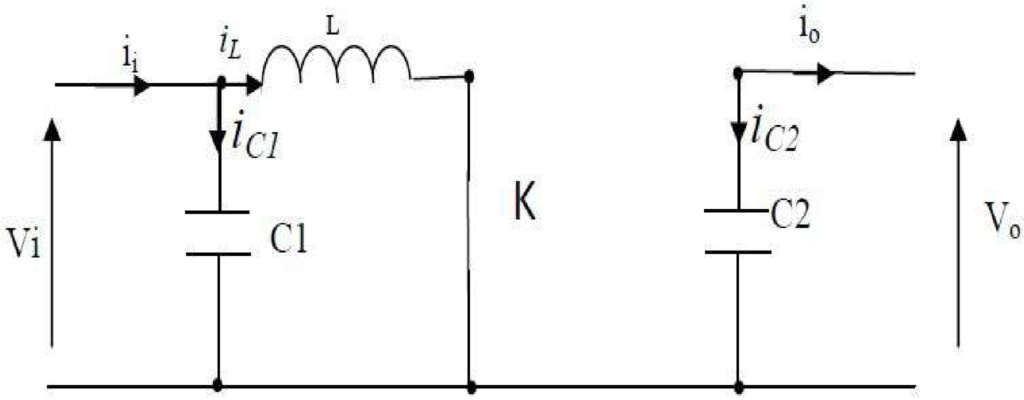

Figure II.7: Equivalent circuit diagram of the boost chopper when t ∈ [0; α,Ts]

Similarly to the buck circuit, applying Kirchhoff's laws to the equivalent circuits of the two operating phases gives:

$$\begin{cases} i_{C1}(t) = C_1 \dfrac{dv_i(t)}{dt} = i_i(t) - i_L(t) \\ i_{C2}(t) = C_2 \dfrac{dv_0(t)}{dt} = -i_0(t) \\ V_L(t) = L \dfrac{di_L(t)}{dt} = V_i(t) \end{cases} \tag{2.5}$$

At the open state of switch K, the equivalent circuit for the operation of the boost converter is as follows

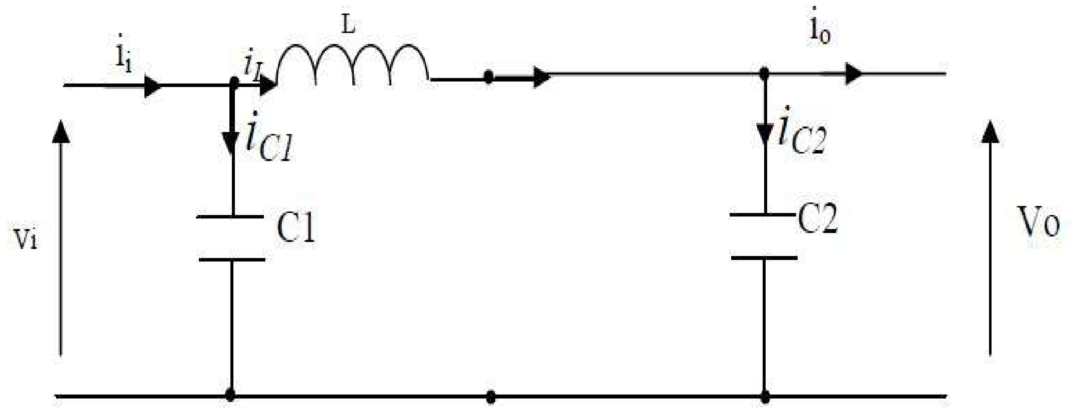

Figure II.8: Equivalent circuit of a boost chopper when t ∈ [α,Ts; Ts]

$$\begin{cases} i_{C1}(t) = C_1 \dfrac{dv_i(t)}{dt} = i_i(t) - i_L(t) \\ i_{C2}(t) = C_2 \dfrac{dv_0(t)}{dt} = i_L(t) - i_0(t) \\ V_L(t) = L \dfrac{di_L(t)}{dt} = V_i(t) - V_0(t) \end{cases} \tag{2.6}$$

II.3.3. Conversion and yield report

We can calculate the conversion ratio $\frac{V_0}{V_i}$ as follows:[63]

$$M(\alpha) = \frac{V_0}{V_i} = \frac{1}{1-\alpha} \tag{2.7}$$

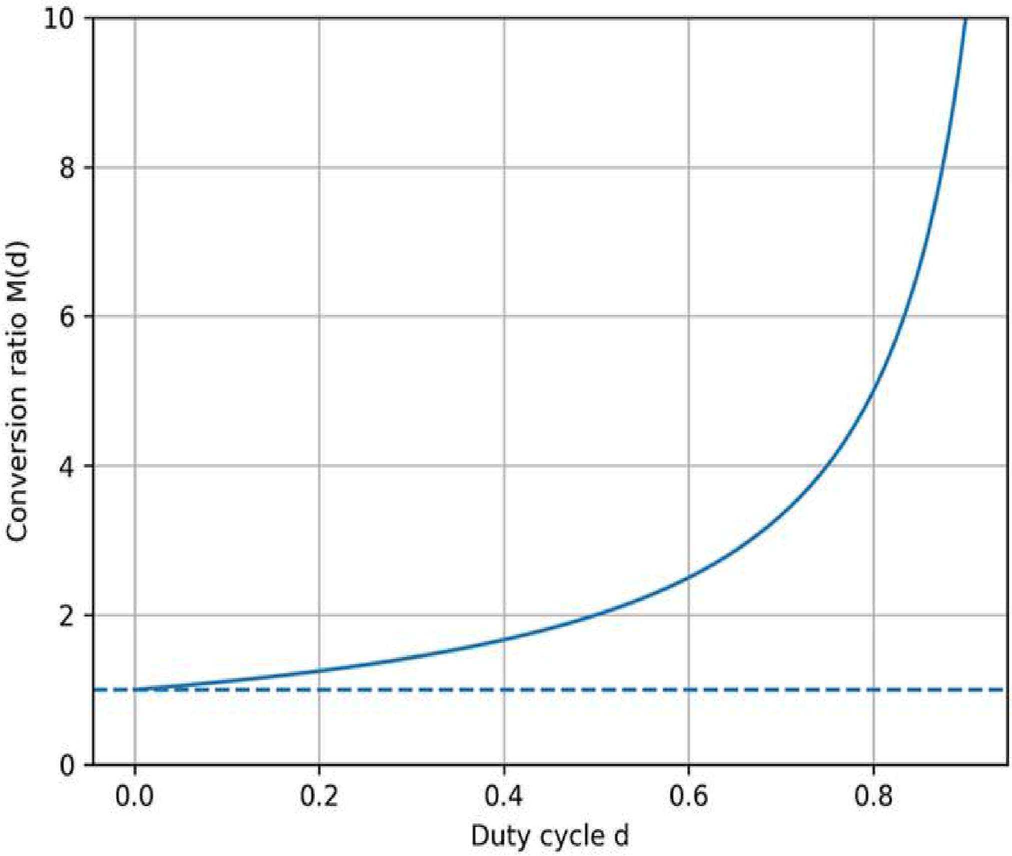

Figure II.9: Shape of the conversion ratio as a function of the duty cycle

II.3.4. Continuous conduction mode

The "Continuous Conduction Mode (CCM)" in a boost converter is defined as the operating state where the inductor current I_L remains strictly greater than zero throughout the entire switching period T_S Physically, this implies that the energy stored in the inductor during the "ON" state of the power switch is not fully depleted into the capacitor and the load during the "OFF" state, ensuring an uninterrupted flow of current. This mode is characterized by lower current ripples compared to the "Discontinuous Conduction Mode (DCM)", which reduces electromagnetic interference and thermal stress on electronic components. Consequently, CCM is preferred for high-power applications requiring stability and high efficiency, such as "Maximum Power Point Tracking (MPPT)" systems in photovoltaic. In this mode, the relationship between the input voltage V_{in} and the output voltage V_{out} is governed by the duty cycle (D) according to the following equation:

$$V_{out} = \frac{V_{in}}{1 - D} \tag{2.8}$$

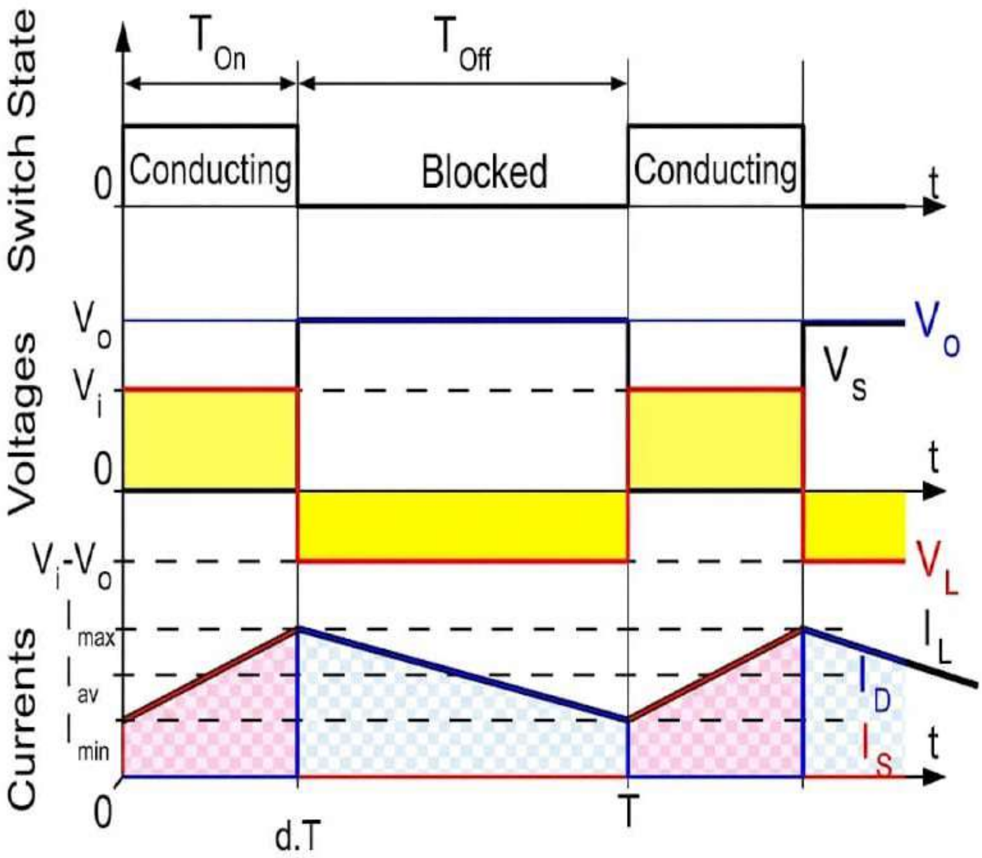

Figure II.10: Current and voltage waveforms in a Boost converter

II.3.5. Discontinuous conduction mode

The "Discontinuous Conduction Mode (DCM)" in a boost converter occurs when the inductor current I_L falls to zero before the end of the switching cycle. This mode typically arises when the converter operates under light load conditions (high load resistance), uses an inductor with low inductance (L), or functions at a lower switching frequency.This mode is characterized by three distinct operational intervals within a single switching period:

•1 ON-State Interval (DT): The switch is closed, energy is stored in the inductor, and the current increases.

•2 OFF-State Interval (D_1T): The switch opens, and the stored energy is transferred to the load through the diode.

•3 IDLE Interval (D_2T): This is the defining feature of DCM, where the inductor current reaches zero and remains there until the start of the next cycle. Consequently, the output voltage gain becomes dependent not only on the duty cycle (D) but also on the load resistance and inductance value, making the converter's dynamic response significantly different from the Continuous Conduction Mode (CCM).

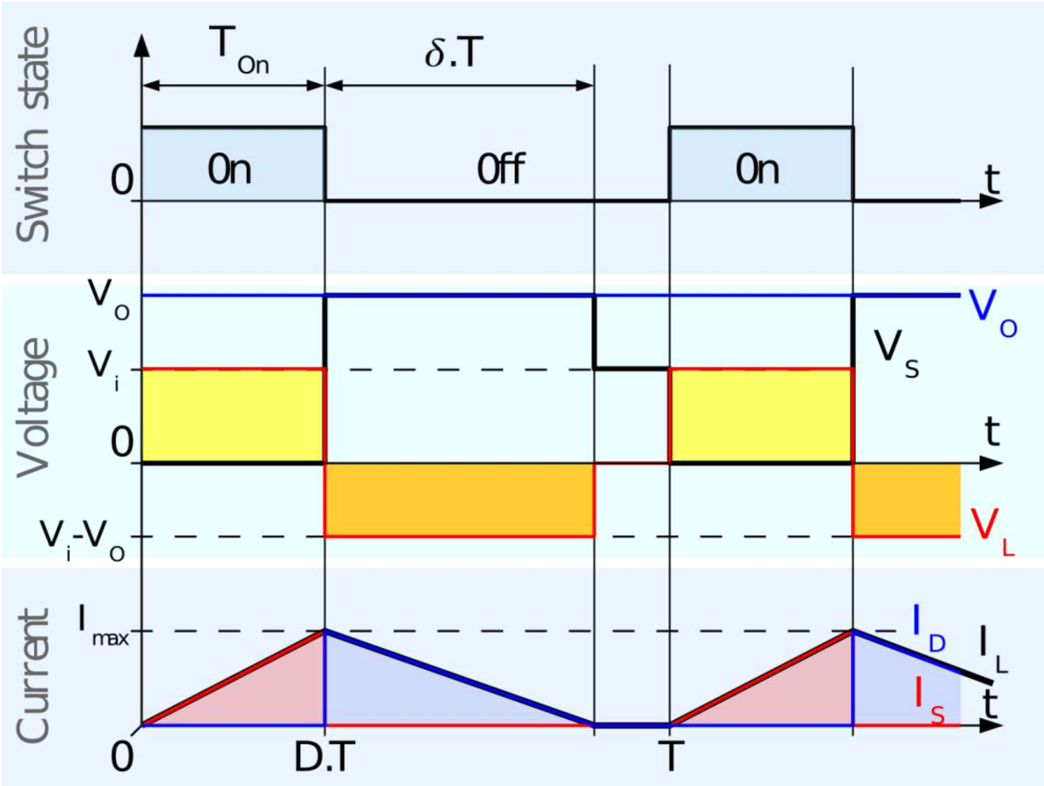

Figure II.11: Waveforms of inductor current and voltage in a boost converter operating in discontinuous mode.

II.4. Buck-Boost Converter

This converter combines the two previous functionalities, namely step-up and step-down. It transforms any input voltage into either a lower or higher output voltage depending on the requirements. Its basic schematic is illustrated in (Figure II.12)[63].

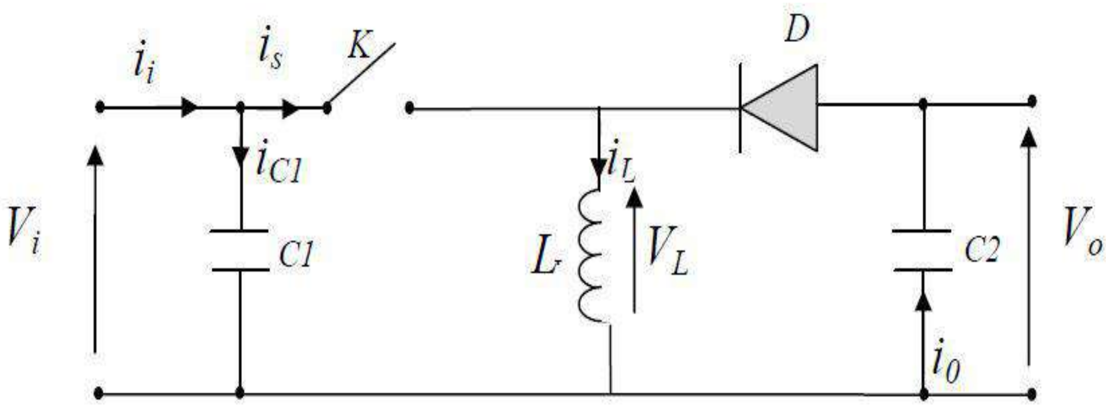

Figure II.12: Buck-Boost Converter

II.4.1. Principle of operation

When the switch K is closed, during the time interval $t_{ON,i,e,}$ t ∈ $[0, \alpha T_S]$ the diode is blocked, while the current increases linearly inside the inductor with a slope equal to $\alpha = \frac{V_i}{L}$. This allows the inductor to store more energy throughout the entire time K remains closed.

When the switch opens, i.e., during t_{OFF} with t∈ $[\alpha T_{S,} T_s]$ the diode conducts through the inductor, in which the current also decreases linearly with a slope equal to $\beta = -\frac{V_0}{L}$ [62]. When the switch K is closed, the equivalent circuit is shown in (Figure II.13).

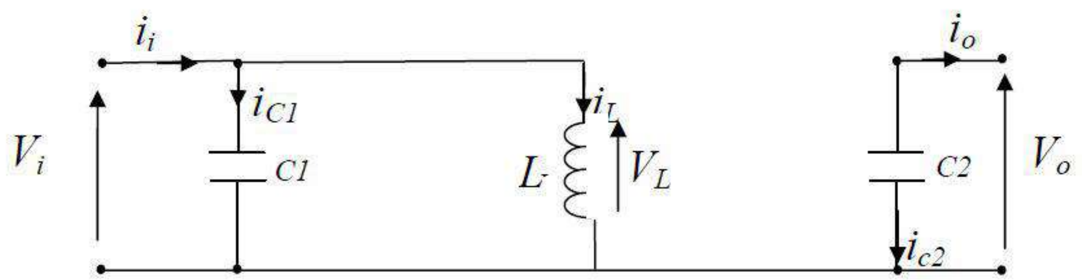

Figure II.13: Equivalent circuit of a Buck-Boost converter when t ∈ [0, αT$_s$]

By applying Kirchhoff's law to this circuit, we obtain the following equations:[60][62]

$$\begin{cases} i_{C1}(t) = C_1 \dfrac{dv_i(t)}{dt} = i_i(t) - i_L(t) \\ i_{C2}(t) = C_2 \dfrac{dv_0(t)}{dt} = -i_0(t) \\ V_L(t) = L\,\dfrac{di_L(t)}{dt} = V_i(t) \end{cases} \quad (2.9)$$

When switch K is open, the equivalent circuit is shown in (Figure II 14).

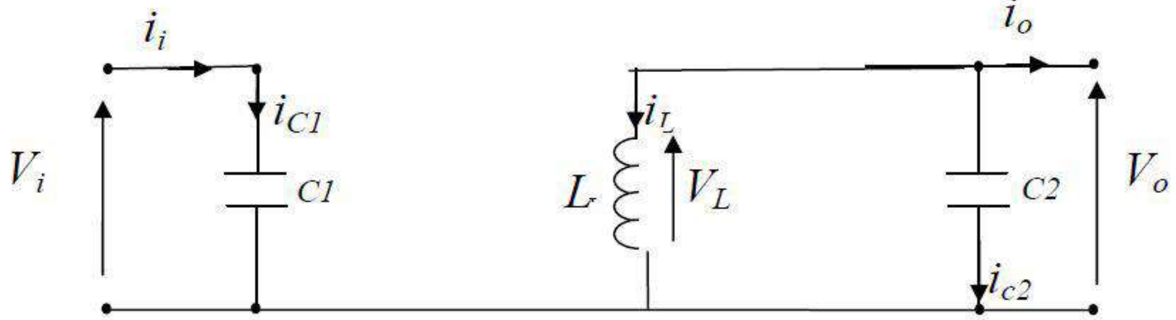

Figure II.14: Equivalent circuit of a Buck-Boost converter when t ∈ [αT$_s$, T$_s$]

The equation model in this configuration is as follows:

$$\begin{cases} i_{C1}(t) = C_1 \dfrac{dv_i(t)}{dt} = i_i(t) \\ i_{C2}(t) = C_2 \dfrac{dv_0(t)}{dt} = i_L(t) - i_0(t) \\ V_L(t) = L \dfrac{di_L(t)}{dt} = V_0(t) \end{cases} \tag{2.10}$$

II.4.2. Conversion and yield report

The conversion ratio is calculated as follows:[63]

$$M(\alpha) = \frac{V_0}{V_I} = \frac{1}{1-\alpha} \tag{2.11}$$

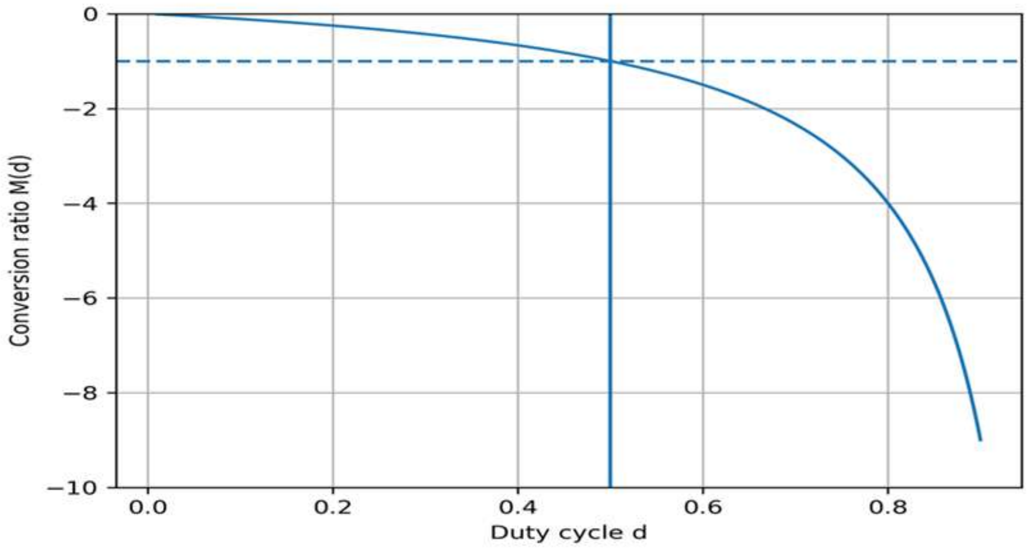

Figure II.15: Conversion ratio as a function of the duty cycle

II.4.3. Continuous conduction mode

The "Continuous Conduction Mode (CCM)" is considered the preferred operational regime for the "Buck-Boost converter" in applications requiring high stability and low output voltage ripple. In this mode, the inductor current i_L remains strictly positive throughout the switching period $(T = T_{ON} + T_{oFF})$, ensuring a consistent energy transfer to the load. Mathematically, maintaining CCM operation depends on selecting an inductance value greater than the critical inductance L_C. This regime simplifies the system's dynamic modeling and the design of feedback control loops, as the converter exhibits a more predictable behavior compared to the Discontinuous Conduction Mode (DCM).

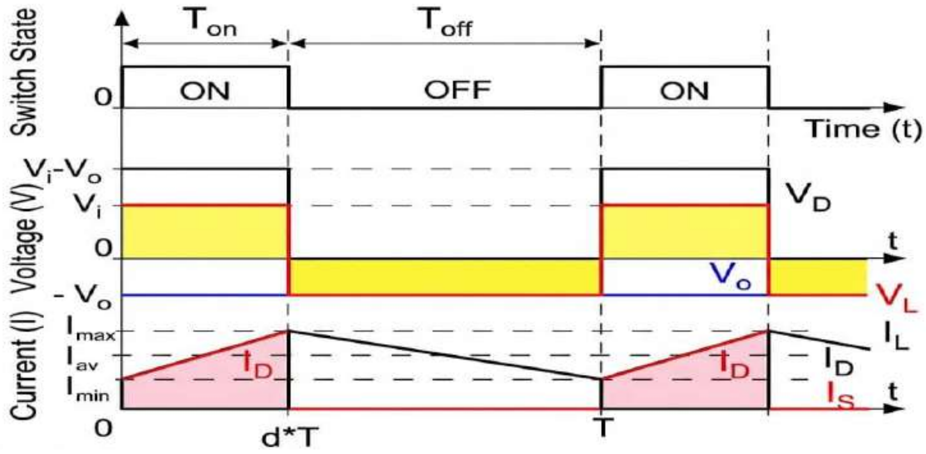

Figure II.16: Current and voltage waveforms in a Buck-Boost converter

II.4.4. Discontinuous conduction mode

The "Discontinuous Conduction Mode (DCM)" in a Buck-Boost converter is characterized by the inductor current i_L dropping to zero during the discharge sub-interval and remaining null until the start of the next switching period. This mode of operation is encountered when the inductance value is lower than the critical inductance (L < L_{crit}) or when the load current is significantly reduced. Structurally, the converter transitions through three distinct states within a single period. In the final state, the inductor is completely depleted of energy, causing the output voltage to become dependent not only on the duty cycle (D) but also on the load resistance and the inductance value. While DCM allows for smaller magnetic components and faster transient response, it requires more complex control analysis due to the increased dependency on operating parameters.

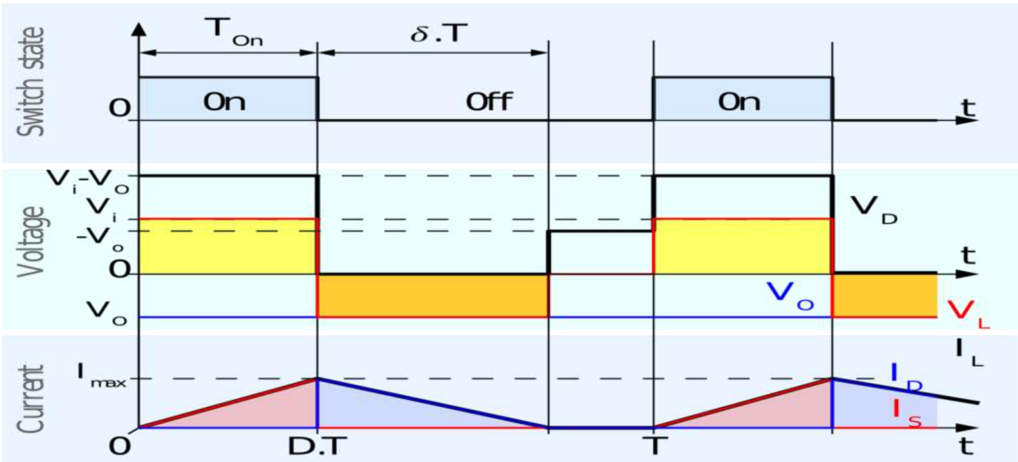

Figure II.17: Waveforms of current and voltage in a buck–boost converter operating in discontinuous mode.

III.5. Simulation results

III.5.1. DC/DC Boost converter simulation

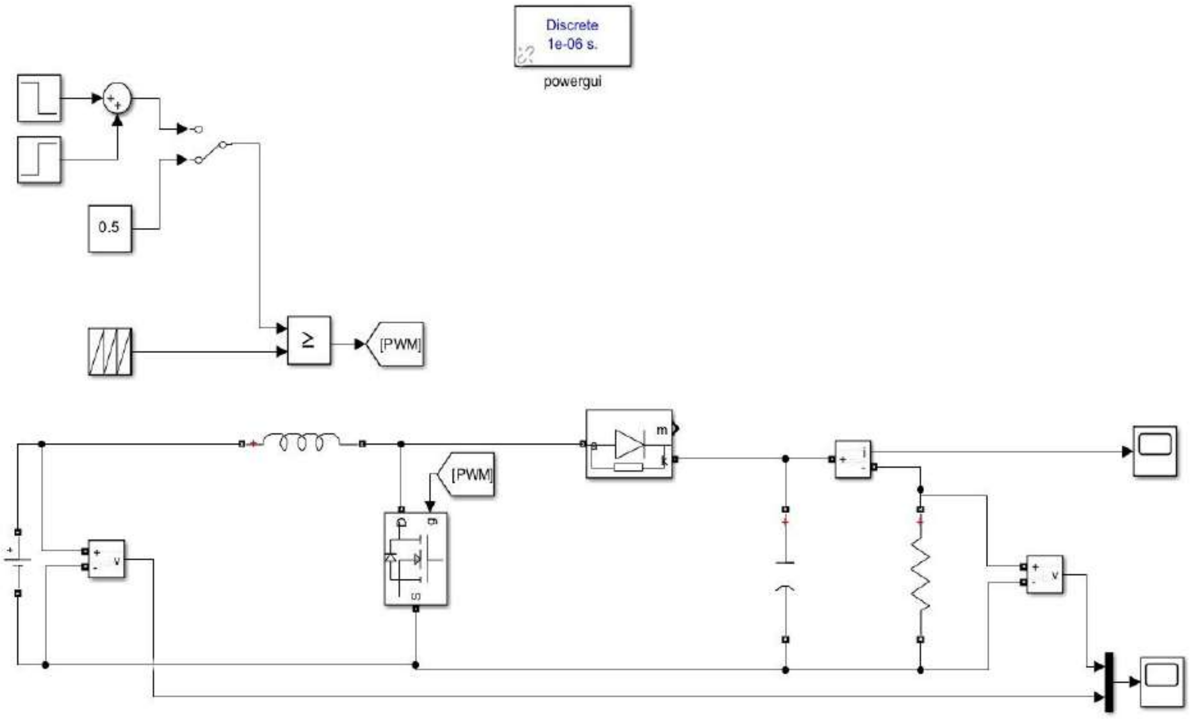

Figure II.18: Block diagram of a Boost converter

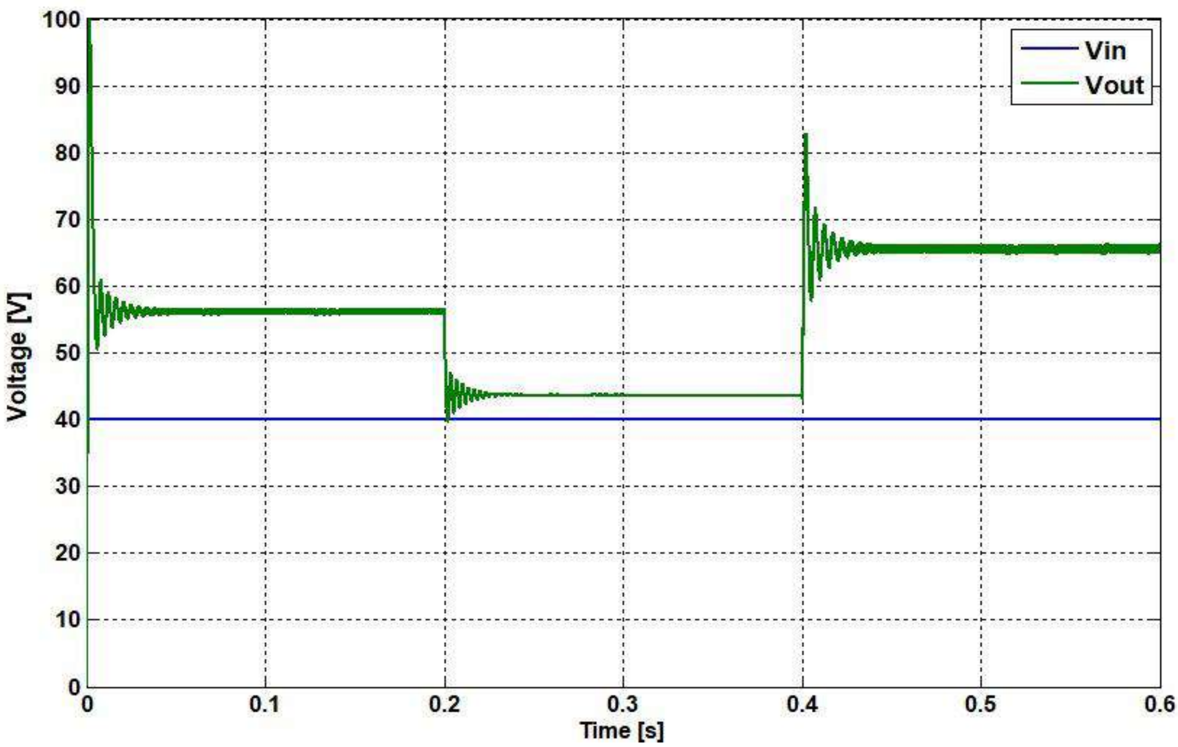

Figure II.19: Time response of the output voltage V_{out} under duty cycle step changes compared to the input voltage V_{in}

The figure (II.19) illustrates the dynamic response of the output voltage V_{out} relative to a constant input voltage V_{in} = 40 V under duty cycle step changes across different time intervals. At the initial and transient instances (t = 0s, t = 0.2s, and t = 0.4s), voltage oscillations and overshoots are observed due to the effect of the circuit's energy storage components.

II.6. Conclusion

In this chapter, we have briefly presented the main DC-DC converters, namely the boost, buck, and buck-boost converters. These serve as the interface stage between the photovoltaic generator and the load. The converter is modeled according to the needs of the application and represents the key element of the system to be controlled. For our application, we have chosen the boost converter, which ensures an output voltage higher than the voltage generated by the photovoltaic panel.

CHAPTER III

MAXIMUM POWER POINT TRACKING PRINCIPLES AND ALGORITHMS

III.1. Introduction

The power delivered by a photovoltaic generator (PVG) depends strongly on the level of solar irradiance, the temperature of the cells, shading conditions, and also on the nature of the load being supplied. Therefore, it is highly unpredictable.

The power characteristic curve of the PVG exhibits a maximum power point (MPP), which corresponds to a specific operating point defined by the voltage VMPP and the current IMPP (see Figure III.1).

Since the position of the MPP depends on the level of irradiance and the temperature of the cells, it is never constant over time. Therefore, an MPPT (Maximum Power Point Tracker) converter must be used to track these changes. An MPPT converter is a power conversion system equipped with an appropriate control algorithm that enables the extraction of the maximum power that the PVG can deliver[31].

III.2. Principle of Maximum Power Point Tracking (MPPT)

(Figure III.2) shows the basic schematic of a conventional MPPT converter. The MPPT control varies the duty cycle of the static converter (SC) using an appropriate electrical signal in order to extract the maximum power that the PV generator (GPV) can provide.

The MPPT algorithm can be more or less complex in searching for the maximum power point (MPP). In general, it is based on adjusting the duty cycle of the SC according to the evolution of its input parameters (current I and voltage V, and consequently the PV generator power) until it operates at the MPP[65].

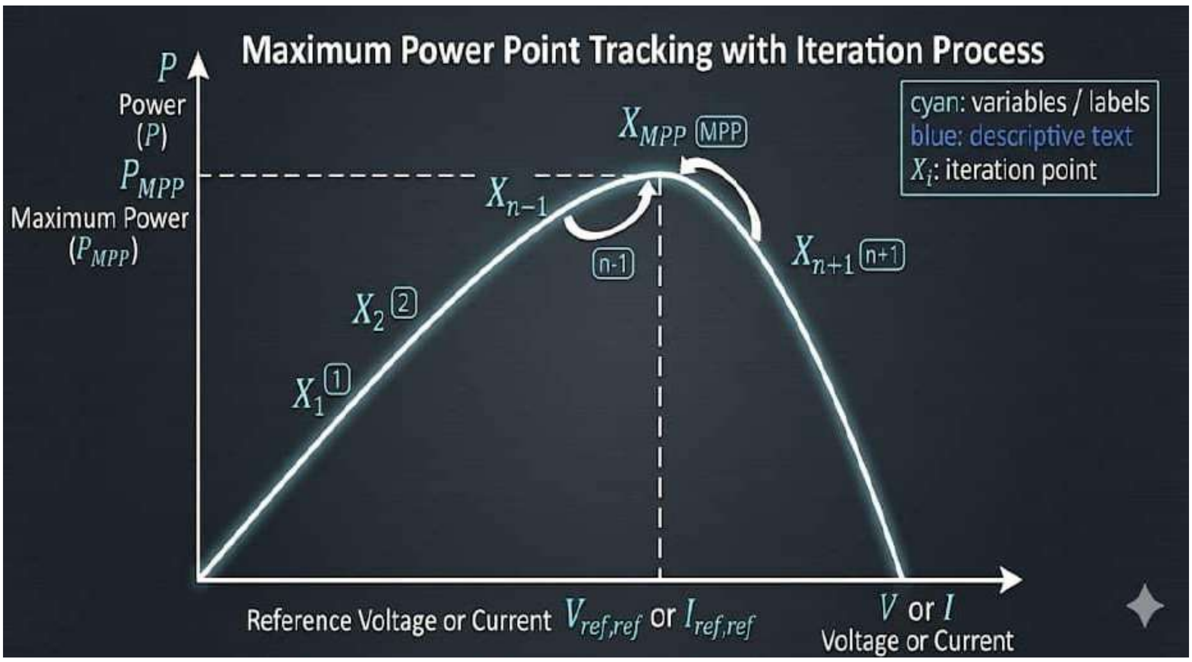

Figure III.1: Power characteristic curve of a PV generator

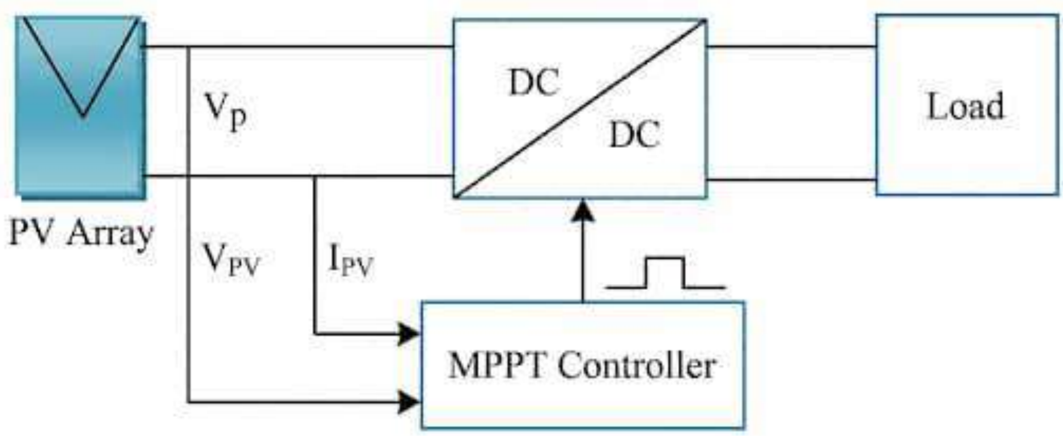

Figure III.2: Principal diagram of an MPPT converter

III.3. Classification of (MPPT) algorithms according to the search method

III.3.1. Direct methods

This type of control determines the optimal operating point (MPP) from the measured currents, voltages, or powers in the system. It can therefore react to unpredictable changes in the operation of the PV generator (PVG). Generally, these procedures are based on a search algorithm, in which the maximum of the power curve is determined without interrupting operation. For this purpose, the operating point voltage is incremented at regular intervals. If the output power increases, then the search direction is maintained for the next step; otherwise, it is reversed. The actual operating point then oscillates around the MPP. This basic principle can be protected against interpretation errors by other algorithms.

These errors may occur, for example, due to an incorrect search direction resulting from a power increase caused by a rapid rise in the level of solar irradiance.

Determining the power value of the PV generator, which is essential for MPP tracking, requires measuring the voltage and current of the generator and multiplying these two variables. Among these methods are the differentiation method, the Perturb and Observe (P&O) method, the incremental conductance method, etc[66].

III.3.2. Indirect methods

This type of control uses the existing relationship between measurable variables (Isc or Voc), which can be easily determined, and the approximate position of the MPP. It also includes control methods based on an estimation of the PV generator operating point, performed using a predefined parametric model.

There are also control methods that track the optimal voltage by taking into account only the variations in cell temperature provided by a sensor. These methods have the advantage of being simple to implement. They are mainly intended for low-cost and low-precision systems operating in geographical areas with little climatic variation. Among these methods, we find the open-circuit voltage method of the generator, the short-circuit method, etc[66].

III.4. MPPT Algorithms

In the literature, several MPPT algorithms exist; the most commonly used ones are:

III.4.1. Perturb and Observe (P&O) Algorithm

The P&O (Perturb and Observe) method is generally the most widely used due to its simplicity and ease of implementation. This algorithm uses the values of voltage Vpv and current Ipv as inputs, and produces the duty cycle α as output [67].

The principle of this algorithm (as its name suggests and as shown in (Figure III.4)) is to apply a perturbation on the voltage Vpv while acting on the duty cycle α. Following this perturbation, the power generated by the panel P(k) is calculated and compared with the previous power value P(k−1) [66].

If the power increases, the operating point moves closer to the Maximum Power Point (MPP), and the variation of the duty cycle is kept in the same direction. On the contrary, if the power decreases, the operating point moves away from the MPP. In this case, the direction of the duty cycle variation must be reversed. As illustrated in (Figure III.3) [68].

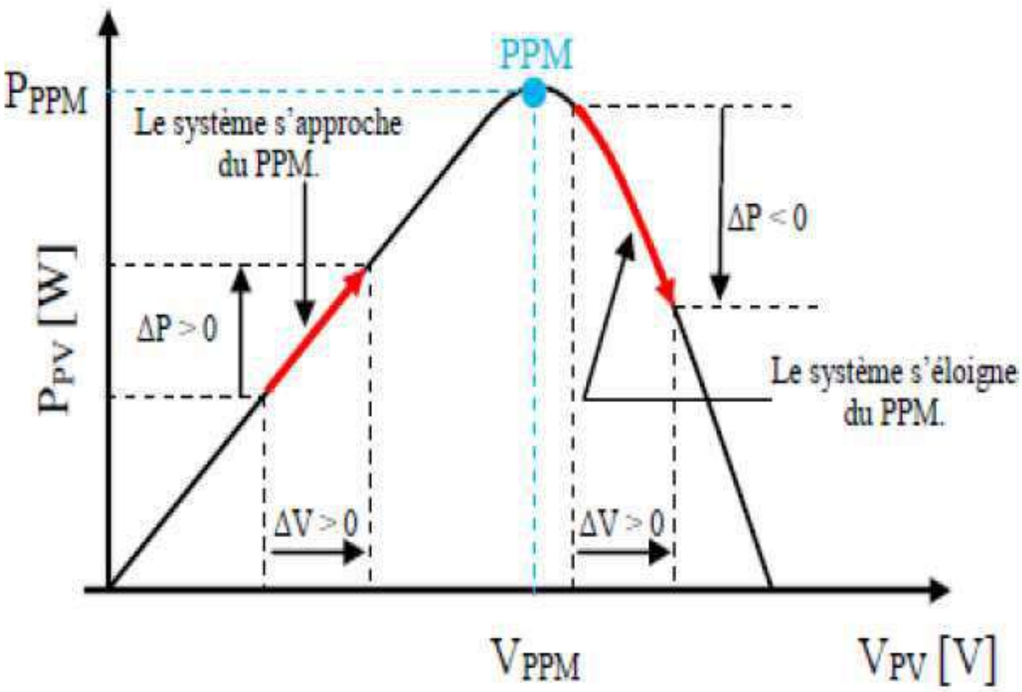

Figure III.3: Search for the MPP using the P&O method.

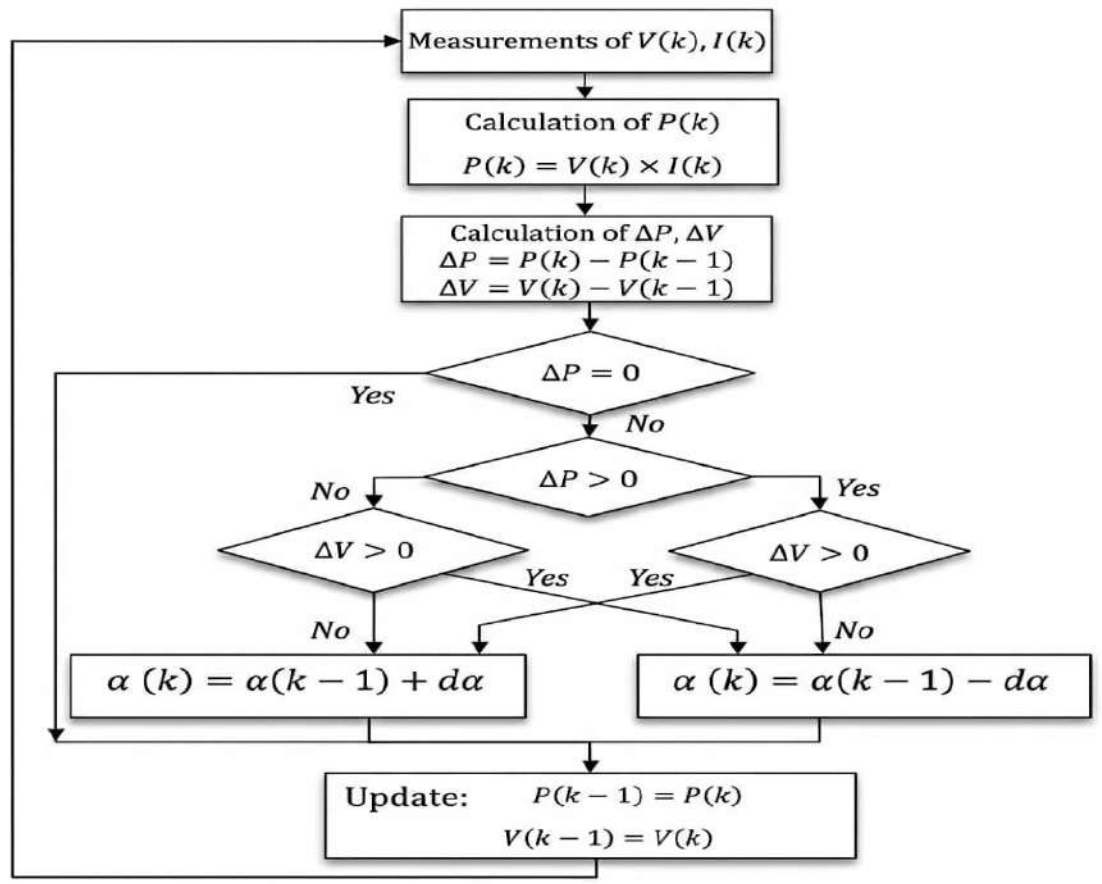

Figure III.4: Flowchart of the P&O algorithm.

III.4.2. Incremental Conductance Algorithm (INC)

The incremental conductance algorithm is an algorithm that adapts well to rapid changes in the site's weather conditions. It is relatively more stable than the P&O method; however, its practical implementation is more difficult [69].

The principle of this algorithm is based on the knowledge of the conductance value G= $\frac{I}{V}$ and the incremental conductance $\frac{\Delta I}{\Delta V}$ in order to determine the position of the operating point relative to the Maximum Power Point (MPP).

• If the incremental conductance $\frac{\Delta I}{\Delta V}$ is greater than the negative of the conductance (−G), the duty cycle is decreased.

• If the incremental conductance is less than the negative of the conductance, the duty cycle is increased.

This process is repeated until the MPP is reached, where the derivative of power is equal to zero (Figure III.5), as indicated in Equation (3.1)[70].

$$\frac{dP_{pv}}{dV_{pv}} = 0 \tag{3.1}$$

This equation can be rewritten as follows:

$$\frac{d(I_{pv} \cdot V_{pv})}{dV_{pv}} = \frac{V_{pv} \cdot dI_{pv}}{dV_{pv}} + \frac{I_{pv} \cdot dV_{pv}}{dV_{pv}} \tag{3.2}$$

$$\frac{dP_{pv}}{dV_{pv}} = V_{pv}\frac{dI_{pv}}{dV_{pv}} + I_{pv} \tag{3.3}$$

This implies that:

$$\frac{dI_{pv}}{dV_{pv}} + \frac{I_{pv}}{V_{pv}} = 0 \tag{3.4}$$

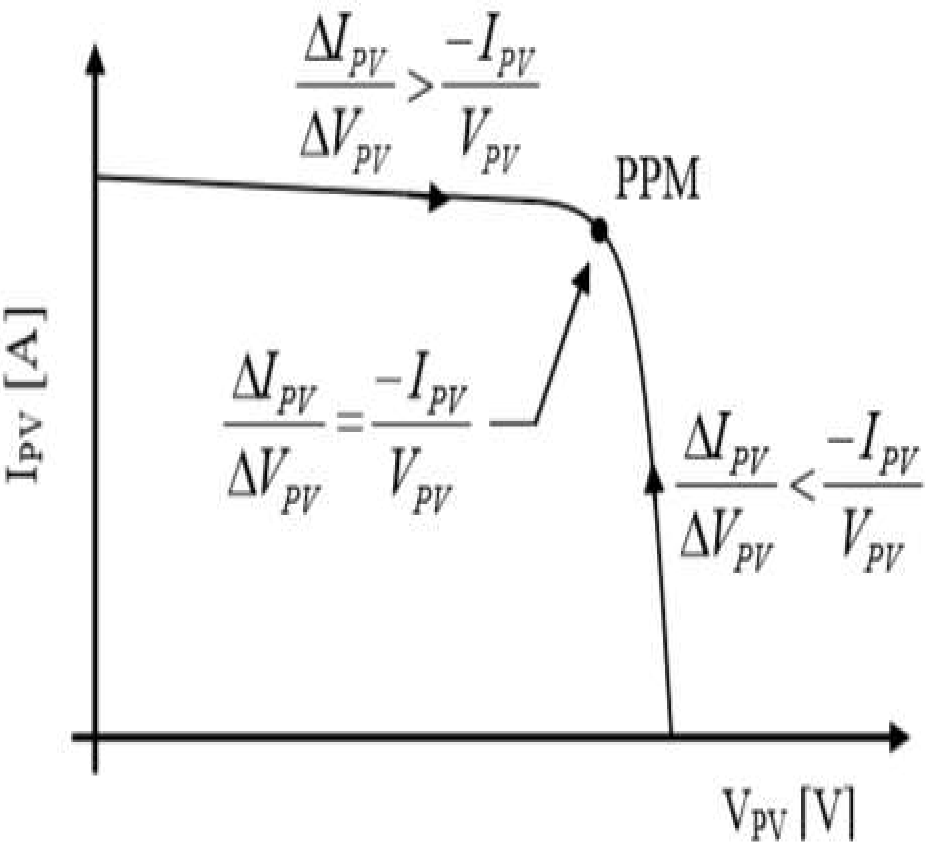

Figure III.5: Positioning of the operating point according to the value of $\Delta I_{pv}/\Delta V_{pv}$ on the I–V characteristics

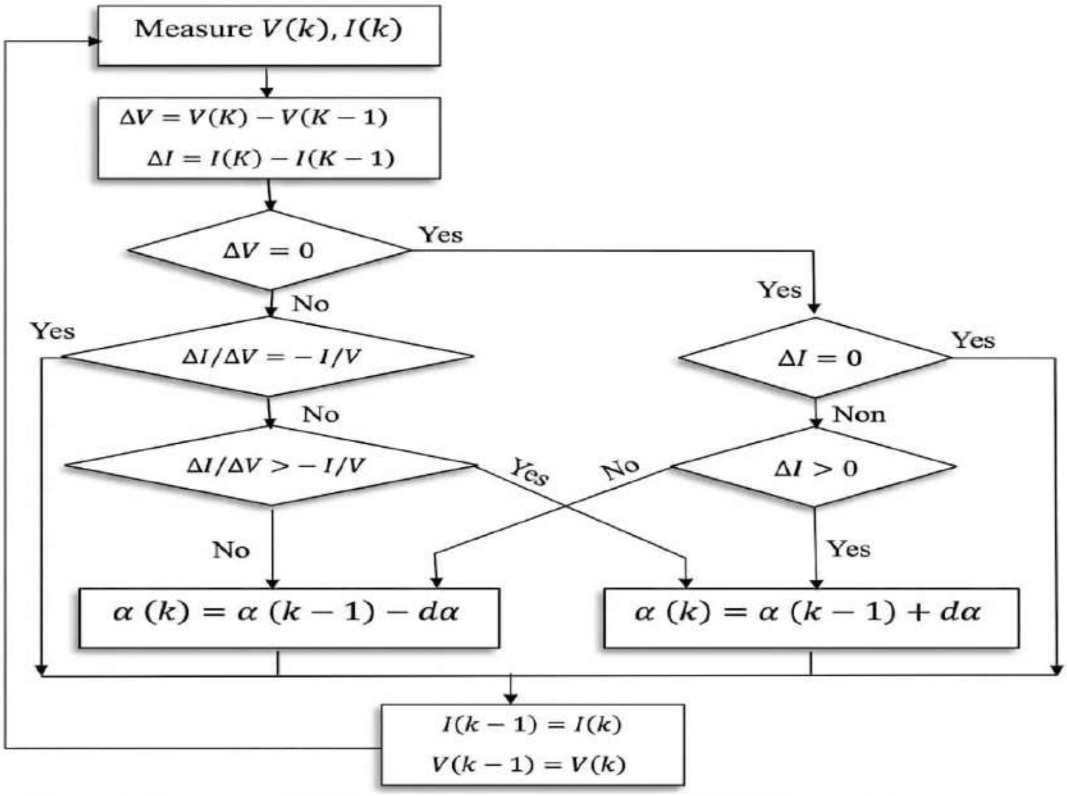

Figure III.6: Flowchart of the INC algorithm

III.4.3. Constant Voltage Algorithm

The approximate linear relationship (3.5) linking the voltages V_{MPP} and V_{OC} of the PV generator (GPV) has led to the so-called Constant Voltage (CV) method[71][72]:

$$V_{\text{MPP}} \approx k_1 \cdot V_{OC} \tag{3.5}$$

where K_1 is a proportionality constant. Since K_1 depends on the characteristics of the panel used, it must be determined in advance by empirically measuring V_{MPP} and V_{OC} under different atmospheric conditions. According to research results, the factor K_1generally lies between 0.71 and 0.78. Once K_1 is determined, V_{MPP}can be calculated using the above expression (3.5), with V_{OC}measured periodically by momentarily opening the power converter (open-circuit condition). The voltage V_{MPP} is then used as the operating voltage for a certain time, after which the cycle is repeated.

The drawback of this algorithm is the loss of available power during the disconnection of the load from the PV generator. Also, the MPP is not always between 71% and 78% of the open-circuit voltage V_{OC} To overcome this issue, pilot cells are used to obtain V_{OC}.

These cells must be carefully selected so as to accurately represent the characteristics of the PV generator.

Once the voltage V_{MPP} has been approximated, a closed-loop control of the power converter can be used to asymptotically reach the desired voltage.

Since the expression is only an approximation, the panel never operates exactly at the MPP. Moreover, in the case of partial shading, K_1 is no longer valid. Although this technique is not truly an MPP method, it is simple and inexpensive to implement.

III.4.4. Constant Current Algorithm

This technique stems from the fact that, under varying atmospheric conditions, the IMPP current is approximately linearly related to the short-circuit current Isc of the PV generator. It has been shown that[71][72].

$$V_{\mathrm{MPP}} \approx K_1 I_{sc} \tag{3.6}$$

Where K_2 is a proportionality constant. As with the CV method, K_2 is determined for the PV generator used. The constant K_2 is generally between 0.78 and 0.92. Measuring the short-circuit current I_{SC} during operation is problematic. A switch is usually added to the power converter to short-circuit the panel and measure the I_{SC} current using a current sensor. This increases the number of components and therefore the cost. The output power is reduced during the measurement of I_{SC}. Moreover, the MPP is never reached.

III.4.5. Hill Climbing Algorithm

The control technique called Hill Climbing is one of the most widely used methods for MPPT control due to its simplicity of implementation [73]. However, it has oscillations around the Maximum Power Point (MPP) in steady-state operation and an occasional loss of MPP tracking when there are rapid changes in weather conditions [74]. The algorithm of this method is illustrated in Figure (2.30) [73].

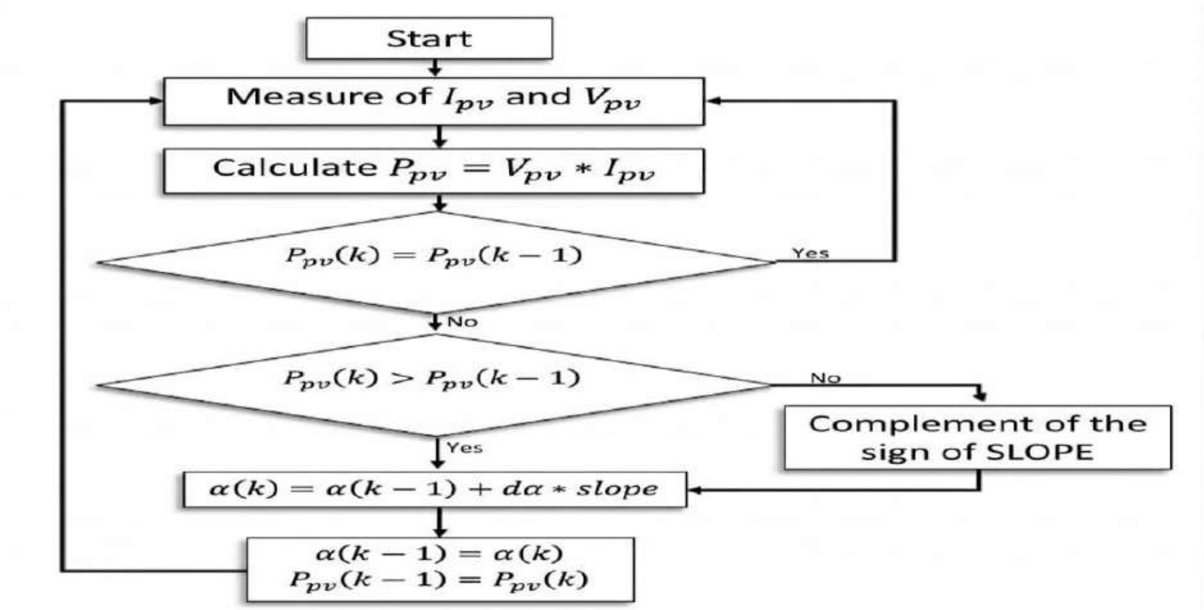

Figure III.7: Flowchart of the Hill Climbing Algorithm

With:

• SLOPE: corresponds to a variable that takes the value “1” or “-1” depending on the direction that must be given to the search in order to increase the output power of the panel.

Periodically, the power of the panel is compared with the previously determined value. Based on the result of this comparison, the sign of the Slope value either changes or remains the same. Once the MPP is reached, the system oscillates around it indefinitely [74].

III.5. Conclusion

This chapter presented the principle of Maximum Power Point Tracking (MPPT) used to maximize the power extracted from photovoltaic systems. The role of the DC–DC converter was explained as an interface that adjusts the PV operating point through duty cycle control. In addition, the classification and types of MPPT algorithms were introduced, highlighting common methods used to track the maximum power point efficiently.

CHAPTER IV

SIMULATION RESULTS AND COMPARATIVE ANALYSIS

IV.1. Introduction

This chapter discusses the modeling and simulation of the photovoltaic generator using the MATLAB/Simulink environment to understand the impact of dynamic changes in solar irradiance and temperature on the electrical characteristic curves (I-V) and (P-V). It also reviews the role of the DC/DC Boost Converter in dynamically matching impedance to direct the system toward the Maximum Power Point (MPP). Finally, the chapter concludes with a comparative study to evaluate the tracking efficiency and transient response speed of three Maximum Power Point Tracking (MPPT) algorithms: Perturb and Observe (P&O), Hill Climbing (HC), and Incremental Conductance (INC) under varying environmental conditions.

IV.2. Simulation Results

IV.2.1. Open circuit PV Panel Simulation Via MATLAB/Simulink

The solar panel block is modeled by electrical equations, with temperature T and irradiation G as inputs, and current I and voltage V as outputs

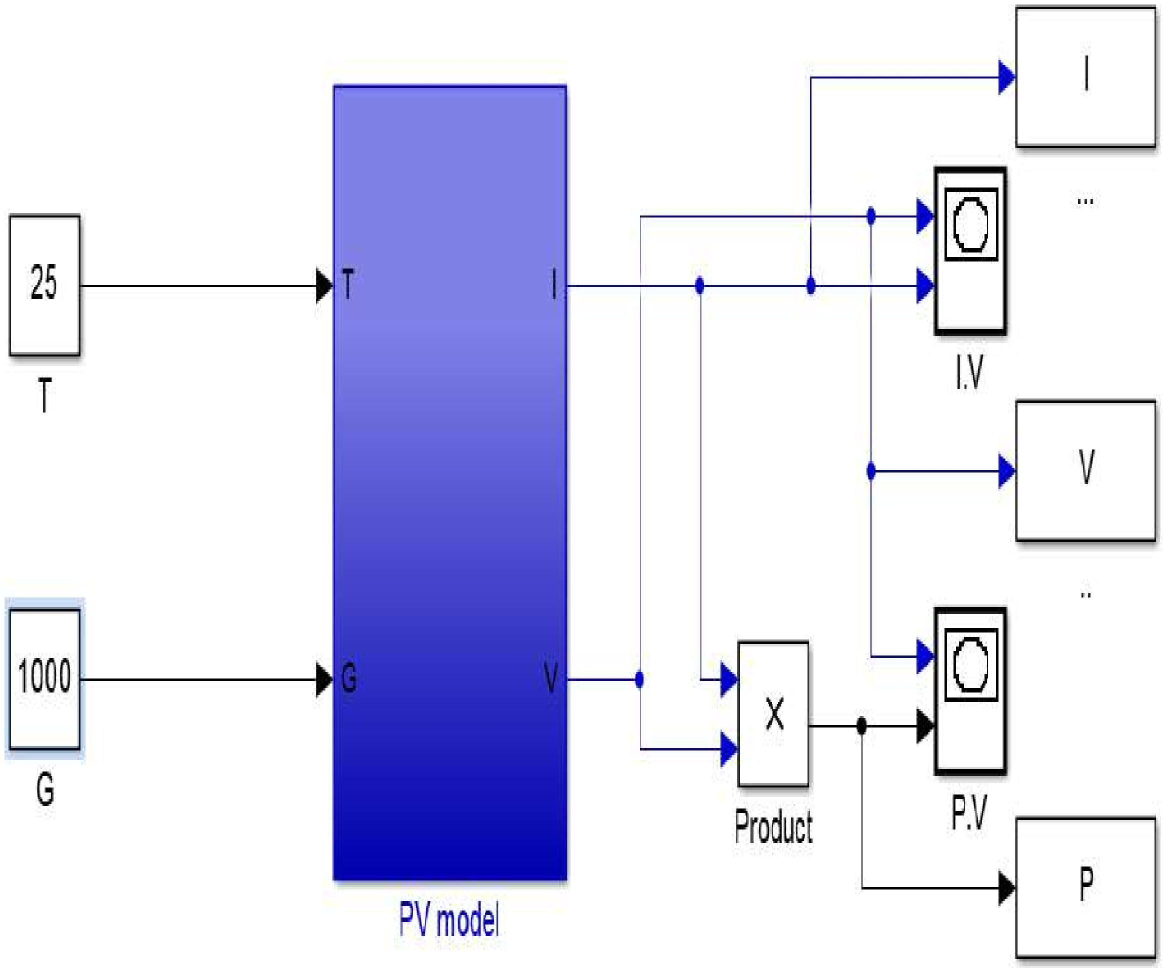

Figure IV.1: Simulation scheme of Open circuit PV Panel

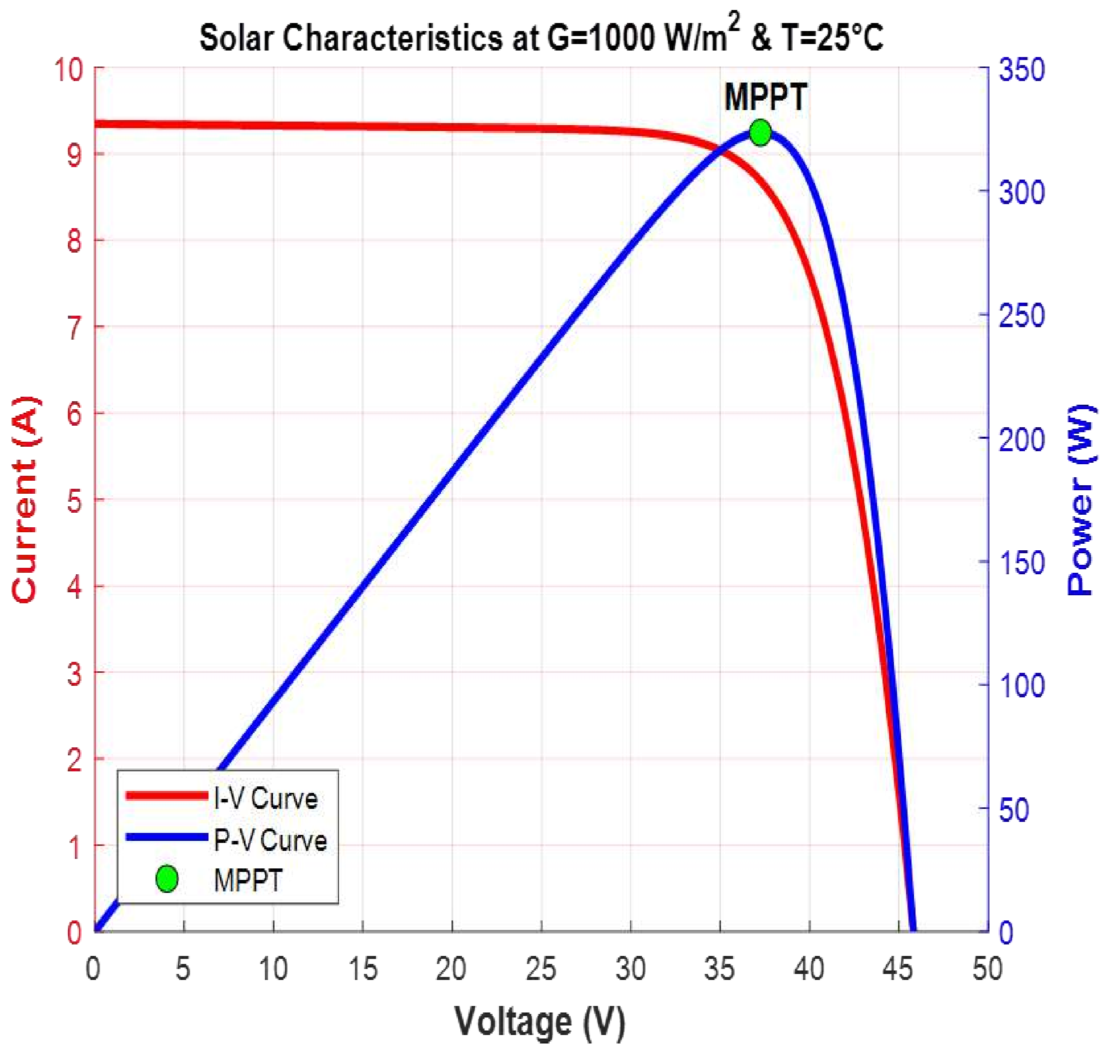

Figure IV.2: Characteristic Curves of a PV Module: Current-Voltage (I-V) and Power-Voltage (P-V) at Standard Test Conditions (STC)

The figure(IV.2) illustrates the electrical characteristics of a PV module under Standard Test Conditions (STC: G = 1000 W/m^2, T = 25°C) using two curves sharing a common Voltage (V) axis. The Current-Voltage (I-V) curve features a short-circuit current $I_{SC} \approx$ 9.3 A and an open-circuit voltage $V_{OC} \approx$ 46 V, showing a sharp exponential current drop after remaining relatively constant at lower voltages. The Power-Voltage (P-V) curve, calculated as P = I•V, rises to its peak at the Maximum Power Point (MPP), which delivers optimal performance at $V_{mp} \approx$ 37.5 V, $I_{mp} \approx$ 8.7A, and a peak power P_{MAX} between 325W and 330W This peak underscores the vital role of Maximum Power Point Tracking (MPPT) algorithms in solar controllers and inverters to continuously extract maximum efficiency under varying environmental conditions.

IV.2.1.1. Irradiance variation test

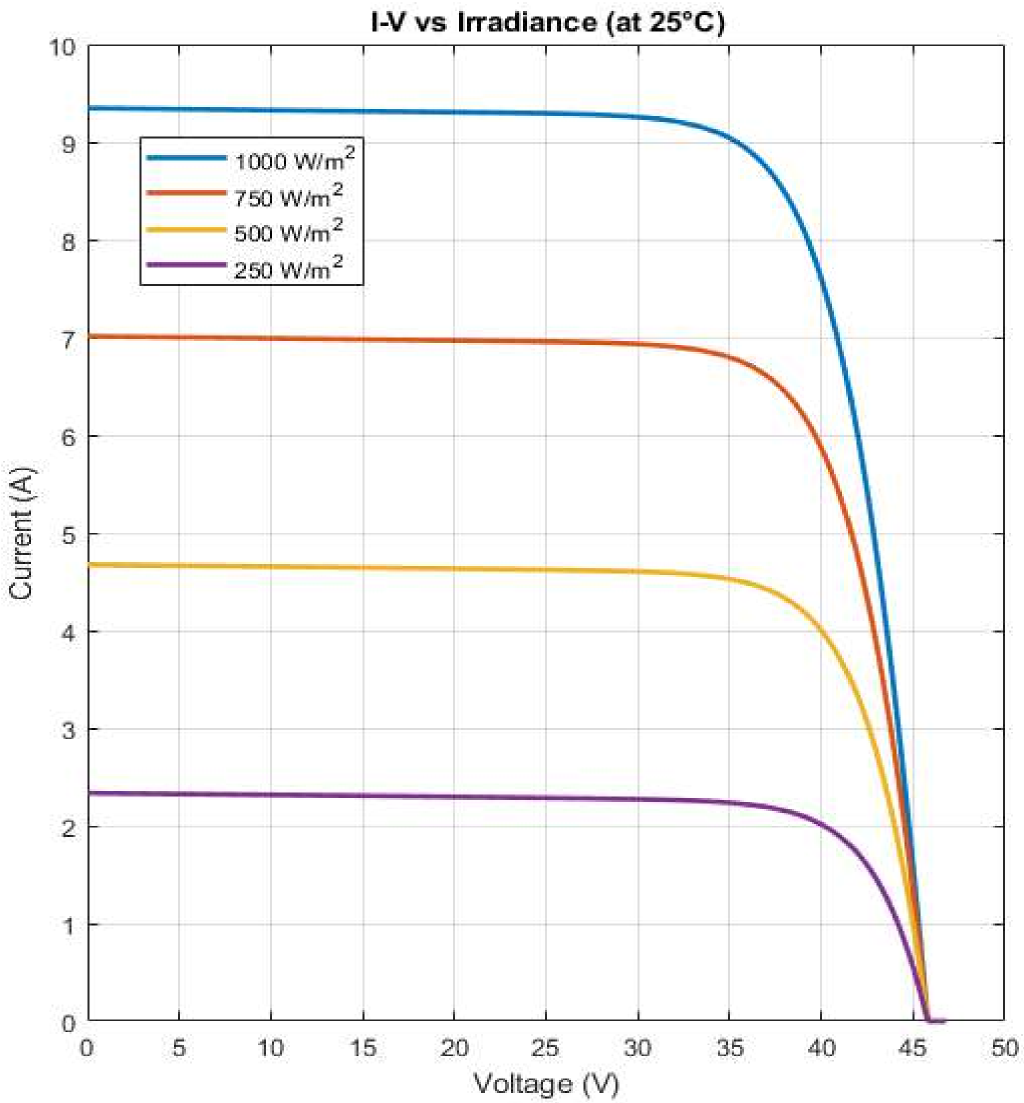

Figure IV.3: I-V Characteristics of the PV module under Solar Irradiance Variation with constant temperature

The figure(IV.3) illustrates the current-voltage (I-V) characteristics of the photovoltaic generator at a constant temperature (25°C) under varying solar irradiance levels (1000, 750, 500, and 250W/m²). A strong direct proportionality is observed between the irradiance intensity and the short-circuit current I_{SC}, which increases linearly with higher irradiance. In contrast, the open-circuit voltage V_{OC} remains minimally affected by these variations, experimentally confirming that solar irradiance is the primary determinant of the current produced by photovoltaic cells.

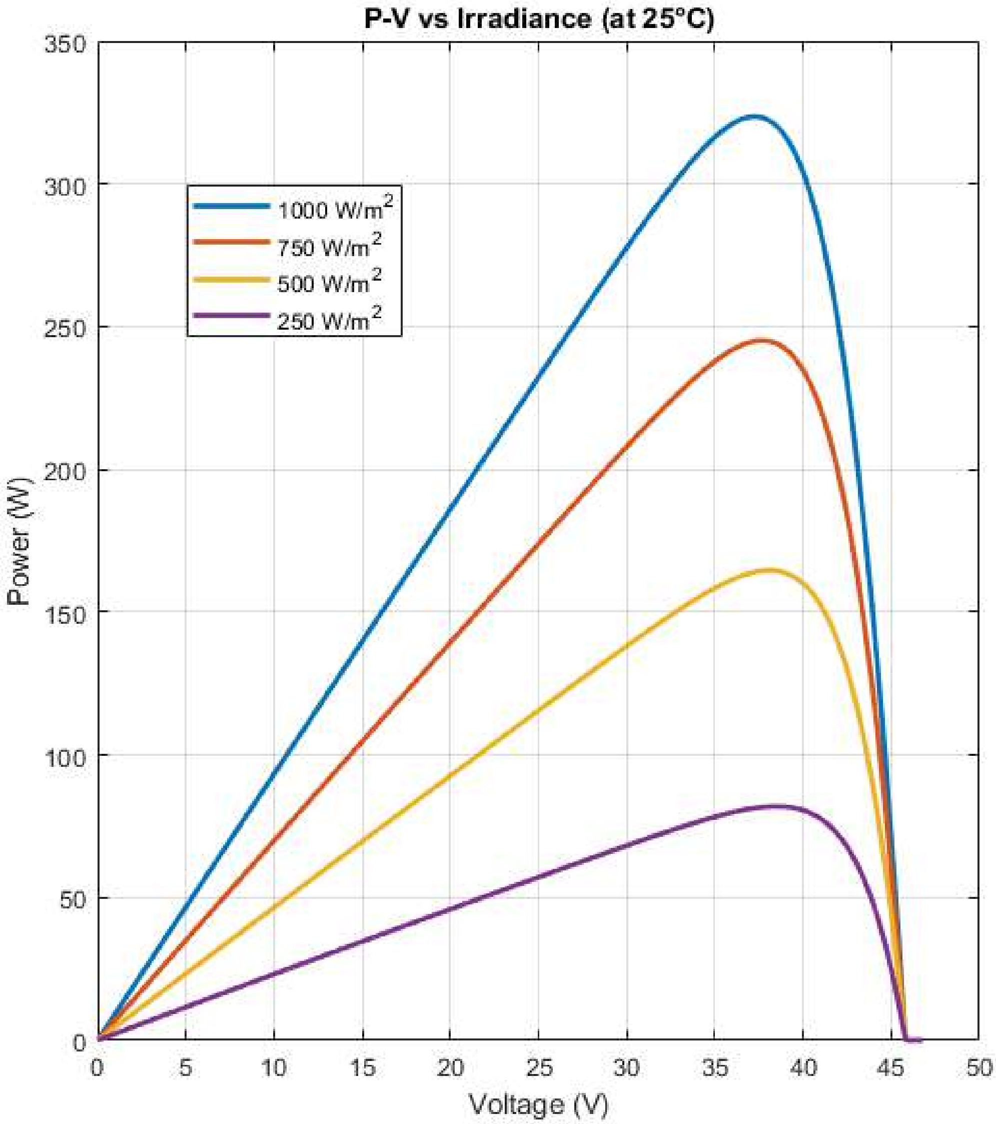

Figure IV.4: P-V characteristics of the PV module under solar irradiance variation with constant temperature

The figure(IV.4) shows the influence of varying solar irradiance on the electrical performance of the PV module through its I–V and P–V characteristics. It can be observed that the maximum power output P_{MAX} is highly dependent on solar irradiance, decreasing significantly from approximately 325 W at 1000 W/m² to 80 W at 250 W/m². Conversely, the open-circuit voltage V_{OC} remains relatively stable with minimal variations around 47V.This non-linear behavior highlights the necessity of implementing Maximum Power Point Tracking (MPPT) techniques to optimize energy extraction under changing atmospheric conditions.

IV.2.1.2. Temperature variation test

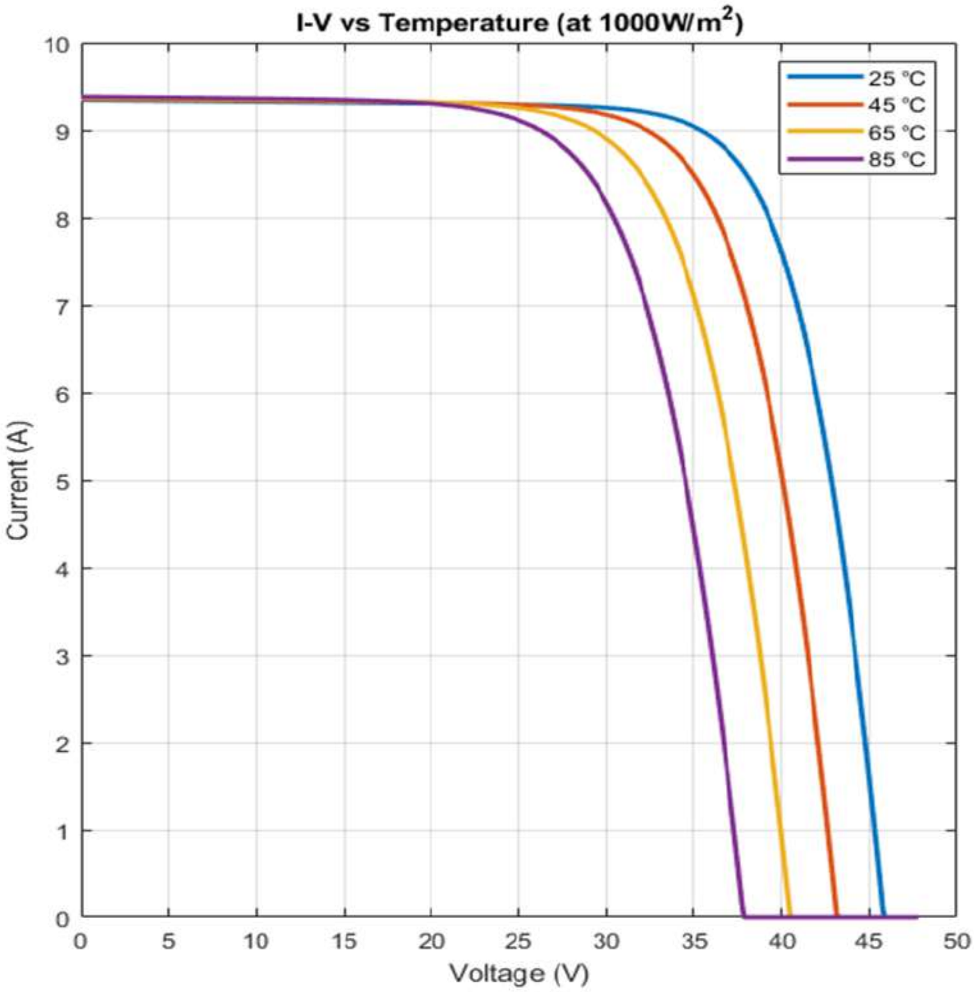

Figure IV.5: I-V Characteristics of a PV module under temperature variation with constant solar irradiance

The figure(IV.5) illustrates the effect of temperature on the current-voltage (I-V) characteristics of the photovoltaic cell under constant irradiance (1000W/m^2). It is observed that an increase in temperature (from 25°C to 85°C) leads to a sharp and significant decrease in the open-circuit voltage V_{OC} contrasted with a very slight and negligible increase in the short-circuit current I_{SC}. As a result of this disparity, the maximum output power P_{MAX} decreases, and the overall performance efficiency of the cell noticeably drops as its operating temperature rises.

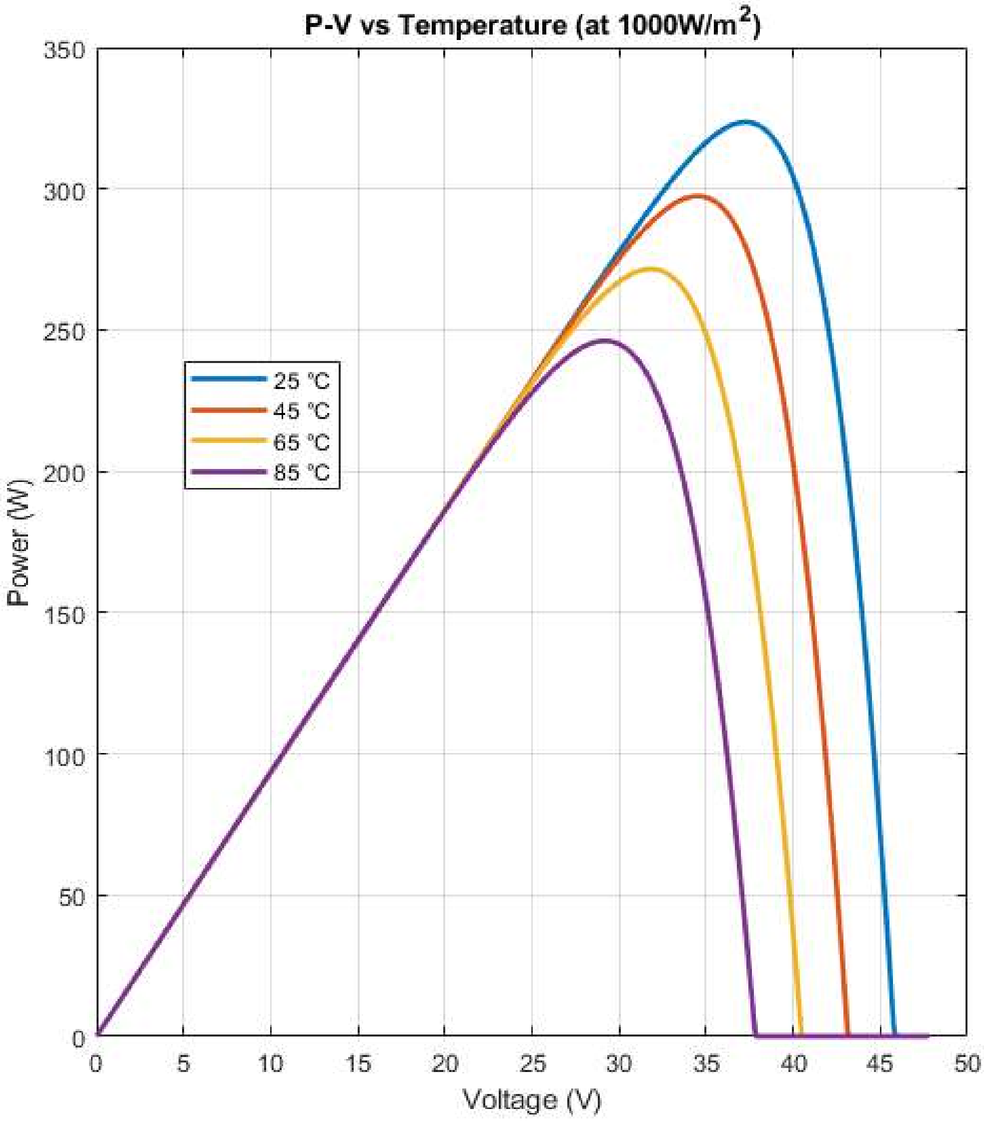

Figure IV.6: P-V Characteristics of a PV module under temperature variation with constant solar irradiance

Figure(IV.6) Power-Voltage (P-V) characteristics of the photovoltaic module under a constant irradiance of 1000 W/m² and varying temperatures (25°C, 45°C, 65°C, 85°C). The curves clearly indicate that an increase in temperature leads to a shift of the Maximum Power Point (MPP) toward lower voltage values, resulting in a direct reduction of the maximum extracted power. This confirms the adverse effect of temperature on the energy efficiency of the PV panel.

IV.2.2. Effect of Load Resistance on Solar Panel Operating Points and Power Output

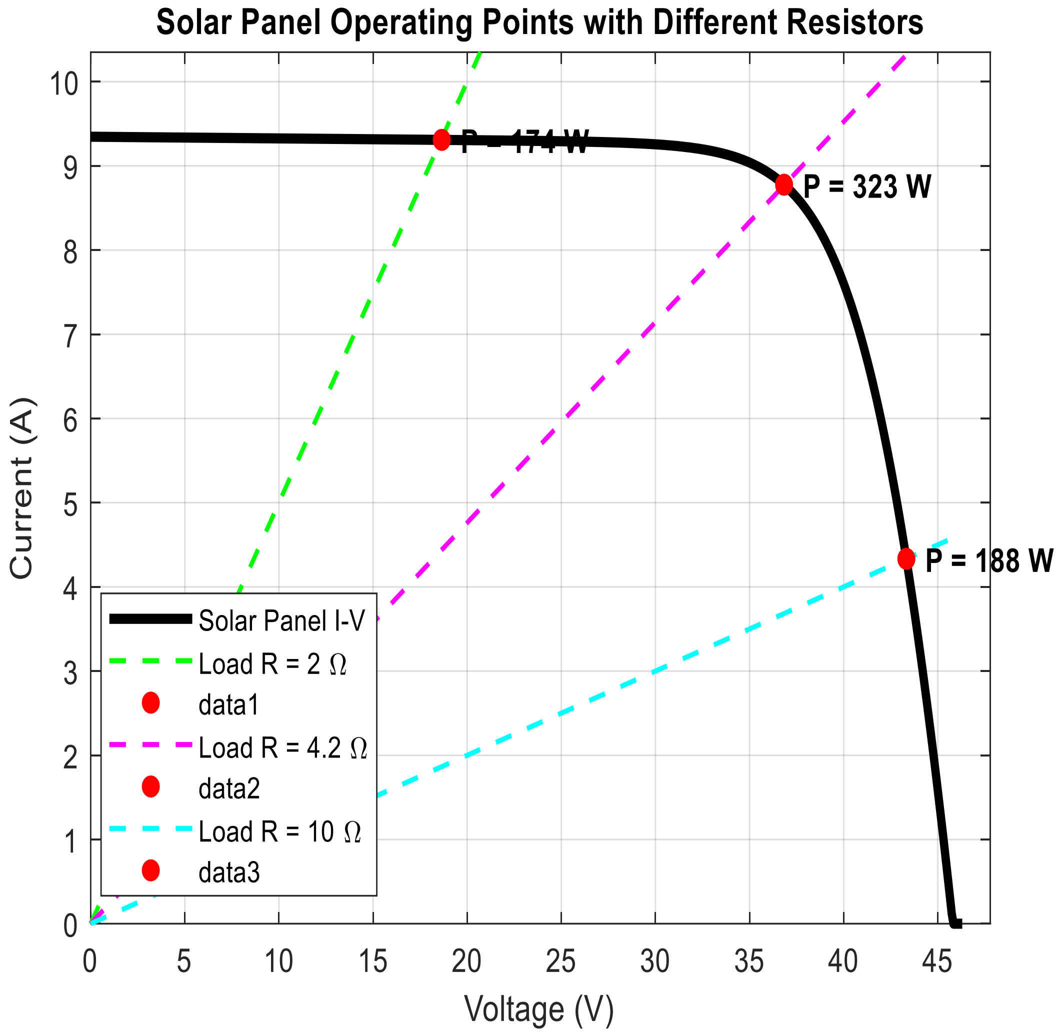

Figure IV.7: I-V characteristics of the PV panel and operating points with different resistors loads

The figure(IV.7) illustrates the impact of varying load resistance values (R) on determining the operating point of the photovoltaic generator along it's I-V characteristic curve. It is observed that shifting the resistance alters the intersection point: a low resistance (2 Ω) drops the voltage, yielding a low power of 174W, while a high resistance (10Ω) restricts the current, resulting in 188W. Conversely, the optimal resistance value (4.2Ω) perfectly matches the maximum power point P_{MPP}= 323W, highlighting the critical importance of impedance matching to ensure maximum system efficiency.

IV.2.3. Effect of DC/DC Boost Converter Duty Cycle on Solar Panel Operating Point

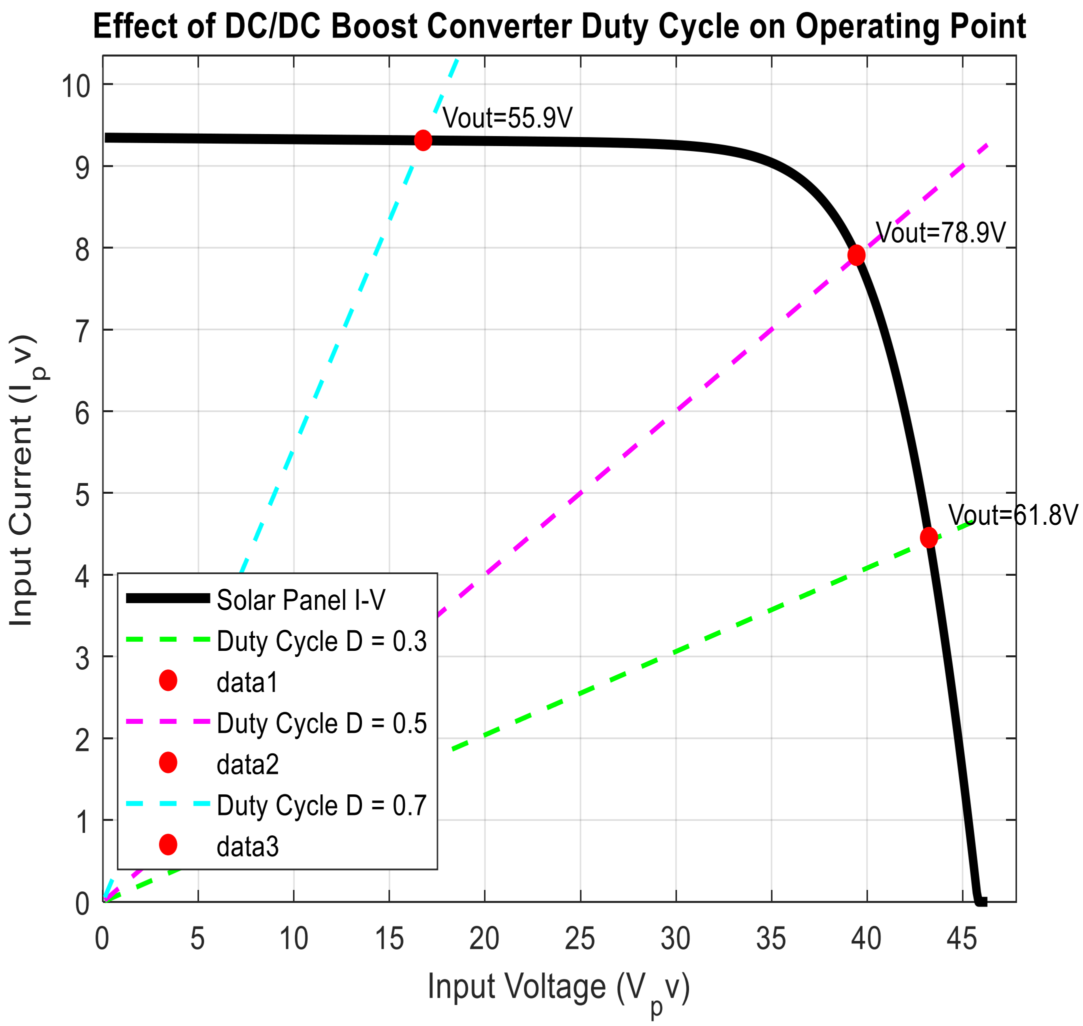

Figure IV.8: Effect of the DC/DC Boost Converter duty cycle on the operating point of the PV solar panel

The figure(IV.8) demonstrates that the DC/DC boost converter acts as a variable impedance matcher, where adjusting the duty cycle (D) shifts the operating point along the PV panel's (I-V) curve. Changing from a low duty cycle (D = 0.3) to a high one (D = 0.7) shifts the system from a high-voltage, low-current region to a high-current, low-voltage region, passing through the Maximum Power Point (MPP) at an intermediate duty cycle (D = 0.5). This highlights the vital role of MPPT algorithms in dynamically optimizing the duty cycle to extract maximum power under varying conditions.

IV.3. Simulation of PV system under Perturb and Observe MPPT method via MATLAB/Simulink

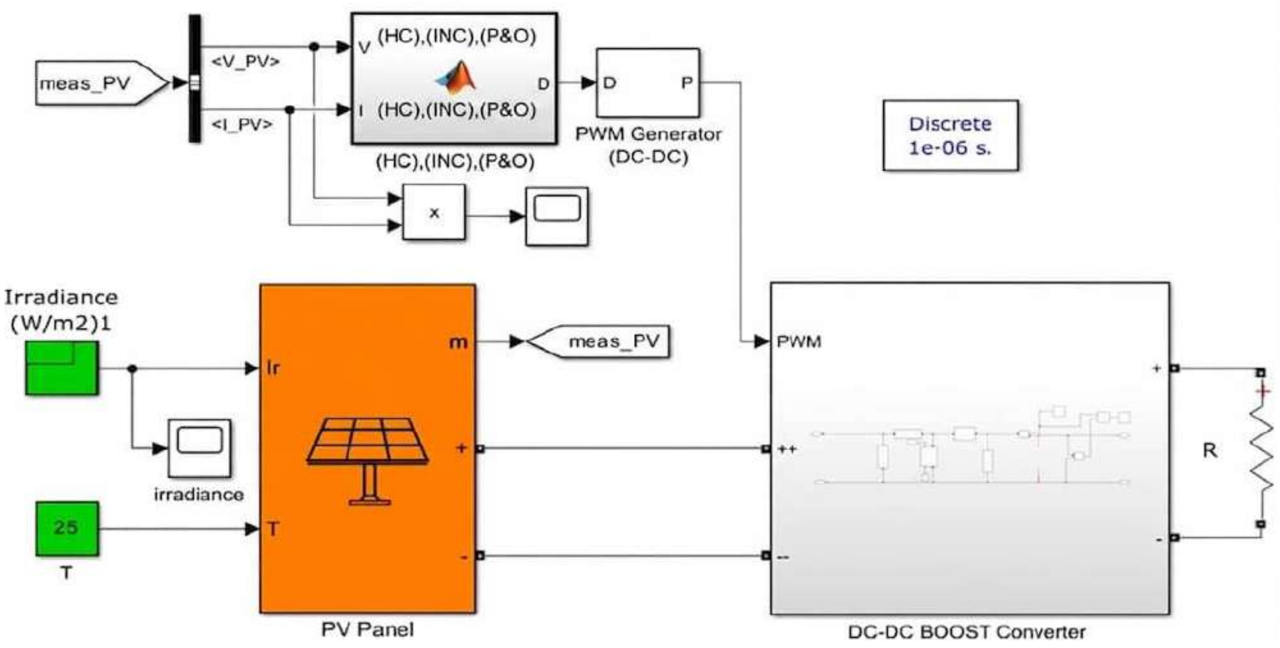

Figure IV.9 :Simulation block diagram of a PV solar system under (P&O),(INC),(HC) algorithm

IV.3.1. Simulation results

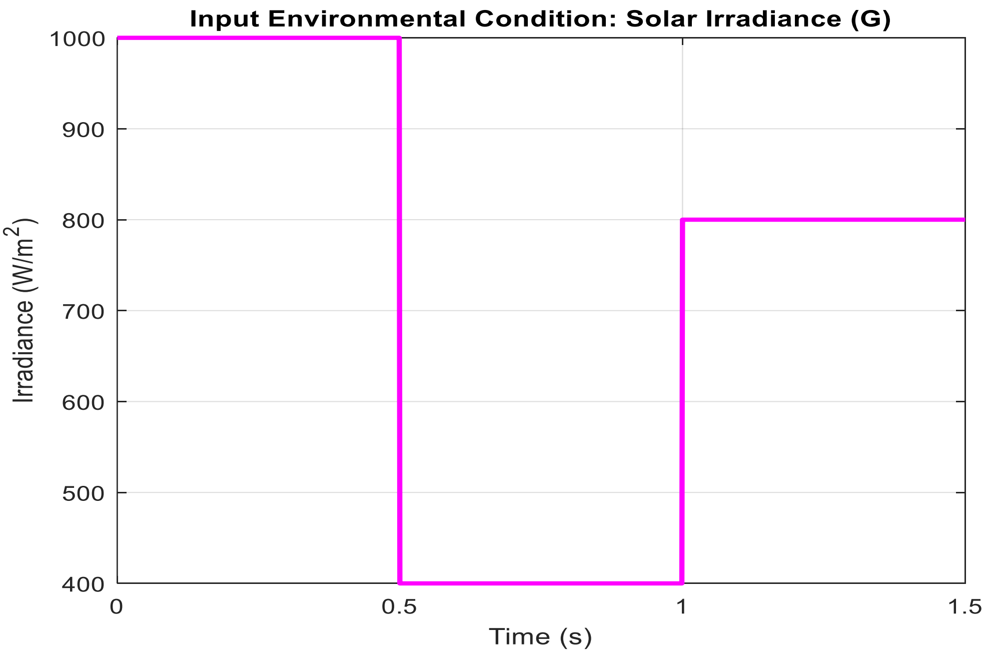

Figure IV.10 : Solar irradiance curve

The figure(IV.10) illustrates the sudden changes (step changes) in solar irradiance as a case study for variable environmental conditions over a time span of 1.5 seconds. The curve goes through three main phases: starting with a high constant irradiance level of 1000 W/m² until 0.5 s, followed by a sharp drop to 400 W/m² lasting until 1 s (simulating cloud passage), and finally recovering to stabilize at 800 W/m². This dynamic profile is utilized to evaluate the transient response and efficiency of Maximum Power Point Tracking (MPPT) algorithms under rapidly changing environmental conditions.

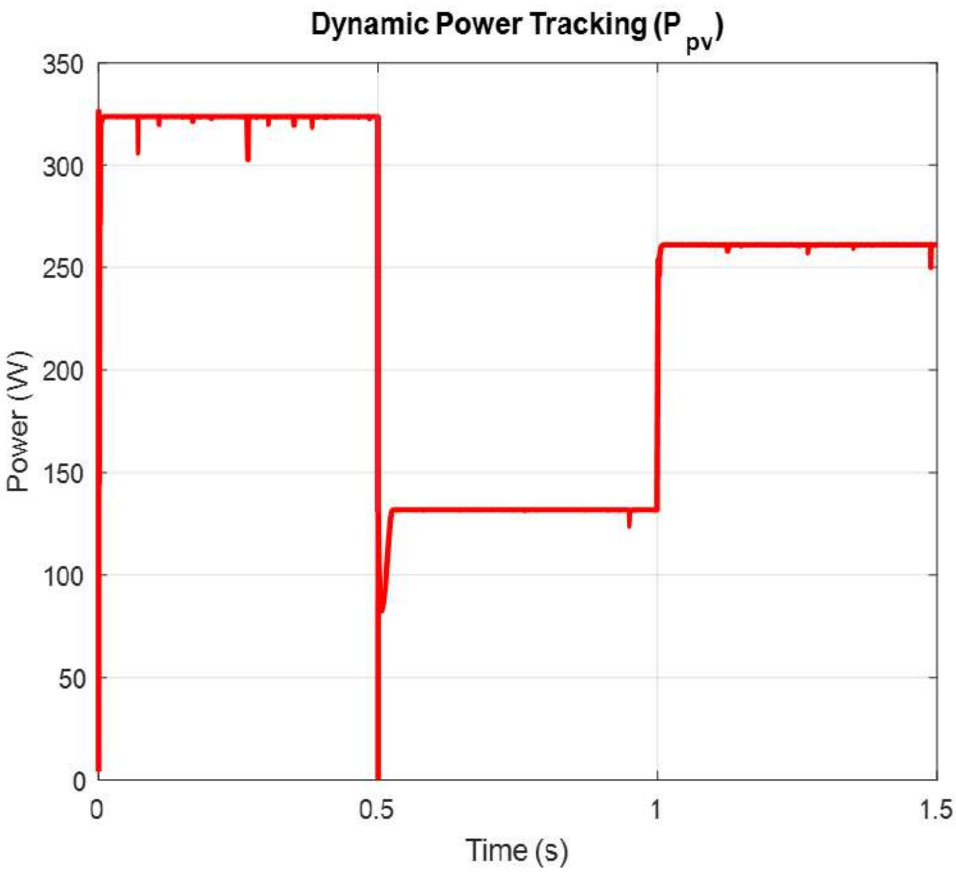

Figure IV.11: Dynamic Power curve with variable irradiance under P&O algorithm

The curve(IV.11) illustrates the dynamic performance of the maximum power point tracking P_{PV} for the photovoltaic generator over time, under sudden variations in operating conditions at 0.5s and 1s. It is observed that the tracking algorithm exhibits a highly rapid dynamic response and a brief settling time when transitioning between different power levels (from 325W to 130W, then to 260W). Furthermore, the system demonstrates near-perfect stability with negligible steady-state oscillations, which proves the high efficiency and robustness of the deployed control system.

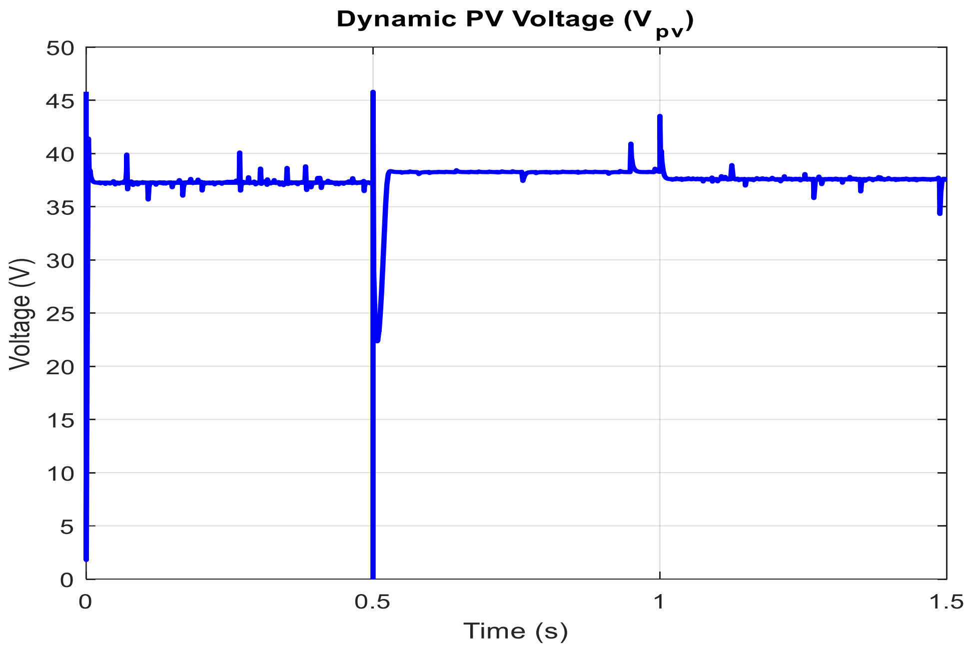

Figure IV.12: voltage curve with variable irradiance under P&O algorithm

The curve(IV.12) illustrates the dynamic response of the photovoltaic generator voltage V_{PV} over time. It is observed that the voltage rapidly stabilizes at its optimal value (around 37.5 V then 38.2 V) following the sudden variations at 0.5s and 1s. The system exhibits minor and brief transient undershoots during transitions, confirming the control system's high capability in voltage regulation and stability maintenance.

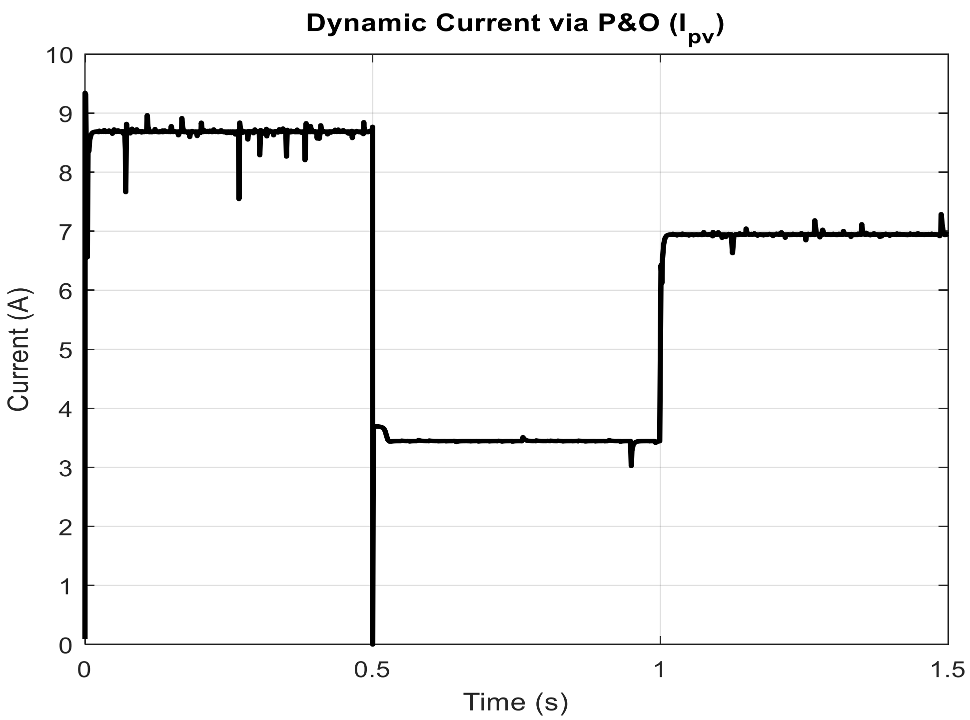

Figure IV.13: current curve with variable irradiance under P&O algorithm

The curve(IV.13) illustrates the dynamic response of the photovoltaic generator current I_{PV} tracked via the P&O algorithm. The system demonstrates fast and accurate tracking under sudden step changes at 0.5s and 1s, where the current smoothly transitions and stabilizes at the new optimal values (around 8.7A, 3.5A, and 7A, respectively). Furthermore, the minimal steady-state oscillations reflect the high efficiency of the algorithm in reducing power losses.

IV.4. Simulation of PV system under Incremental Conductance (INC) MPPT algorithm via MATLAB/Simulink

IV.4.1. Simulation results

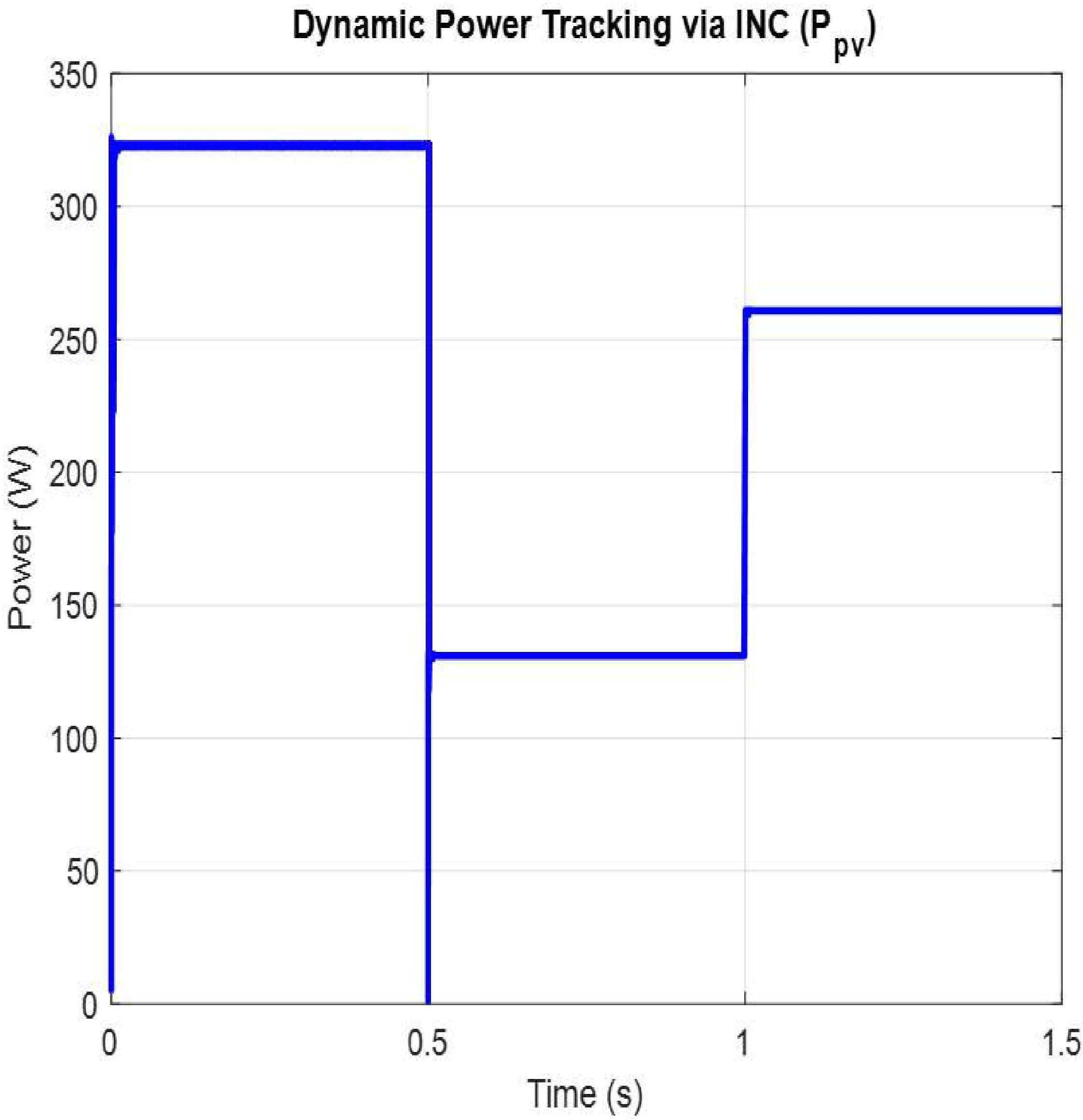

Figure IV.14: Dynamic Power curve with variable irradiance under INC algorithm

The curve(IV.14) illustrates the dynamic performance of the maximum power point tracking P_{PV} using the Incremental Conductance (INC) algorithm. The results display an instantaneous and highly rapid response during sudden step changes at 0.5s and 1s, with the power transitioning accurately between the three levels (325W, 130W, and 260 W). Furthermore, the curve exhibits ideal stability with zero steady-state oscillations, proving the superior tracking efficiency of the INC algorithm.

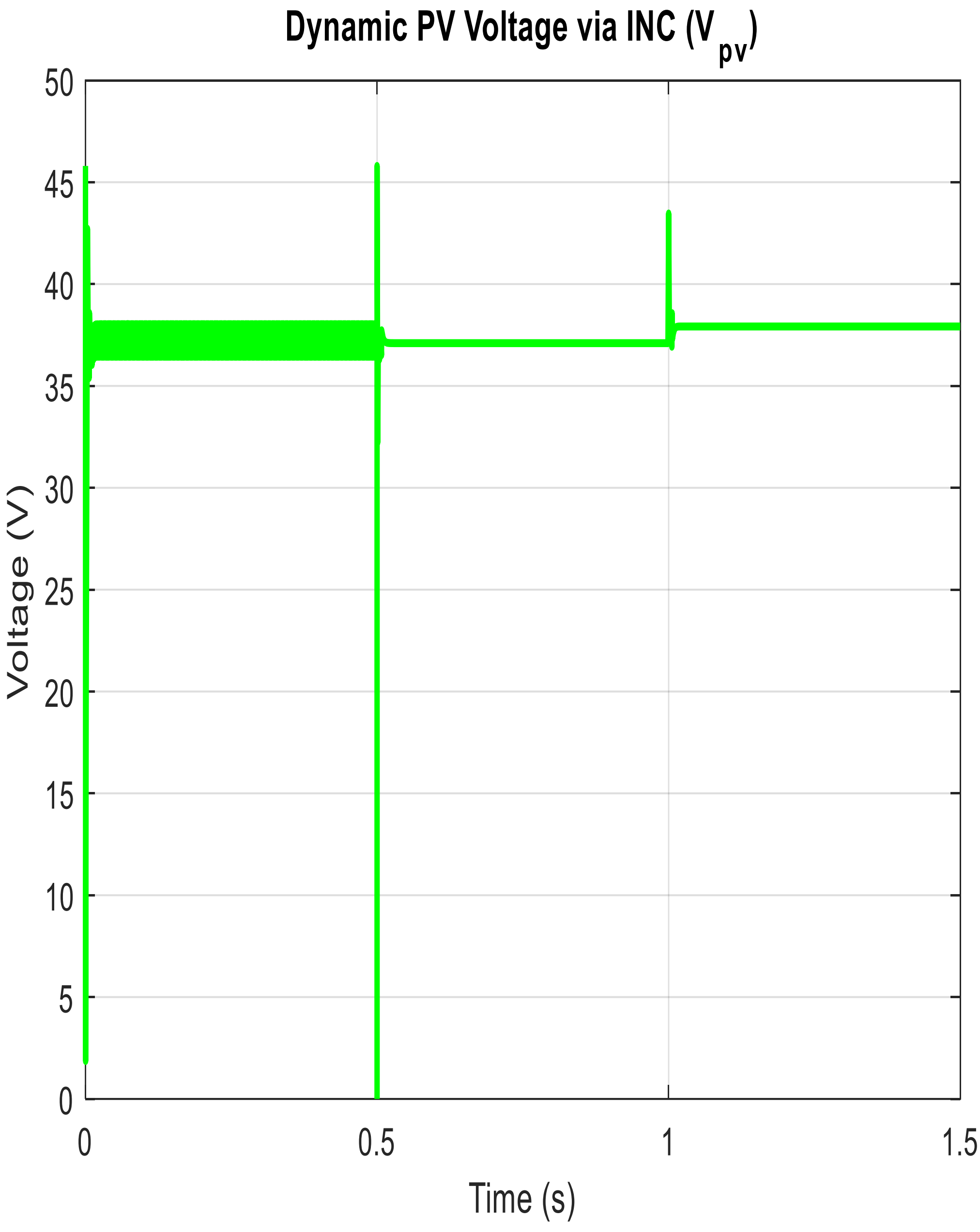

Figure IV.15: Dynamic voltage curve with variable irradiance under INC algorithm

The curve(IV.15) illustrates the dynamic response of the photovoltaic generator voltage V_{PV} using the Incremental Conductance (INC) algorithm. It shows minor oscillations in the initial interval [0s - 0.5s] during the search for the optimal point, followed by a highly rapid response at the transition times of 0.5s and 1s. The voltage directly settles with robust stability at the new reference values (37V and 38V) with zero steady-state ripples, highlighting the algorithm's strong capability in precise voltage regulation.

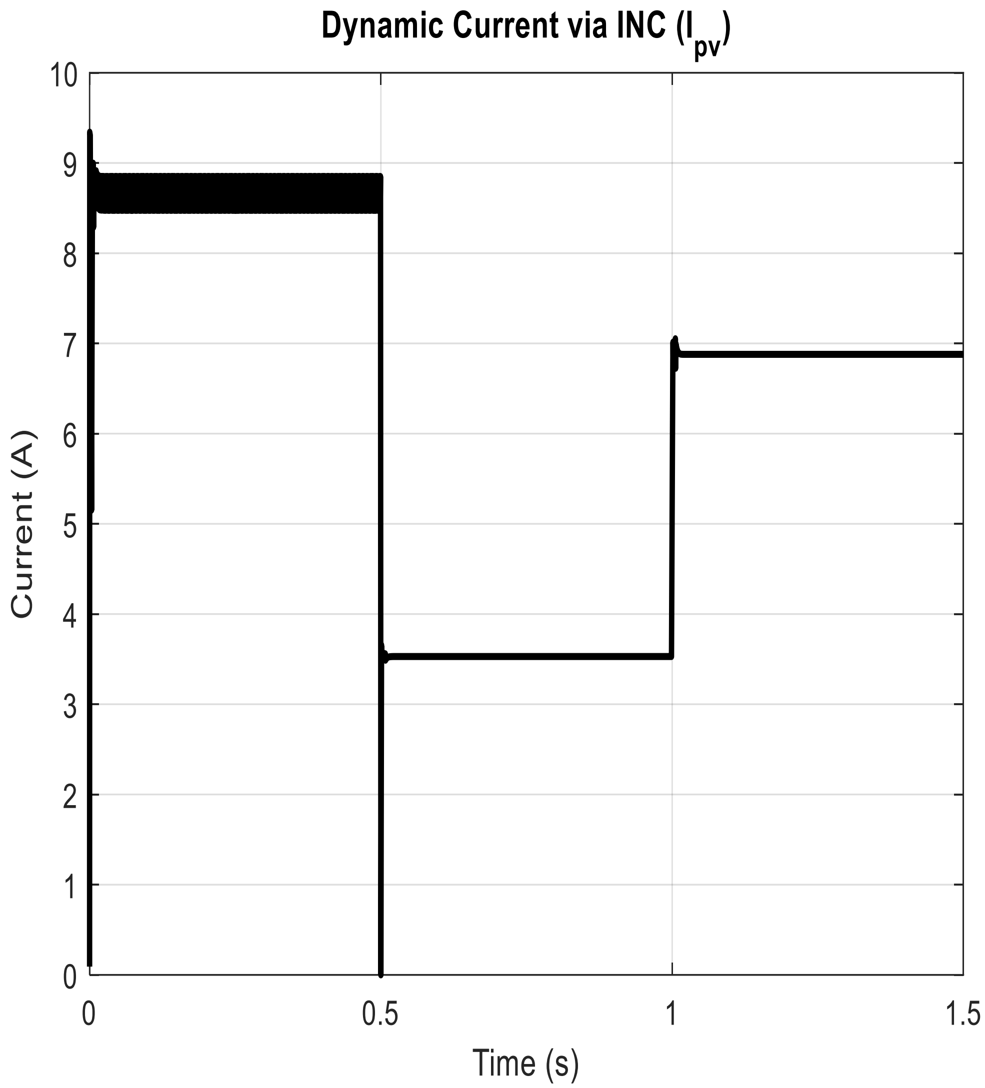

Figure IV.16: Dynamic current curve with variable irradiance under INC algorithm

The curve(IV.16) illustrates the dynamic response of the photovoltaic generator current I_{PV} tracked via the Incremental Conductance (INC) algorithm. Minor initial oscillations are observed in the interval [0s - 0.5s] during the primary tracking phase, followed by a highly rapid and accurate response to sudden step changes at 0.5s and 1s. The current transitions smoothly and settles immediately at the new optimal values (3.5A and 6.9A) with zero steady-state ripples, confirming the algorithm's high efficiency in maximum power point tracking and system stability.

IV.5. Simulation of PV system under Hill Climbing (HC) MPPT algorithm via MATLAB/Simulink

IV.5.1. Simulation results

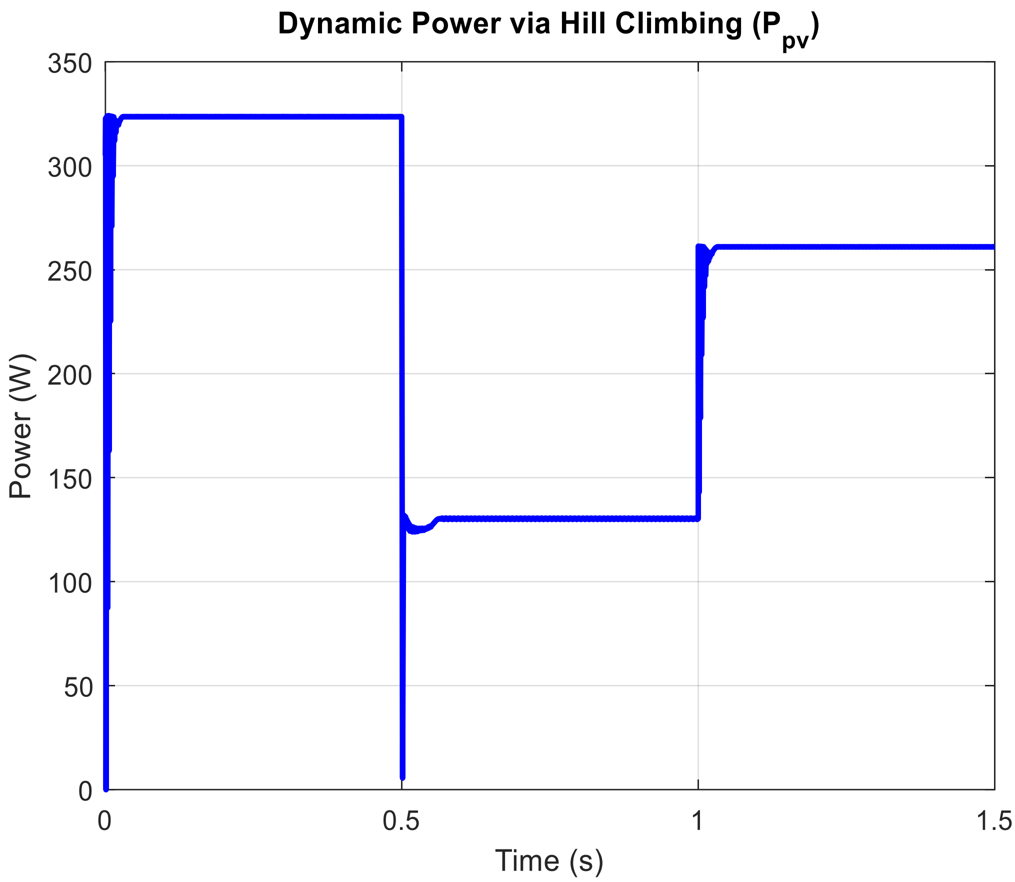

Figure IV.17: Dynamic power curve with variable irradiance under Hill Climbing (HC) algorithm

The curve(IV.17) illustrates the dynamic performance of the maximum power point tracking P_{PV} using the Hill Climbing technique. The results demonstrate a highly rapid and accurate response to sudden step changes at 0.5s and 1s. The power smoothly transitions between the three levels (325W, 130W, and 260W) with nearly zero steady-state oscillations, highlighting the algorithm's effectiveness in maintaining maximum power extraction.

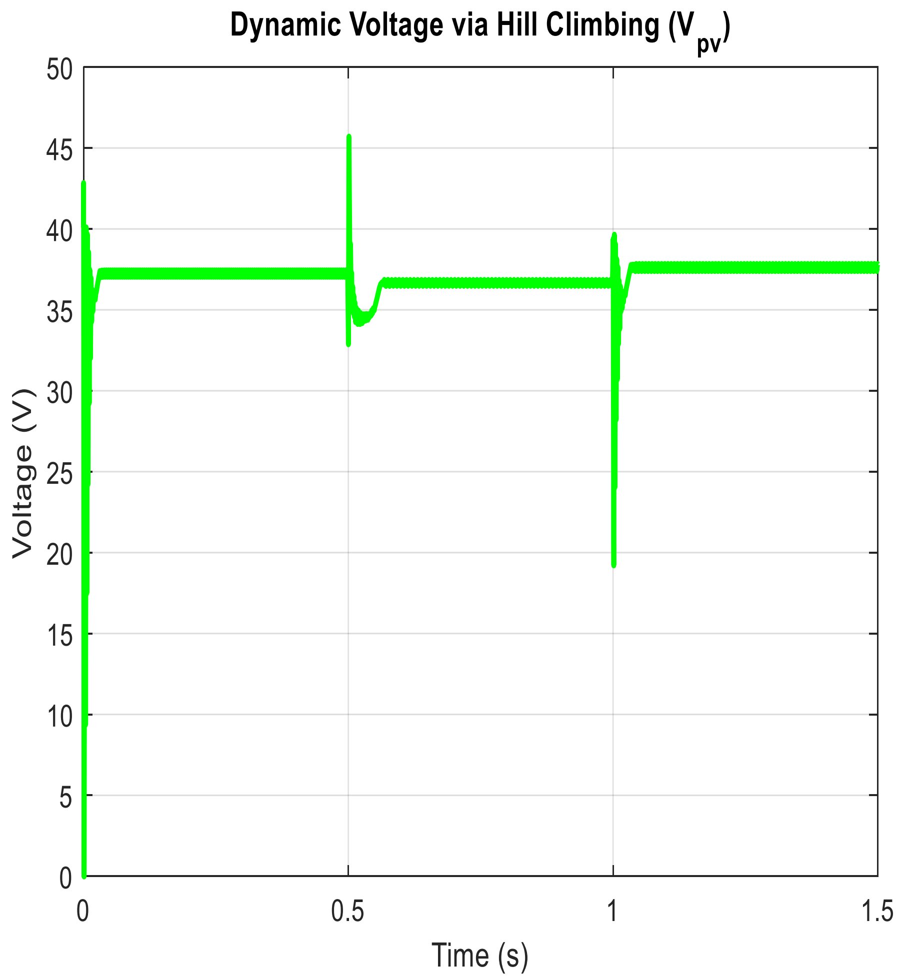

Figure IV.18: Dynamic voltage curve with variable irradiance under Hill Climbing (HC) algorithm

The curve(IV.18) illustrates the dynamic behavior of the photovoltaic generator voltage V_{PV} using the Hill Climbing technique. The system demonstrates excellent stability around the optimal voltage values (approximately 37.2V, 36.6V, and 37.5V). Although brief transient overshoots and undershoots occur during the step changes at 0.5s and 1s, the rapid settling time highlights the algorithm's robustness and efficiency in voltage regulation under dynamic conditions.

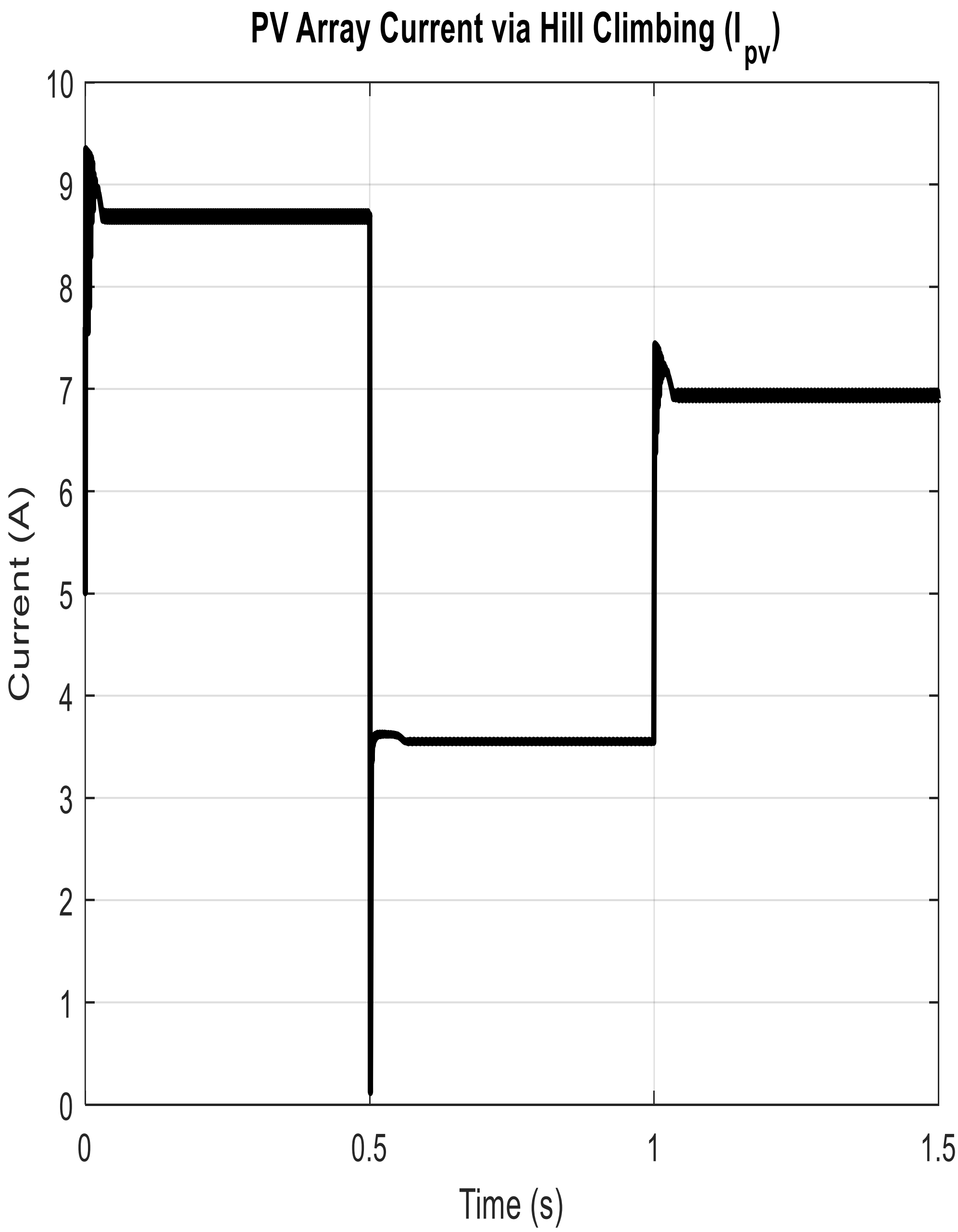

Figure IV.19: Dynamic current curve with variable irradiance under Hill Climbing (HC) algorithm

The curve(IV.19) illustrates the dynamic performance of the photovoltaic generator current I_{PV} tracked via the Hill Climbing technique. The system exhibits a highly rapid response during sudden step changes at 0.5s and 1s, where the current smoothly transitions and directly settles at the new optimal values (around 8.7A, 3.5A, and 6.9A, respectively). The stable and smooth steady-state profile indicates negligible oscillations, ensuring an efficient reduction in power losses

IV.6. Comparison between Perturb & Observe (P&O), Incremental Conductance (INC), and Hill Climbing methods

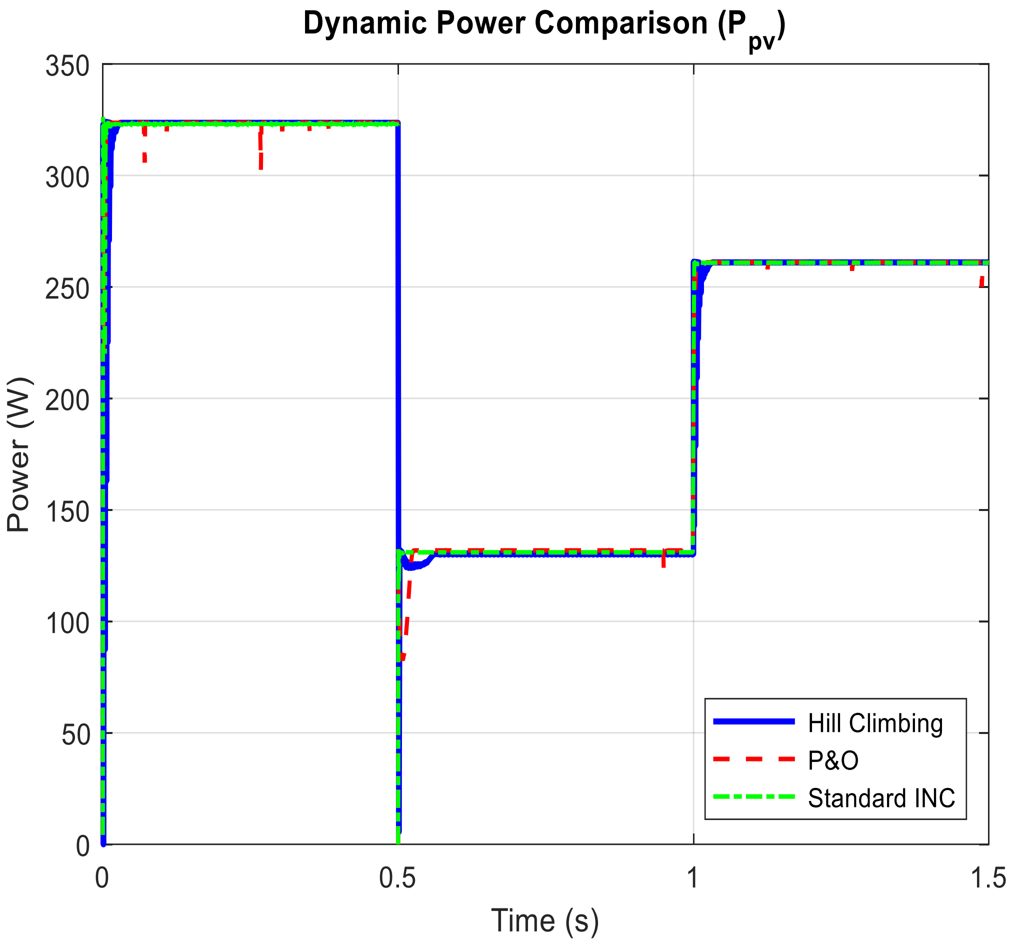

Figure IV.20: Dynamic power comparison between P&O, INC and Hill Climbing MPPT algorithms under varying irradiance

The curve(IV.20) presents a dynamic performance comparison of the maximum power point tracking P_{PV} among three algorithms: Hill Climbing, P&O, and Standard INC. While all three methods successfully track the maximum power point across different levels, the Standard INC algorithm demonstrates superior performance in terms of instantaneous response, perfect stability, and zero steady-state oscillations. The Hill Climbing technique follows with a smooth transition, whereas the P&O algorithm exhibits minor transient drops and oscillations during the step changes at 0.5s and 1s. This confirms the technical superiority and higher efficiency of the INC approach under dynamic operating conditions.

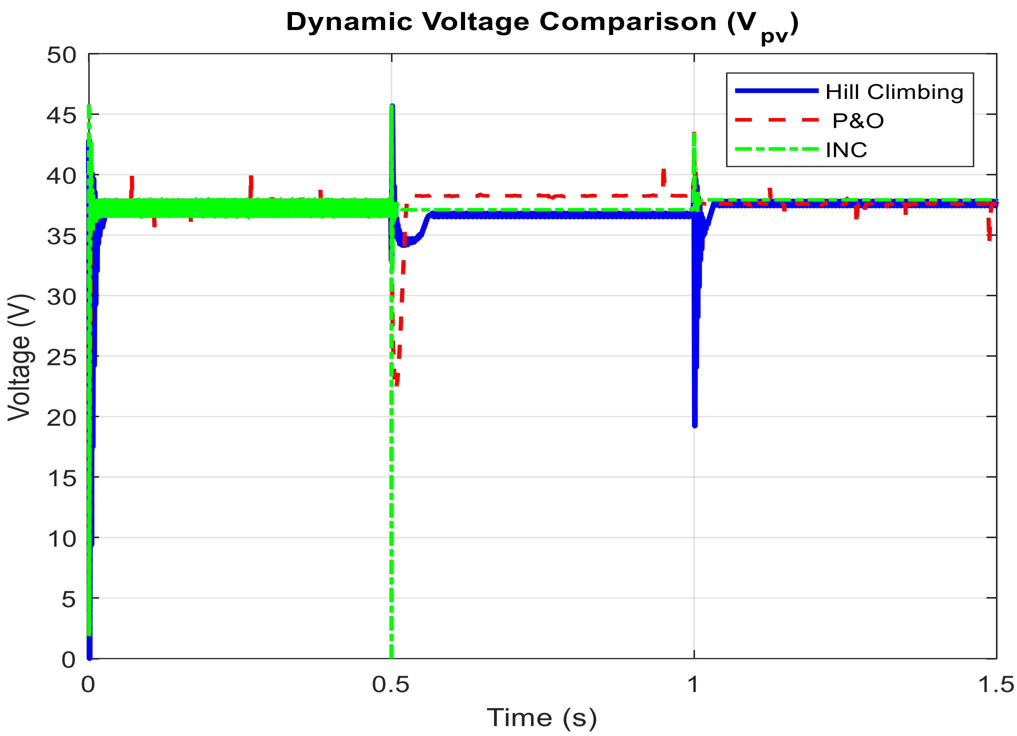

Figure IV.21: Dynamic voltage comparison between P&O, INC and Hill Climbing MPPT algorithms under varying irradiance

The curve(IV.21) presents a dynamic response comparison of the photovoltaic generator voltage V_{PV} among the three algorithms: Hill Climbing, P&O, and INC. The results highlight distinct behaviors in voltage regulation during the step changes at 0.5s and 1s. The INC algorithm demonstrates the fastest settling time and the highest steady-state stability despite the initial peak. Conversely, the P&O method exhibits a sharp drop and continuous steady-state ripples, while the Hill Climbing technique shows a significant transient undershoot at 1s before recovering. This confirms the superior capability of the INC approach in precise and robust voltage regulation.

IV.7. Conclusion

This chapter concluded with a dynamic study demonstrating the direct proportional effect of solar irradiance on current and the adverse effect of temperature on the PV generator's voltage and efficiency, while confirming the pivotal role of the boost converter as an impedance matcher. Although the comparative simulation results showed that all tracking techniques successfully extracted maximum power, the Incremental Conductance (INC) algorithm proved its technical superiority by delivering an instantaneous response, the fastest settling time, and zero steady-state ripples in both power and voltage compared to the P&O and Hill Climbing methods.

General Conclusion

In conclusion, this dissertation has focused on the study of photovoltaic systems as one of the most important renewable energy sources that have experienced significant development in recent years due to the increasing demand for clean and environmentally friendly energy. The work mainly concentrated on improving the performance of photovoltaic systems through the use of DC–DC power converters and Maximum Power Point Tracking (MPPT) techniques in order to increase energy conversion efficiency and minimize power losses caused by changing environmental conditions.

First, a general study of photovoltaic cells and panels was presented, including their operating principles, electrical characteristics, and the main factors affecting their performance such as solar irradiance and temperature. In addition, the different components of a photovoltaic system and its practical applications were discussed, highlighting the important role of solar energy in meeting the growing global demand for electrical power.

Next, DC–DC converters were studied with particular emphasis on the Boost Converter. Its operating principle, different operating modes, and mathematical modeling were explained in detail. The study showed that this converter plays a vital role in increasing and regulating the output voltage of photovoltaic panels according to load requirements, thereby improving system stability and efficiency.

Furthermore, Maximum Power Point Tracking (MPPT) techniques were investigated as one of the most effective methods for enhancing photovoltaic system efficiency. These techniques allow the extraction of the maximum available power from solar panels despite continuous changes in weather conditions. The most commonly used MPPT algorithms were presented, together with their operating principles, advantages, and limitations, which helped in understanding the importance of selecting the appropriate algorithm depending on system requirements and operating conditions.

In the practical part of this work, the photovoltaic system was modeled and simulated using MATLAB/Simulink in order to analyze its behavior under varying irradiance and temperature conditions. The simulation results demonstrated the effectiveness of combining MPPT techniques with the Boost Converter in improving the extracted power, stabilizing the output voltage, and increasing the overall efficiency of the photovoltaic system.

Finally, this study confirms that the integration of photovoltaic systems with modern control techniques represents an effective solution for developing renewable electrical energy systems. Moreover, this field remains open to many future research opportunities, particularly in the development of more intelligent and faster MPPT algorithms, the improvement of power converter performance, and the integration of artificial intelligence and energy storage systems to achieve more efficient and reliable solar energy systems.

List of References

[1]. Sarvi, M., & Azadian, A. (2022). A comprehensive review and classified comparison of MPPT algorithms in PV systems. Energy Systems, 13(2), 281-320.

[2]. Nadeem, Ahsan, and Afaq Hussain. "A comprehensive review of global maximum power point tracking algorithms for photovoltaic systems." Energy Systems 14.2 (2023): 293-334..

[3]. Chabani, A., Makhloufi, S., & Lachtar, S. (2021). Overview and impact of the renewable energy plants connected to the electrical network in southwest Algeria. EAI Endorsed Transactions on Energy Web, 8(36), e7-e7.

[4]. Belboul, Z., Toual, B., Kouzou, A., Mokrani, L., Bensalem, A., Kennel, R., & Abdelrahem, M. (2022). Multiobjective optimization of a hybrid PV/Wind/Battery/Diesel generator system integrated in microgrid: A case study in Djelfa, Algeria. Energies, 15(10), 3579.

[5]. Fezzani, A., Hadj-Mahammed, I., Kouzou, A., Zaghba, L., Drid, S., Khennane, M., ... & Abdelrahem, M. (2022). Energy efficiency of multi-technology PV modules under real outdoor conditions—an experimental assessment in ghardaïa, Algeria. Sustainability, 14(3), 1771.

[6]. Sakhraoui, K., Awopone, A. K., von Hirschhausen, C., Kebir, N., & Agadi, R. (2023). Toward a systemic approach to energy transformation in Algeria. Euro-Mediterranean Journal for Environmental Integration, 8(2), 365-379.

[7]. Benkhaled, M., Benmessaoud, M. T., & BoudgheneStambouli, A. (2023). High Penetration of Solar Energy to the Algerian Electricity System in the Context of an Energy Roadmap Toward a Sustainable Energy Paradigm by 2030.

[8]. Boukli Hacene, M. E. A., Lucache, D., Rozale, H., & Chahed, A. (2020). Renewable energy in Algeria: desire and possibilities. Journal of Asian and African Studies, 55(7), 947-964.

[9]. Deriche, M. A., Hafaifa, A., Tahri, A., Mohammedi, K., & Tahri, F. (2020). Energy and environmental performance analysis of grid-connected photovoltaic systems under similar outdoor conditions in the Saharan environment. Diagnostyka, 21(2), 13-23.

[10]. Djibrillah, M. (2021). Sustainable Energy Solution in Algeria: a Collection of Good Practices from SSB Japan's Project to Provide Effective Solutions for Energy Paradigm Shift (Master's thesis, PAUWES).

[11]. Aman, B. (2021). Selection Strategy of Rational Zones for Installation of Photovoltaic Solar Panels in Algeria.

[12]. Hassan, M. A., Bailek, N., Bouchouicha, K., Ibrahim, A., Jamil, B., Kuriqi, A., ... & El-kenawy, E. S. M. (2022). Evaluation of energy extraction of PV systems affected by environmental factors under real outdoor conditions. Theoretical and Applied Climatology, 150(1), 715-729.

[13]. Lagouch, A., Maouedj, R., & Benatiallah, A. (2024). A 5-MWp grid-connected photovoltaic plant's performance analysis and challenges under Algerian Sahara conditions. International Journal of Ambient Energy, 45(1), 2304732.

[14]. Bouchiba, O., Merizgui, T., Gaoui, B., Chettih, S., & Cheknane, A. (2021). Artistic feasibility research on a standalone hybrid solar/wind system based on IncCond algorithm under variable load demands-a case study: South Algeria. International Journal of Electrical and Computer Engineering (IJECE), 11(6), 4649-4658.

[15]. Bouznit, M., Pablo-Romero, M. D. P., & Sánchez-Braza, A. (2020). Measures to promote renewable energy for electricity generation in Algeria. Sustainability, 12(4), 1468.

[16]. Khadir, M. T., & Bouziane, S. E. (2020). Artificial Neural Networks modeling of electrical renewable energy both photovoltaic and wind for the region of Adrar Algeria. In 4th International Conference on Artificial Intelligence in Renewable Energetic Systems. Tipaza, Algeria.

[17] Bouhired F.2004. Commande et contrôle d'un installation solaire thermique . Mémoire de Magister,Université, Boumerdès

[18] OUKAF A et Abdelkrim B.2021. Amélioration de la commande MPPT d'un système photovoltaïque par les techniques intelligentes. Mémoire présenté pour l'obtention du diplôme de Master Académique Université MOHAMED BOUDIAF.

[19] https://www.ef4.be/fr/pv/composants dun systeme/systemes photovoltaiques.html

[20] https://fr.scribd.com/document/509165099/energie-photovoltaique-introduction (28.03.2024)

[21] -N. AIT KHELIFA « Modélisation d'un système de pompage photovoltaïque utilisant un moteur synchrone à commutation naturelle», Mémoire de Maste2, Université de Bejaïa, 2011.

[22]-P. BESSEMOULIN, J. OLIVIERI,«Rayonnement solaire et sa composante ultraviolette», la météorologie série 8-N° 31, pp (42-59), 2000.

[23] -S. NAOUAL, «Modélisation et Extraction Automatique des Paramètres d'un Générateur, » Université Ferhat Abbas de Sétif Mémoire de Magister, Département d'électrotéchnique 2010.

[24] -Uni. Kassel,«PhotovoltaicSystemsTechnology», Kassel, Germany, 2003, www.uni-Kassel.de/re.

[25] VisionL earning, Web 19 June 2021

https://www.visionlearning.com/en/library/Earth-Science/6/Factors-that-Control-Earths-Temperature/234

[26] M.Krimi , le gisement solaire (présentation sur power point), Institue de formation en électricité et gaz (IFFEG) ,13 mai Blida, Algérie.

[27] Yves Roulet Ingénieur Environnement « differentes utilisations de l "energie solaire et integration des capteurs solaires » département des infrastructures service des bâtiments, monuments et archéologie, mai 2005

[28] Liman A et Soukane S. 2012.Etude et modélisation d'un système photovoltaïque autonome, mémoire d'Ingéniorat, UMMTO.

[29] HELALLI K:2012 Modélisation d'une cellule photovoltaïque étude comparative.Mémoire de Magister, Université Mouloud Mammeri.

[30] -BENDJOUDI Faouzi ,LAKHDARI Farid , «Etude et Conception D'un Système de Pompage Photovoltaïque Avec Stockage Electrochimique»,mémoire de master , UNIVERSITE ABDERAHMANE MIRA DE BEJAÏA,2014

[31] Milles Abdessamd ,«Réalisation d'un convertisseur à accumulation capacitive" Cuk" Pour les applications solaires», Mémoire de Maste2, Université de Batna,2014

[32] ZAIRI S et BOUBIADA.S.2020.Etude et Dimensionnement d'un centrale Photovoltaïque. Université Mohamed Khidre , Biskra

[33]: K.HELALI, Modélisation d'une Cellule Photovoltaïque: Etude Comparative, mémoire de magister, université MOULOUD MAMMERI de TIZI-OUZOU 2012.

[34] TIHAR RAZKI, KHALFALLAH ALI, «Etude comparative par simulation des différents algorithmes de commande MPPT dans une chaine de conversion PV», Mémoire de Maste2, UNIVERSITE MOHAMED BOUDIAF - M'SILA,2022

[35] Cheikh Abd Erazek, «Modélisation d'une station de pompage photovoltaïque», Mémoire de Maste2, UNIVERSITÉ BADJI MOKHTAR- ANNABA,2019

[36] GHERRAZ FERIEL, MEDJDOUB RIM, « Maximum power point trackers (MPPT) pour un système PV par des méthodes classiques et des méthodes intelligentes. » , Mémoire de Maste2, Universitaire BOUSSOOUF Abdelhafid –Mila,2024

[37] Y.Pankow, „"Étude de l"intégration de la production décentralisé dans un réseau basse tension „", Thèse de doctorat de l"école nationale supérieure d"Art et Métiers, France, décembre 2004.

[38]-BOUALEM, DENDIB, «Technique conventionnelles et avancée de poursuite MPPT pour des application photovoltaïque : étude comparative. », Université Ferhat Abbes-Sétif Mémoire de Magister, Département d'électronique TS4/6338, 2007.

[39] https://www.digikey.fr/fr/product-highlight/p/panasonic/amorphous-silicon-solar-cells (02.03.2024)

[40] Boudjema Mohammed et Belhaouas Nasreddine, „" Commande d"une poursuite du point de puissance maximal (MPPT) par les réseaux de neurones et implémentation

[41] https://fr.linkedin.com/pulse/module-5-les-principaux-%C3%A9l%C3%A9ments-dun-syst%C3%A8me-solaire-mbainaiwala (03.03.2024)

[42] BOUCHETAB AHMED, «Commande d'un onduleur photovoltaïque Connecté au réseau électrique. » , Mémoire de Maste2, Université de Jijel,2012

[43] Zaiem K.2019. Commande d'un système photovoltaïque par controleur Neuro-flou Réduit. MEMOIRE MASTER, UNIVERSITE BADJI MOKHTAR,ANNABA.

[44] Alternative Energy Tutorials, Web 19 June 2021

https://www.alternative-energy-tutorials.com/photovoltaics/bypass-diode.html

[45] Electronic tutorial, Web 19 June 2021

https://www.electronics-tutorials.ws/diode/bypass-diodes.html

[46] MERAOUAH M et Ali M.2020 Application du contrôle intelligent d'un hacheur Boost dans un système de conversion d'énergie solaire. MEMOIRE MASTER . UNIVERSITÉ IBN-KHALDOUN,TIARET.

[47] Yann R.2009. Gestion des flux énergétiques dans un système photovoltaïque avec stockage connecte au réseau.Thèse de Doctorat, Université Joseph Fourier.

[48] BOUCHTER A et MOKRANE C.2020 .Comparaison entre différentes techniques de commande MPPT d'un système solaire. Université 8Mai 1945 – Guelma

[49] A. Goetzberger V.U. Hoffmann, „"Photovoltaic Solar Energy Generation""", Springer Verlag, 2005.

[50] Fatima B.2018 Modélisation et simulation des sources de production décentralisée Application à l'intégration d'un générateur PV à stockage dans un réseau électrique . Thèse de doctorat, Université Abdelhamid Ibn Badis, Mostagane.

[51] Eric RANGA, Macdonald PHIRI, «STUDY AND SIMULATION OF A PHOTOVOLTAIC WATER PUMPING SYSTEM», Mémoire de Maste2, University of Abou Bakr Belkaïd – Tlemcen,2021

[52] https://www.researchgate.net/figure/Symbole-dun-convertisseur-DC-DC_fig12_320910708 (04.03.2024)

[53] M. HARAOUIBA, «étude et simulation d'un générateur de panneau,» FACULTE DE SCIENCE DE L'INGENIORT, ANNABA, 2019

[54] KHECHIBA ABDELDJALIL, HAOUAMED SAAD, «Implémentation Et Simulation D'un Contrôleur MPPT Dans Les Systèmes Photovoltaïques» , Mémoire de Maste2, Université Echahid Hamma Lakhdar-El Oued,2024

[55] G. F. E. S. AMEL, «commode de panneau solaire à l'aide d'un carte à pic,» BISKRA, 2010.

[56] TOUMI N ,KOUDA I .2021.ÉNERGIE SOLAIRE PHOTOVOLTAÏQUE ET SYSTEME PHOTOVOLTAIQUE AUTONOME. Université Badji Mokhtar ,Annaba.

[57] Mohamed Arrouf, „‟ Optimisation de l‟ensemble onduleur, Moteur et Pompage branché sur un générateur photovoltaïque ", thèse de doctorat, Spécialité électronique, Université Mentouri de Constantine, 2007.

[58] Babaei E, Esmaeel M, Mahmoodieh S. Electrical Power and Energy Systems Systematical method of designing the elements of the Cuk converter. Int J Electr Power Energy Syst, Vol 55, pp 351–361. 2014.

[59] J. M. Enrique, E. Duran, Theoretical assessment of the maximum power point tracking efficiency of photovoltaic facilities with different converter topologies,Solar Energy, Vol 81, pp 31-38, 2007.

[60] J. David Irwin. The Power Electronics Handbook. TIMOTHY L. SKVARENINA, 2002.

[61] Robert W. Erickson and Dragan Maksimovic. Fundamentals of Power Electronics (Second Edition). Springer, 2nd edition, 2001.

[62] Abouchabana Nabil. Etude d'une nouvelle topologie buck-boost appliquée à un MPPT. These de magister, ENP, Alger, 2009.

[63] M. Belkacemi Mohamed Lamine, M. Sifi Redouane, «Etude et réalisation d'un convertisseur DC-DC avec contrôleur MPPT destiné au pompage photovoltaïque», Mémoire de fin d'études, E.N.P- 10, Avenue Hassen Badi, 16200 El Harrach, Alger,2014

[64] Benoit Issartel. Conception d'un convertisseur DC/DC de type boost. Thése de doctorat, Polytech Clermont-Ferrand, France 2006.

[65] M.Angel Cid Pastor, "Conception et Réalisation de Modules Photovoltaïques Electroniques", Institut National des Sciences Appliquées de Toulouse, 2006

[66]: F.BENADEL, Etude et Simulation D'une Commande MPPT Pour Système PV, mémoire de Master, université de Mohamed Boudiaf - M'SILLA, 2016.

[67]: A.Talha, Développement d'une Méthode MPPT pour un Système Photovoltaïque, Premier Séminaire International sur les Energies Nouvelles et Renouvelables, SIENR'2010, Ghardaïa, Algeria, October 2010.

[68]: A.Hanen, H.Abid, K.Loukil, A.Toumi et M. Abid, Etude comparative de cinq algorithmes de commande MPPT pour un système photovoltaïque, Conférence Internationale des Energies Renouvelables (CIER'13) Tunisie, 2013.

[69]: A.Rhif, Etudes et Applications sur les Energies Renouvelables, Proceedings of Engineering & Technology, ISSN: 1737-9334, 2019.

[70]: H. H. MOLINARO et B. MULTON, Energie électrique: génération photovoltaique, Culture Sciences de l'Ingénieur, Paris, 2020.

[71] V. Salas, E. Olias, A. Barrado, A. Lazaro, "Review of the maximum power point.tracking algo-rithms for stand-alone photovoltaic systems", Solar Energy Materials & Solar Cells ….90 (2006)1555.1578

[72] Trishan Esram, Student Member, IEEE, and Patrick L. Chapman, Senior Member, IEEE, "Comparison of Photovoltaic Array Maximum Power Point Tracking Techniques", IEEE TRANSACTIONS ON ENERGY CONVERSION, 2006

[73]: A. BENSLIMANE et A.MERABTI, A comparative study between hill clibing algorithm and fuzzy logic controller algorithm of MPPT for GPV system, EasyChairperprint № 2695, 2020.

[74]: C.CABAL, Optimisation énergétique de l'étage d'adaptation électronique dédié à la conversion photovoltaïque, Thèse Doctorat, universite de TOULOUSE, 2008.

[75] Government of Algeria. (2014). Executive Decree No. 14-203 of 13 July 2014 establishing the conditions and procedures for benefiting from guaranteed tariffs for electricity produced from solar photovoltaic and wind energy installations. Official Journal of the People's Democratic Republic of Algeria

Appendix 01

The Electrical Parameters of the PV Generator

Parameter	Symbol	Value & Unit
Maximum Power	Pmax	330 W
Short-Circuit Current	Isc	9.35 A
Open-Circuit Voltage	Voc	45.8 V
Current at Maximum Power	Imp	8.85 A
Voltage at Maximum Power	Vmp	37.3 V
Number of Cells in Series	Ns	72
Series Resistance	Rs	0.22 Ω
Shunt Resistance	Rsh	500 Ω
Temperature Coefficient of Isc	α	0.0006 A/K
Temperature Coefficient of Voc	β	-0.133 V/K
Diode Ideality Factor	A	1.3
Load/Circuit Resistance	R	20 Ω
Filter Inductance	L	0.001 H (1 mH)
Filter Capacitance	C	0.00022 F (220 µF)